UNIVERSITÀ DEGLI STUDI DI PALERMO

Dottorato di Ricerca in Scienze Fisiche
Dipartimento di Fisica e Chimica - Emilio Segrè
Settore Scientifico Disciplinare FIS/02

Quantum identical particle indistinguishability: concepts and applications

IL DOTTORE
ALESSIA CASTELLINI

IL TUTOR
PROF. GIUSEPPE COMPAGNO

IL COORDINATORE
PROF. GIOACCHINO MASSIMO PALMA

CICLO - XXXII
ANNO CONSEGUIMENTO TITOLO - 2020

A mia madre

Contents

List of publications

1. G. Compagno, A. Castellini, and R. Lo Franco,
   "*Dealing with indistinguishable particles and their entanglement*",
   Philosophical Transactions of the Royal Society A 376, 20170317 (2018).

2. A. Castellini, B. Bellomo, G. Compagno, and , R. Lo Franco,
   "*Activating remote entanglement in a quantum network by local counting of identical particles*",
   Physical Review A 99, 062322 (2019).

3. A. Castellini, R. Lo Franco, L. Lami, A. Winter, G. Adesso, and G. Compagno,
   "*Indistinguishability-enabled coherence for quantum metrology*",
   Physical Review A 100, 012308 (2019).

4. A. Castellini, R. Lo Franco, and G. Compagno,
   "*Effects of indistinguishability in a system of three identical qubits*",
   Proceedings 12, 23 (2019).

5. F. Nosrati, A. Castellini, G. Compagno, and R. Lo Franco,
   "*Control of noisy entanglement preparation through spatial indistinguishability*",
   arXiv:1907.00136 (2019).

6. K. Sun, Y. Wang, Z-H. Liu, X-Y Xu, J-S Xu, C-F Li, G-C Guo, A. Castellini, F. Nosrati, G. Compagno, and R. Lo Franco,
   "*Experimental control of photon spatial indistinguishability to realize entanglement and teleportation*",
   submitted.

7. A. Castellini, F. Nosrati, R. Lo Franco and G. Compagno,
   Deformations of identical particle systems
   to be submitted.

- **Information paper**

- G. Compagno, A. Castellini, and R. Lo Franco,
  "*Are identical quantum twins distinguishable?*",
  Atlas of Science (2019).

- **Paper not included in this thesis**

- A. Castellini, H. R. Jauslin, B. Rousseaux, D. Dzsotjan, G. Colas des Francs, A. Messina, and S. Guérin,
  "*Quantum plasmonics with multi-emitters: application to stimulated Raman adiabatic passage*",
  The European Physical Journal D 72, 223 (2018).

Introduction

Identical quantum systems (e.g. photons, electrons, atoms, qubits, plasmons ...), for which all the intrinsic properties, as mass and charge, are the same, constitute a crucial element on which networks for quantum information processes are based [1, 2, 3, 4]. Let me take some examples. By treating a system of bosons as a gas of quantum identical systems, Einstein showed that at low temperatures, particles are "trapped" in the ground state of the global system, forming a "condensate" [5, 6]. Quantum correlated electrons are naturally created by split Cooper pair in systems of quantum dots [7] coupled to superconductor structures [8]. Optical setups [9, 10] have identical systems as building blocks and recent researches try to exploit plasmonic platforms for the development of quantum technologies, sensing and computing [11, 12, 13]. All the cited identical particles-based systems, i.e. Bose-Einstein condensates, superconducting circuits, quantum dots, optical setups and plasmonic platforms, are today essential to deploy quantum communication, quantum metrology and quantum computing. As a result, the characterization of features and correlations of identical quantum systems (particles) is essential from both the conceptual and practical view points.

Classically, both nonidentical and identical particles (NIP and IP, respectively) are always addressable. being possible to identify them by means of labels or to follow their trajectories without affecting their dynamics. Therefore, both NIP and IP are always *distinguishable* and their dynamics, given the same initial conditions, is the same. On the other hand in quantum mechanics, IP systems present physical properties that significantly differentiate them from NIP ones. This is due to the fact that now IP cannot be addressed by any physical label, since labels are quantum numbers rendering particles nonidentical, and moreover the concept of trajectory is lost. The IP unaddressability thus should require an approach different from the one used for NIP. Nevertheless, curiously, the standard quantum mechanical description of IP, firstly, attributes to them unphysical (mock) labels which make them nonidentical [14, 15] and secondly, introduces a symmetrization postulate with respect to these labels. The latter do not correspond physically to any measurable quantum property that really differentiates particles. This introduces problems in the characterization not only of their quantum states but mostly of their quan-

tum correlations. The symmetrization postulate establishes that the only allowed IP states are the ones symmetric (*fermions*) or antisymmetric (*bosons*) with respect to the exchange of mock labels, however, it gives place to some effects apparently in contrast for example, with relativistic causality. As an example of this, consider the case of spatially separated and independently generated IP: according to the symmetrization postulate, quantum states seem to imply that the mere presence of particles of the same species in remote locations leads to nonzero probability amplitudes that each particle occupies all the involved locations immediately after their generation, even if the events creating them are space-like separated. Moreover, the structure of IP quantum states looks entangled with respect to mock labels.

Entanglement [16, 17] is another crucial feature of quantum-enhanced technologies [18, 19, 20, 21]. When quantum particles are entangled, single-particle measurements on different particles are correlated even if they are noninteracting and space-like separated. Thus, entanglement can lead to non local behaviors, that is ones which cannot be reproduced by a classical local hidden variable model [17, 22]. And it is just this purely quantum trait which is at the basis of several protocols and instruments to implement quantum information, such as key distribution, teleportation and quantum algorithms.

Being both IP and entanglement the core of quantum-enhanced devices, it is really essential to characterize the IP-quantum correlations. However, as already said, ordinarily the structure of IP quantum states in the particle-based standard approach is such that they look always entangled, even when physically one expects that they must be uncorrelated, for example when they are independently prepared at space-like separated locations [14]. This is due, as said before, to the presence of unphysical labels characterizing the single-particle states, which leads the Hilbert space of composite IP systems to lose the tensorial structure that, instead, characterizes NIP systems. As a result, the usual criteria and tools used to characterize NIP-entanglement, such as the separability criterion, Schmidt rank, partial trace and von Neumann entropy are not well defined for IP and brings to physical inconsistencies [23, 24]. With the purpose of separating the real physical correlation to the unphysical one due to labels, several different theories, both in the standard particle-based [25, 24, 26] and second quantization approach [27, 28, 29, 30], have been proposed for both spatially overlapping and nonoverlapping independently prepared particles. However, some of these theories [23, 24], which use new concepts as the Slater rank and the von Neumann entropy for bosons and fermions, give results in contrast with some experimental evidences: as an example, the affirmation that two noninteracting IP in the same site prepared in orthogonal single-particle states are not entangled is in contrast to recent the experimental results of [31]. Furthermore, in the standard approach, there is not for IP the analogous of the operational framework based on local operations and classical communication (LOCC) through which correlations of NIP are identified and exploited [17, 32]. The reason is due to the unaddressability of spatially overlapping IP, which makes the concept

of particle-locality as used in LOCC meaningless.

Recently, a different particle-based approach has been introduced [33], named *no-label approach*, that does not use from start unphysical labels to characterize IP states. In this way the problem of the unphysical entanglement present in the standard treatment is avoided from the very beginning. The advantage of the no-label formalism is that, to quantify IP entanglement, it exploits the same criteria and tools known for NIP, without conceptual and physical inconsistencies. As a starting point, it gave the possibility of obtaining the following results: the identification of the physical origin of IP-entanglement for pure states of two independently prepared IP (both spatially separated and overlapping) [33, 34]; the existence of the Schmidt decomposition for IP (showing that it is universally valid for any type of particles) [35]; a new efficient generation scheme of multipartite W entangled states [36]; the definition of an operational framework for IP based on *spatially* localized operations and classical communication (sLOCC), in order to directly exploit IP entanglement in a Bell-like scenario of separate locations, also when IP spatially overlap [34]. Recently in the literature, the no-label approach has been confronted with alternative methods both in first [37] and second quantization [38, 39] and it has also been applied to treat effects as the Hanbury Brown-Twiss with IP [40] and quantum entanglement in one-dimensional systems of anyons [41].

This thesis is the result of my research work during the PhD in Physical Sciences at the University of Palermo, under the supervision of Professor Giuseppe Compagno. My scientific contributions are in the context of IP quantum systems, with the purpose of identifying, by means of the no-label approach, the properties exploitable for quantum information processing.

- **Part I: Background and new formalism for identical particles**

In the first part of the thesis, I will analyse the basic concepts of the standard quantum mechanical approach to IP that lead to difficulties in the characterization of their quantum correlations. I will recall different theories, both in the standard first and second quantization formalisms, proposed to overcome these drawbacks.
Then, original research results will be presented. I will generalize, to the case of N IP, the no-label formalism and the operational framework based on *spatially localized operations and classical communication* (sLOCC). This will give the possibility to quantify, in a Bell-like scenario with separated locations, the role played by particle indistinguishability in the emergence of the operationally exploitable entanglement in a generic mixed state of IP. Finally I will introduce a measure for particle indistinguishability. This will permit to quantify its effects on the implementation of quantum protocols.

- **Part II: Consequences of indistinguishability: concepts and applications**

In the second part of the thesis, first of all, I will show an experiment implemented in collaboration with the research group of Guan-Can Guo at the CAS Key Laboratory of Quantum Information of Hefei (China). The aim of the experiment is to show if and how one can practically control the degree of spatial indistinguishability of two IP and eventually exploit it for quantum teleportation.

Then, I will deal with the role of particle statistics in the implementation of an entanglement transfer in a large-scale quantum network.

After having shown how indistinguishability affects the emergence and the transfer of entangled states, I will examine the possibility to use it also to preserve the preparation of correlations in presence of an environment.

Successively, I will deal with the generalization to IP of the basic concepts of the resource Theory of quantum coherence known for NIP and I will investigate the exploitation of coherence due to indistinguishability for quantum information processes.

Finally, a new class of operations, called "deformations", will be introduced for IP systems, showing some of their physical effects.

Part I

Background and new formalism for identical particles

Chapter 1

Standard description of identical particles in quantum mechanics

1.1 Introduction

In this Chapter, first of all I will recall the basic concepts of the ordinary standard approach (SA) to quantum identical particles (IP) in first quantization, i.e. the exchange degeneracy due to the presence of unphysical labels associated to each particle and the symmetrization postulate introduced to remove it. Then the drawbacks coming from this treatment in the characterization of IP entanglement will be highlighted, showing that the usual tools and concepts used for nonidentical particles (NIP), such as the separability criterion, the Schmidt decomposition and the von Neumann entropy, cannot be directly exploited for IP. When this is done, in fact, it presents some physical inconsistencies or is meaningless. Some theories developed within the SA, both in first and second quantization, to identify and quantify IP quantum correlations, will be presented.

1.2 Exchange degeneracy and symmetrization postulate

"Two particles are said to be identical
if all their intrinsic properties (mass, spin, charge, etc...) are exactly the same."[15]

In classical physics, the fact that a system consists of IP or NIP is irrelevant for the description of its configuration and evolution. In fact, even if particles are exactly of the same type, they follow different spatial trajectories and I can always look at each of them without disturbing its dynamics. I can also differently label them (using for example numbers), keeping them always identical without modifying their physical behavior. No matter how I label them: all the

configurations obtained exchanging labels follow the same dynamics, making all the physical predictions unaffected by these labels [15].

Consider now quantum IP. In quantum mechanics, IP can be considered truly elementary or not. In fact, any quantum system of interacting particles which is able to form a bound state has a discrete energy spectrum. These systems in their ground states can be endowed with fixed unchanging properties as long as the energy exchanges with their environment are much less than the difference between the first excited state and the ground state. Under these conditions, such systems act as elementary particles and if they are of the same species, they can be considered IP. All composed systems stop to being considered elementary and identical when excited levels enter into play. As an example, helium atoms up to few kelvin, hydrogen atoms up to $T \sim 10^3\ K$ and nucleons up to $T \sim 10^5\ K$ are elementary. On the other hand, particles without internal structure (elementary excitations of quantum fields) are truly elementary. Therefore, from now on, with IP I will mean systems of at least two elementary systems under the previously presented condition, e.g. qubits, atoms, quantum dots, photons, electrons, quasi-particles, etc...

Contrary to the classical case, in quantum physics the trajectories of IP not only cannot be observed without modifying their behavior, but also cannot be uniquely associated to a given particle, if there are spatial regions in which the probability of finding more than one particle is different from zero. The SA to deal with quantum IP assume that they are not [15], marking them with labels which do not correspond to physical properties. Even if they are unphysical (mock), formally the operation of labelling quantum IP makes them different and modifies the description of their dynamics. As an example, let us consider two IP sharing a spatial region: following the SA, I assign to one of them the number 1 and to the other the number 2. According to the first postulate of quantum mechanics [42], the physical state of our system has to be described by a ket $|\Psi\rangle$ belonging to the Hilbert space associated to the two particles. Let us suppose that one particle is in the single-particle state $|\{\alpha\}\rangle$, where $\{\alpha\}$ are the eigenvalues associated to a set of commuting observables [1], and analogously, the other one is in $|\{\beta\}\rangle$. Performing a two-particle measurement on the system, I will obtain $\{\alpha\}$ from one particle and $\{\beta\}$ from the other. But I don't know if the state of our system is

$$|\Psi\rangle = |\{\alpha\}\rangle_1 \otimes |\{\beta\}\rangle_2 \,, \tag{1.1}$$

or

$$|\Psi\rangle = |\{\alpha\}\rangle_2 \otimes |\{\beta\}\rangle_1 \,, \tag{1.2}$$

[1] In quantum mechanics, physical quantities associated to a system are called "observables" and they are essential in defining its quantum state.

or even one of their possible linear combinations

$$|\Psi\rangle = a\,|\{\alpha\}\rangle_1 \otimes |\{\beta\}\rangle_2 + b\,|\{\alpha\}\rangle_2 \otimes |\{\beta\}\rangle_1 \tag{1.3}$$

with $|a|^2 + |b|^2 = 1$. This is known as *exchange degeneracy*. Even if the physical state is the same, the mathematical descriptions are different because of the presence of labels 1 and 2, which are physically unobservable but mathematically quantum numbers rendering particles nonidentical. These labels not only cause the association of different kets to the same sets of eigenvalues, but also different physical predictions. In fact, if I try to calculate the probability of finding our system initially prepared in $|\Psi\rangle = a\,|\{\alpha\}\rangle_1 \otimes |\{\beta\}\rangle_2 + b\,|\{\alpha\}\rangle_2 \otimes |\{\beta\}\rangle_1$ in a different state $|\Psi'\rangle$, it will depend on the coefficients a and b. As a result, the exchange degeneracy given by the presence of mock labels does not give us the possibility to write uniquely the ket associated to a specific physical state and to calculate probabilities to find the system in a different quantum state. The fact is that no complete measurement performed on each particle will give us the possibility to know which is exactly the form of the state $|\Psi\rangle$, since the different mathematical possibilities depends on quantities that are not physically observable and come only from the purely formal attempt to describe IP analogously to NIP [43].

The exchange degeneracy is removed by the symmetrization postulate [15], that gives us a rule to associate to a physical state of IP a single ket: it can be completely symmetric or antisymmetric, depending on the nature of particles, with respect to permutation of the unphysical labels. Particles for which the kets are symmetric are called *bosons* and the ones described by antisymmetric kets are called *fermions*. As a result, in the previously considered two-particle example, the state $|\Psi\rangle$ is uniquely represented setting $a = b = \frac{1}{\sqrt{2}}$ for bosons and $a = -b = \frac{1}{\sqrt{2}}$. An immediate consequence of the symmetrization postulate is that two or more fermions cannot occupy simultaneously the same quantum state (Pauli's exclusion principle).

In systems of N noninteracting IP, the physical states are (anti)symmetric, with respect to unobservable labels, linear combinations of $N!$ tensor products of labelled single-particle states. For bosons (fermions) they have the structure of a Slater permanent (determinant), and the bigger is the number of particles, the more complicated is the expression of the state in the SA.

1.3 No general agreement on entanglement of identical particles

In this section, I will show some examples of how the SA gives rise to methodological and practical difficulties in the characterization of the IP entanglement. These difficulties arise because of the adoption of unphysical labels marking particles and of the required (anti)symmetrization

of states with respect to them. Usual tools and criteria to study NIP entanglement cannot be used for IP. Many theories have been developed for this purpose, giving however contradictory results, which in certain cases, are also in contrast with experimental evidences.

1.3.1 Failure of usual tools to characterize identical particle entanglement

Consider a system S composed by a particle 1 and a particle 2. If they are nonidentical, this labels are associated to physical observables. Suppose that the global system is described by the two-particle pure state $|\Psi\rangle \in \mathcal{H}_S = \mathcal{H}_1 \otimes \mathcal{H}_2$, where $\mathcal{H}_S$ is the Hilbert space of the system and $\mathcal{H}_i$ is the i-single-particle one ($i = 1, 2$). The state $|\Psi\rangle$ is *separable* if it reflects the tensor product structure of the total Hilbert space, i.e. if it can be written as

$$|\Psi\rangle = |\phi\rangle_1 \otimes |\chi\rangle_2 \,, \tag{1.4}$$

where $|\phi\rangle_1 \in \mathcal{H}_1$ and $|\chi\rangle_2 \in \mathcal{H}_2$. In this case, no measurement performed on the subsystem 1 affects the number 2 and I know exactly the state of each particle. Otherwise, the state $|\Psi\rangle$ is *entangled*. An important tool linked to the identification and quantification of the amount of entanglement in bipartite systems is the Schmidt decomposition of the state [24]

$$|\Psi\rangle = \sum_{i=1}^{r} \sqrt{\lambda_i}\, |\phi_i\rangle_1 \otimes |\chi_i\rangle_2 \,, \tag{1.5}$$

where $\{|\phi_i\rangle\}_1$ and $\{|\chi_i\rangle\}_2$ are basis in $\mathcal{H}_1$ and $\mathcal{H}_2$, respectively, and are the eigenstates of the single-particle reduced density matrices

$$\begin{aligned} \rho_1 &= \mathrm{Tr}_2[|\Psi\rangle \langle\Psi|], \\ \rho_2 &= \mathrm{Tr}_1[|\Psi\rangle \langle\Psi|], \end{aligned} \tag{1.6}$$

respectively, which have the same spectrum $\{\lambda_i\}$. The value r, that is the number of nonzero coefficients in the decomposition, is called *Schmidt rank*, and it goes from 1 (for separable states) to $d = \min\left[\dim(\mathcal{H}_1), \dim(\mathcal{H}_2)\right]$ (maximally entangled states). A well known measure of the entanglement of the two particles, which is a function of the Schmidt coefficients λ_i, is the *von Neumann entropy* of the single-particle reduced density matrices

$$S(\rho_1) = S(\rho_2) = -\sum_i \lambda_i \log_2 \lambda_i. \tag{1.7}$$

It represents our ignorance about the states of the single subsystems. A pure state of a bipartite system is separable if and only if its Schmidt rank is 1, i.e. if it can be written in terms of a single tensor product of one-particle states associated to the two subsystems, and if and only if

the von Neumann entropy of the reduced density matrices is zero.

On the other hand, consider now the case in which the two particles are *identical* and suppose that one of them occupies the single-particle state $|\phi\rangle$ and the other one the state $|\chi\rangle$. Labels 1 and 2, introduced before, while for NIP are physical properties distinguishing them, for IP are not physically meaningful. In the SA, for both independently prepared space-like separated and spatially overlapping particles, the two-particle state $|\Psi\rangle$ is [14]

$$|\Psi\rangle_{\pm} = \frac{1}{\sqrt{2}}(|\phi\rangle_1 \otimes |\chi\rangle_2 \pm |\phi\rangle_2 \otimes |\chi\rangle_1), \tag{1.8}$$

where $+$ stands for bosons and $-$ for fermions. The application of the symmetrization postulate due to the presence of labels 1 and 2 implies that the previously presented tools characterizing entanglement of pure states for two NIP cannot be directly applied. In fact not only they give rise to unphysical results in some cases, but also they are not well defined, as I am going to show.

- **Separability**
  The fermionic (bosonic) Hilbert space is the antisymmetric (symmetric) subspace of the Hilbert space $\mathcal{H} = \mathcal{H}_1 \otimes \mathcal{H}_2$. As a result, the tensor product structure (on which the concept of particle-locality is based), associated to the total Hilbert space of NIP, is lost for IP.

  "*An immediate consequence of the symmetrization postulate is that two particles of the same type are always entangled, even if they were prepared independently, far away from each other, in different laboratories.*"[14]

  This is the obvious mathematical conclusion, based on the separability criterion, coming from the formal label-based SA. However,

  "we must now convince ourselves that this entanglement is not a matter of concern: no quantum prediction, referring to an atom located in our laboratory, is affected by the mere presence of similar atoms in remote parts of the universe."[14]

  Independently prepared space-like separated (noncausally related) IP are clearly physically uncorrelated [24], that is measurements on one of them are independent on the results of measurements performed on the other one. Therefore separability of the state is a mathematical tool that gives, already for the simplest presented case, unrealistic interpretations of quantum correlations when the symmetrization postulate is applied.

- **Schmidt rank**
  When particles are independently prepared and space-like separated, $|\phi\rangle$ and $|\chi\rangle$ of Eq. (1.8) are orthonormal. The Schmidt rank of the state with respect to mock labels of Eq. (1.8) is 2 and according to the Schmidt criterion for NIP, this state is entangled. Even then, the direct exploitation of a well known tool used for NIP would give unphysical correlations. Moreover, if $|\phi\rangle$ and $|\chi\rangle$ spatially overlap, it is not clear if the entangled structure of the state of Eq. (1.8) represents a real physical correlation or it is only a result of the SA with labels.

- **von Neumann entropy**
  The operation of tracing out the particle 1 (2) to obtain the single-particle reduced density matrix is a physically meaningless operation for IP, given thay are not addressable and thus the concept of particle-locality is lost. As a result, the interpretation of von Neumann entropy is no more directly linked to the presence of real physical correlations between IP and a more careful analysis of it is required. As I will show, a certain link between von Neumann entropy and IP entanglement has been proposed. However, in first quantization it requires separate treatments for bosons and fermions, that give contradictory results [23, 24, 44], and in second quantization it is based on an algebric concept of locality [30, 44, 45], different from the particle one (used for NIP).

1.3.2 New standard tools: first quantization approach

Different theories have been developed in order to characterize the role played by the identity of particles in the emergence of quantum correlations. Except for someone thinking that "all identical particles are inherently correlated from the outset, regardless of how far apart their creation took place" [46] because of the symmetrization postulate, the greater part of physicists mathematically and physically agree that states of spatially separated identical particles, which never interacted before, are intrinsically uncorrelated and this remain valid also after spatially separated operations on the system. In this case, *particles act as nonidentical ones and their statistics does not play any role, neither in their dynamics nor in their correlations.*

The situation is more confused when two IP have a certain probability to occupy the same site (e.g. in systems of quantum dots, where electrons can tunnel towards different dots with tunable probabilities [47, 48, 49]). In this case the effect of the particle statistics cannot be ignored. As an example, it is not clear how to quantify the *intrinsic* (i.e. linked to the quantum state, regardless of measurements) physical entanglement in states of IP in the same spatial regions with opposite pseudospins, eventually separating it from the possible formal correlations due only to the presence of mock labels. Therefore, are IP in the same site physically entangled or not? Given a certain amount of entanglement, how can I separate the fictitious entanglement

due to mock labels from the real physical one? These are the main questions to which they have tried to reply, using different tools and new concepts. In the following, I recall some of them with the corresponding conclusions.

- **Slater rank**

  For bipartite systems of multilevel IP, the Schmidt rank has been substitued by the Slater rank [24, 23, 25], which gives different results for fermions and bosons.

  A generic state of 2 identical fermions with spin S can be written in its Slater decomposition, i.e. as a linear combination of a number $1 \leq r \leq (2s+1)/2$ of terms, each of which obtained antisymmetrizing with respect to mock labels tensor products of orthonormal 1-particle states [23]. *r* is the corresponding Slater rank of the state. If $r = 1$, the state is of the form of $|\Psi\rangle\_$ of Eq. (1.8), where $\{|\phi\rangle, |\chi\rangle\}$ is an orthonormal basis of the 1-particle Hilbert space $\mathbb{C}^{2s+1}$. In this case, the two fermions are considered physically uncorrelated, independently on their spatial configuration, since the sole origin of the entanglement in the state is formal and linked to unobservable labels. Two-particle fermionic entangled states correspond to a Slater rank strictly greater than 1, in perfect analogy with the Schmidt rank for NIP.

  On the other hand, for bosons the situation is less straightforward. In fact, in contrast to fermions satisfying the Pauli exclusion principle [15], two bosons can occupy the same quantum state and the global system can be described by the tensor product of the same single-particle states (e.g. $|\Psi\rangle = |\phi\rangle_1 \otimes |\phi\rangle_2$), with the corresponding Slater rank $r = 1$. In analogy with the case of nonidentical particles, $r = 1$ represents a nonentangled state. However, if the two bosons occupy two different single-particle states, I can have two different situations, corresponding to $r = 2$: the global state can be obtained symmetrizing a single tensor product of

  (i) two 1-particle orthogonal states and, analogously to the fermionic case, the apparent entangled structure is considered purely due to the symmetrization postulate. The state is thus physically nonentangled;

  (ii) two 1-particle nonorthogonal states: in this case "no definite property can be attributed to both subsystems" [23] and the state is entangled.

  Finally $r > 2$ corresponds to the case in which the global state cannot be obtained symmetrizing a single tensor product of single-particle states and also in this case, the state is considered entangled. As a result, for bosons, it is not always sufficient to know the Slater rank to establish if two bosons are entangled or not.

- **Fermionic and bosonic von Neumann entropy**

  The physical interpretation of this quantity, which is based on the 1-particle reduced den-

sity matrix, is intrinsically different from the one for NIP. Moreover, as the Slater rank, it requires separate treatments for bosons and fermions.

For the latters, von Neumann entropy is bounded from below by 1, instead of zero (NIP): it happens for $r = 1$, i.e. for nonentangled states according to the previously presented criterion [23]. The interpretation of this difference relies on the fact that, in contrast to uncorrelated NIP, single Slater determinants of the form of Eq. (1.8) contain an uncertainty about which is the particle (1 or 2), which is reflected on the reduced density matrix $\rho^{(1 \text{ or } 2)} = \mathrm{Tr}_2[|\Psi\rangle \langle\Psi|] = \mathrm{Tr}_1[|\Psi\rangle \langle\Psi|]$. As a result, the von Neumann entropy $S(\rho^{(1 \text{ or } 2)})$, representing a measure of the lack of knowledge of the state corresponding to the single particle, is different from zero. However, this ignorance is not linked to a real physical correlation between particles, but only to the mathematical labels-dependent description of the state. In some way, it is considered a measure of the unphysical entanglement due only to mock labels. Instead, when $r > 1$, von Neumann entropy is greater than 1 and measures the presence of a real entanglement between IP [24]. Finally, for fermions the connection between Slater rank and von Neumann entropy is analogous to the one between the Schmidt rank and the von Neumann entropy for NIP, but the corresponding values and the interpretations are different.

For bosons, the situation is more complicated because of the fact that nonentangled systems can be characterized by two different values of the von Neumann entropy : (i) 0 for $r = 1$ and (ii) 1 for $r = 2$. The interpretation of the second case is analogous to the one presented for fermions.

As illustrated above, both for bosons an femrions, some difficulties arise trying to interpret the von Neumann entropy of the reduced density matrix of Eq. (1.8): in fact, not only it seems to take into account another form of ignorance about the single particle quantum states (different from the one characterizing states of NIP), intrinsically associated to the meaningless question about which particle is the number 1 or the number 2, but it requires different treatments of bosons and fermions [23, 24].

It is important to make a remark. Even if the previous tools give physical results for independently prepared and spatially separated IP, they give predictions which contrast with some recent experimental evidences when particles overlap. As an example, let us consider the case of two IP in the same site, one in the state $|\phi\rangle = |\mathrm{A} \downarrow\rangle$ where A is the spatial mode and $\downarrow$ is the pseudospin, and the other one in $|\chi\rangle = |\mathrm{A} \uparrow\rangle$. The global quantum state has the form of Eq. (1.8) and according to the criteria presented before, since $\langle\phi|\chi\rangle = 0$, the state is unentangled for both bosons and fermions [26, 23, 24]. However, recently, it has been experimentally shown that entangled states can be obtained by moving two IP with opposite pseudospins in the same site [31], in contrast to what is expected from the theory previously treated.

The previously presented tools have been introduced in order to characterize, both for in-

dependently prepared space-like separated and spatially overlapping IP, the so-called *a priori* entanglement, i.e. the one strictly linked to the quantum state of the system, regardless of the measurements that can be performed on it to reveal and exploit the correlations.

In the following, I will give an example of theories according to which, on the contrary, IP entanglement depends on both the state and measurements.

- **Measurement-induced entanglement**

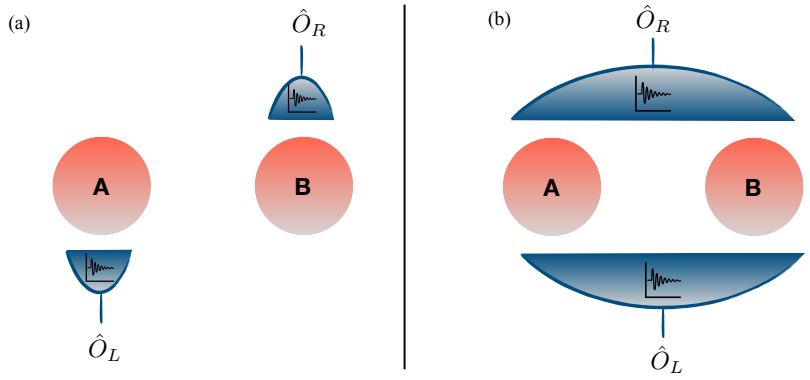

Figure 1.1: **Measurement-induced entanglement**. A and B are two independently prepared and spatially separated IP (a): Unambiguous choice of detectors $\hat{O}_L$ and $\hat{O}_R$, in which each of them can be triggered only by one particle. (b): Ambiguous choice of detectors, each of which can be triggered by both particles.

When particles are nonidentical, "only interaction between particles can lead to an entangled state."[24]. On the other hand, if they are identical, measurements play an important role in the emergence of entanglement, also between independently prepared and spatially separated particles. Let us consider, as an example, two independently prepared identical bosons, which never interacted before, in the following pure state

$$|\Psi\rangle = \frac{1}{\sqrt{2}}(|\mathrm{A}\uparrow\rangle_1 \otimes |\mathrm{B}\downarrow\rangle_2 + |\mathrm{A}\uparrow\rangle_2 \otimes |\mathrm{B}\downarrow\rangle_1), \tag{1.9}$$

where $|\mathrm{A}\rangle$ and $|\mathrm{B}\rangle$ are two spatially separated wavefunctions. According to the previously presented criteria, this state is *a priori* physically unentangled. Let us now perform a measurement, using two detectors $\hat{O}_L$ and $\hat{O}_R$, spatially separated and localized in the regions in which $|A\rangle$ and $|B\rangle$, respectively, are peaked (Fig. 1.1(a)). This set-up is called unambiguous, since each detector can be triggered by a single particle and measurement's results are uncorrelated.

Let us now suppose that the two detectors $\hat{O}_L$ and $\hat{O}_R$ project in the delocalized spatial states $|L\rangle = \frac{1}{\sqrt{2}}(|A\rangle + |B\rangle)$ and $|R\rangle = \frac{1}{\sqrt{2}}(|A\rangle - |B\rangle)$, respectively. This choice of

detectors is called $ambiguous$, since they can be triggered by both particles (Fig. 1.1(b)): post-selecting the cases in which both detectors measure a particle, the apparatus is not able to say to which particle the result of each detector is associated (such an experimental configuration is known as deleting which-way information setup [15, 24], like the Hong-Ou-Mandel apparatus) and an intrinsically probabilistic *measurement-induced* entanglement appears, even if the "a priori" (before the measurement) entanglement was zero.

1.3.3 New standard tools: separability in second quantization approach

Some theories, showing that entanglement is not an absolute concept, recover the separability criterion (not applicable to IP states) associating it to expectation values of observables, in the second quantization formalism [28, 27]. In this context, physical observables are expressed as self-adjoint polynomials of creation and annihilation operators defined in the single-particle Hilbert space [24, 50, 27, 51].
Consider the Fock space $\mathcal{H}$ of a many-body system and the algebra $\mathcal{B}(\mathcal{H})$ generated by the creation and annihilation operators acting on $\mathcal{H}$. These operators create and annihilate, respectively, particles in the different *modes* of the system: a mode is a single-particle vector state. Let us define an algebraic bipartition of $\mathcal{B}(\mathcal{H})$ consisting of any pair $(\mathcal{A}_1, \mathcal{A}_2)$ of commuting subalgebras $\mathcal{A}_1$, $\mathcal{A}_2 \subset \mathcal{B}(\mathcal{H})$ ($\mathcal{A}_i$, with $i = 1, 2$, is a subset of the creation and annihilation operators generating $\mathcal{B}(\mathcal{H})$). An operator is said *local* with respect to the bipartition $(\mathcal{A}_1, \mathcal{A}_2)$ if it is the product $A_1 A_2$ of an operator A_1 in $\mathcal{A}_1$ and some A_2 in $\mathcal{A}_2$ [30, 45]. This definition recover, at the level of observables, the concept of locality used for NIP and that cannot be used at the level of states because of the unaddressability of IP.
A state ρ is said to be *separable with respect to the bipartition* $(\mathcal{A}_1, \mathcal{A}_2)$ if the expectation of any local operator $A = A_1 A_2$ can be decomposed into a convex combination of products of local expectation values as

$$\mathrm{Tr}(\rho A) = \sum_k \lambda_k \mathrm{Tr}(\rho_k^{(1)} A_1)\mathrm{Tr}(\rho_k^{(2)} A_2), \qquad \lambda_k \geq 0, \quad \sum_k \lambda_k = 1, \tag{1.10}$$

where $\rho_k^{(1)}$ and $\rho_k^{(2)}$ are admissible states for the systems leaving in the Hilbert subspaces 1 and 2 associated to the subalgebras $\mathcal{A}_1$ and $\mathcal{A}_2$, respectively. Otherwise the state is entangled.

Following this approach, a difference between the entanglement between particles and the one between sets of modes has been proposed [29].

As a specific example, consider N bosons filling M different modes and define the annihilation and creation operators of a particle in the j_{th}-mode ($j = 1, ..., M$), $\hat{a}_j$ and $\hat{a}_j^\dagger$ respectively, satisfying the commutation rules $[\hat{a}_j, \hat{a}_l^\dagger] = \delta_{jl}$. Consider a bipartition of this set of operators

$$\begin{aligned} &\{\hat{a}_j, \hat{a}_j^\dagger \mid j = 1, 2, ...m\}, \\ &\{\hat{a}_j, \hat{a}_j^\dagger \mid j = m+1, m+2, ...M\}, \end{aligned} \tag{1.11}$$

representing two commuting subalgebras $\mathcal{A}_1$ and $\mathcal{A}_2$, respectively. A pure state is Mode-separable with respect to $(\mathcal{A}_1, \mathcal{A}_2)$ if and only if [30, 45]

$$|\psi_{\mathrm{M}}\rangle = \mathcal{P}(\hat{a}_1^\dagger, ..., \hat{a}_m^\dagger) \cdot \mathcal{Q}(\hat{a}_{m+1}^\dagger, ..., \hat{a}_M^\dagger) \, |0\rangle \, , \tag{1.12}$$

where $\mathcal{P}$ and Q are arbitrary functions of the creation operators. Otherwise, it is Mode-entangled with respect to the chosen algebraic bipartition.

The state of Eq. 1.12 can be written also in terms of the mode occupation number as follows

$$|\psi_{\mathrm{M}}\rangle = \sum_{n,\sigma,\sigma'} c_{n\sigma\sigma'} \, |n, \sigma\rangle_{\mathcal{A}_1} \otimes |N-n, \sigma'\rangle_{\mathcal{A}_2} \, , \tag{1.13}$$

where n is the *local* number of particles occupying the first m modes, σ (σ') is the index associated to the different configurations in which n ($N-n$) particles occupy the first m modes (the modes $m+1, ..., M$). The mode-entanglement of $|\psi_{\mathrm{M}}\rangle$ is

$$E_{\mathrm{M}}(|\psi_{\mathrm{M}}\rangle) = S(\rho_{\mathcal{A}_1}) = -\mathrm{Tr}(\rho_{\mathcal{A}_1} \log_2 \rho_{\mathcal{A}_1}), \tag{1.14}$$

with $S(\cdot)$ the von Neumann entropy of the reduced density matrix $\rho_{\mathcal{A}_1} = \mathrm{Tr}_{\mathcal{A}_2}(|\psi_{\mathrm{M}}\rangle \langle\psi_{\mathrm{M}}|)$. It can be shown that bipartite mode-entanglement may be reduced if there are restrictions on allowed *local* [2] operations, i.e. if there are super selection rules (SSR) [52]. Generical SSR limit the operations which can be implemented on a quantum system. The restriction to LOCC gives rise to entanglement as a nonlocal resource, therefore particle number conservation, additionally confining the possible operations, should give rise to a new resource [53].

[2] The term *local* is here used differently from how it is presented in quantum field theory (QFT), where it has a spatial connotation. In fact, two configurations that are locally equivalent with respect to a subalgebra $\mathcal{A}_i$ ($\mathcal{A}_i$-locally equivalent) are not locally equivalent with respect to the QFT (QFT-locally equivalent). As an example, let us consider two physical configurations, $\sigma = 1$ and $\sigma = 2$, with 3 particles in the 3-modes subalgebra $\mathcal{A}_1$. In the configuration labeled by σ_1, two particles are in the mode 1 and the other one in the mode 2. In the configuration labeled by σ_2, two particles are in the mode 2 and the other one in the mode 3. These two configurations are $\mathcal{A}_1$-locally equivalent, since there is the same number of particles in $\mathcal{A}_1$, but they are not QFT-locally equivalent, since occupying different modes, particles are differently distributed in space.

Let us now assume that the *local* number of particles, i.e. the number of particles associated to each of the two subalgebras, is a superselected observable, in the sense that the corresponding operator commutes with all observables. This SSR implies that if Alice has access to the m $\mathcal{A}_1$-modes and Bob to the $\mathcal{A}_2$-ones, each of them cannot prepare superposition of states of different local number of particles by LOCC. Since $|\psi_{\mathrm{M}}\rangle$ is a linear combination of states with different local particle numbers (see Eq. (1.13)), the arbitrary local manipulation will mean violating the SSR for particle number. Therefore, E_{M} does not take into account this SSR and so it does not represent the amount of entanglement to which Alice and Bob have affectively access. According to the chosen particle-number SSR, I call the operationally available entanglement E_{P} where the subscript P stands for *particle*. E_{P} is the minimal amount of entanglement which Alice and Bob can produce between their quantum states by local operations and it can be obtained by averaging over the entropy obtained by first projecting the density matrix into a subspace with fixed local numbers of particles n and $N-n$ [29],

$$E_{\mathrm{P}}(|\psi_M\rangle) = \sum_n p_n E_{\mathrm{M}}(|\psi_M^{(n,N-n)}\rangle). \tag{1.15}$$

In particular, I project the state of Eq. 1.12 into a specific subspace with fixed local (with respect to subsalgebras) numbers of particles and it is entangled if

$$|\psi_{\mathrm{P}}\rangle \neq \Pi_{\mathcal{A}_1}^{(n)} \Pi_{\mathcal{A}_2}^{(N-n)} \mathcal{P}(\hat{a}_1^\dagger, ..., \hat{a}_m^\dagger) \cdot \mathcal{Q}(\hat{a}_{m+1}^\dagger, ..., \hat{a}_M^\dagger) \, |0\rangle \, . \tag{1.16}$$

It can be shown that $E_{\mathrm{P}} \leq E_{\mathrm{M}}$.
In this context, a new point of view arises in the debate about the entanglement in systems of particles in the same site:

"Any entanglement formally appearing amongst the identical particles, including entanglement due purely to symmetrization, can be extracted into an entangled state of independent modes, which can then be applied to any task. In fact, the entanglement of the mode system is in one-to-one correspondence with the entanglement between the inaccessible identical particles."[54]

This theory exploit the concept of extraction of the "symmetrization entanglement" [54] by means of operations performed on the system.

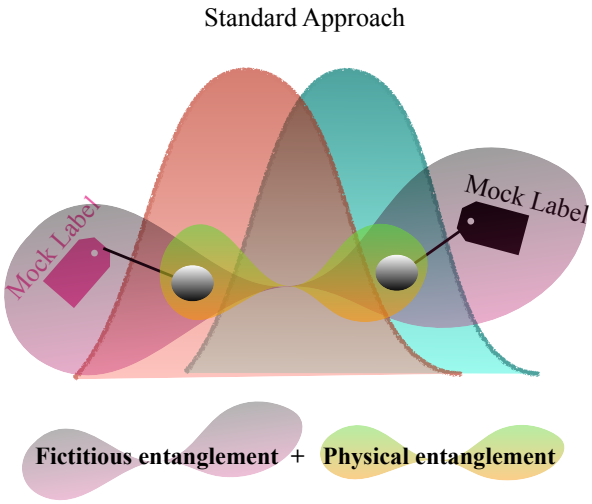

Figure 1.2: **Ambiguity due to the standard approach to IP**. System of two entangled spatially overlapping IP. Using the SA it is not clear how to separate the fictitious entanglement, coming from the symmetrization postulate with respect to mock labels, from the true physical entanglement. The red and green clouds represent the single-particle wave functions.

1.4 Discussions

In conclusion, as a starting point I have recalled the essential ingredients of the SA to treat IP: even if IP are not addressable in quantum mechanics, the allowed physical configuration in which they can live are described by assuming, at first, that they are nonidentical, by labelling them with *mock labels*, and exploiting then the symmetrization postulate with respect to these labels. However, some ambiguities and inconsistencies arise in treating IP entanglement by means of the tools usual for NIP. In fact, according to some of them, such as the separability criterion, the Schmidt rank and von Neumann entropy, IP quantum states should be always entangled. Understanding, by physical considerations, that this cannot by true in general, it has been necessary to propose new concepts, tools, methods and entanglement definitions. Yet, these theories require different treatments for bosons and fermions and, further, it remains unclear how to separate fictitious entanglement coming from *mock labels* from the real physical one (Figure 1.2). Moreover, some of these theories [24, 23, 26] are in contrast with experimental evidences [31] and troubles under general conditions of scalability remain.

New concepts, such as *entanglement of modes*, in the context of second quantization have been proposed, increasing the difference between the treatment of NIP and IP entanglement.

Finally, both in in the standard first and second quantization, the debate about entanglement of spatially overlapping IP is still open. In addition, second quantization becomes purely formal when not truly elementary IP, such as atoms, are considered, since they cannot be considered as excitations of any field.

Chapter 2

No-label approach to identical particles

2.1 Introduction

In the previous chapter, I have shown how the symmetrization postulate makes it the debate about IP correlations still heated. In order to introduce the core of this chapter, let us start making a first consideration, recalling the following Cohen-Tannoudji's sentences [15],

"If application of the symmetrization postulate were always indispensable, it would be impossible to study the properties of a system containing a restricted number of particles, because it would be necessary to take into account all the particles in the universe which are identical to those in the system. Under certain special conditions, identical particles behave as if they were actually different and it is not necessary to take the symmetrization postulate into account in order to obtain correct physical predictions."[15]

It is well known that when two IP are independently prepared in two well separated spatial regions, $\mathcal{L}$ and $\mathcal{R}$, one in the state $|\phi\rangle$ and the other in $|\chi\rangle$, respectively, and single-particle measurements are performed using devices localized in $\mathcal{L}$ and $\mathcal{R}$, the effects on the physical predictions of the symmetrization postulate are null [55, 25, 15, 26, 56]. In this case, all the probability amplitudes or matrix elements of an operator can be calculated considering $\mathcal{L}$ and $\mathcal{R}$ as distinguishing real labels, and writing a global initial state without symmetrizing with respect to these labels. In fact, the result of a measurement performed in the region $\mathcal{L}$ ($\mathcal{R}$) cannot come from particle in $\mathcal{R}$ ($\mathcal{L}$) [15, 26]. The initial state of the system can be thus written as a factorized state $|\Psi\rangle = |\phi\rangle_{\mathcal{L}} \otimes |\chi\rangle_{\mathcal{R}}$, both for bosons and fermions, and as a result IP behave as NIP. Analogously, studying the thermodynamical statistics of a many IP system, it is well known that at high densities, the system follows the Bose-Einstein statistics if they are bosons or the Fermi-Dirac one if fermions. However in the limit of low densities (well separated particles), the two distributions reduce to the Maxwell-Boltzmann one, valid for NIP [57].

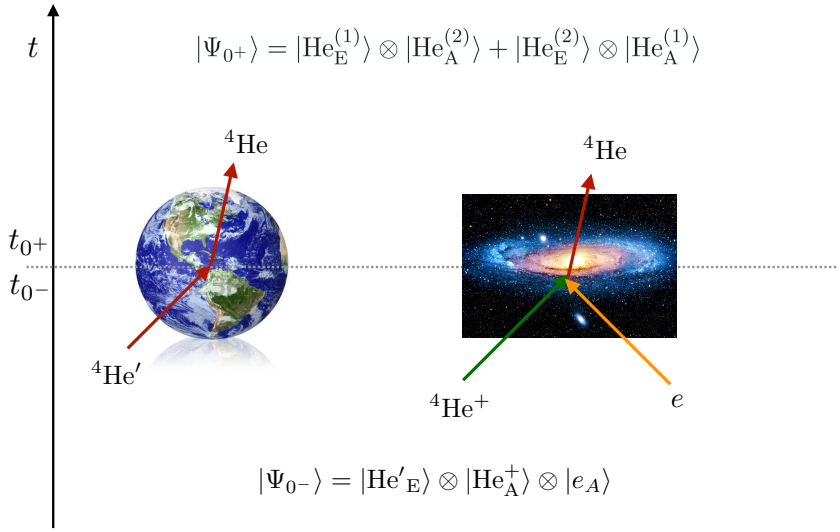

Figure 2.1: Simultaneous generation on the Earth and on the Andromeda galaxy of two identical helium atom states.

In this case, one can qrite IP states without respecting the bosonic of fermionic symmetry, when the symmetrization postulate is useless [15, 24, 26, 56]: for example, see the antisymmetric Bell state $|\Psi^-\rangle = \frac{1}{\sqrt{2}}(|0\rangle_1 \otimes |1\rangle_2 - |0\rangle_2 \otimes |1\rangle_1)$ for nonoverlapping photons (that are bosons!) [24].

However, even in thise type of physical situations, in many works it seems that people do not want to renounce formally to the symmetrization postulate when particles behave as nonidentical. Thus, instead of eliminate the symmetric structures of the states, specific theories have been developed to neutralize it, but in certain cases some counterintuitive aspects remais, for example when ones considers time dependent problems.

In fact, in the SA when a particle is generated locally, it must instantaneously appear in a far away location provided that another identical particle is already present there. To make this point clear, consider an helium atom ^{4}He in the state $|\mathrm{He}'_{\mathrm{E}}\rangle$ on the Earth and the ionized atom $^4\mathrm{He}^+$ in the state $|\mathrm{He}^+_{\mathrm{A}}\rangle$ plus an electron in the state $|e_{\mathrm{A}}\rangle$ on the Andromeda galaxy (subscripts E and A representing the spatial localisation of states on Earth and Andromeda). Being at the beginning all the involved particles distinguishable, the global state is the tensor product $|\Psi_{0^-}\rangle = |\mathrm{He}'_{\mathrm{E}}\rangle \otimes |\mathrm{He}^+_{\mathrm{A}}\rangle \otimes |e_{\mathrm{A}}\rangle$. At the universal time $t = 0$, $^4\mathrm{He}'$ is scattered in ^{4}He and simultaneously ion $^4\mathrm{He}^+$ on Andromeda absorbs the electron e forming the atom ^{4}He (see Fig. 2.1). At $t = 0^+$ on the Earth and on Andromeda two identical bosons appear in the states $|\mathrm{He}_{\mathrm{E}}\rangle$ and $|\mathrm{He}_{\mathrm{A}}\rangle$. Being in the SA the identical atoms distinguished with labels 1 and 2, the global state is $|\Psi_{0^+}\rangle = \frac{1}{\sqrt{2}}(|\mathrm{He}_{\mathrm{E}}^{(1)}\rangle \otimes |\mathrm{He}_{\mathrm{A}}^{(2)}\rangle + |\mathrm{He}_{\mathrm{E}}^{(2)}\rangle \otimes |\mathrm{He}_{\mathrm{A}}^{(1)}\rangle)$. Thus, while at $t = 0^-$ each particles is separately localised on either E or A, at $t = 0^+$ each of the two helium atoms simultaneously occupies both states on E and A, as it can be easily seen in terms of

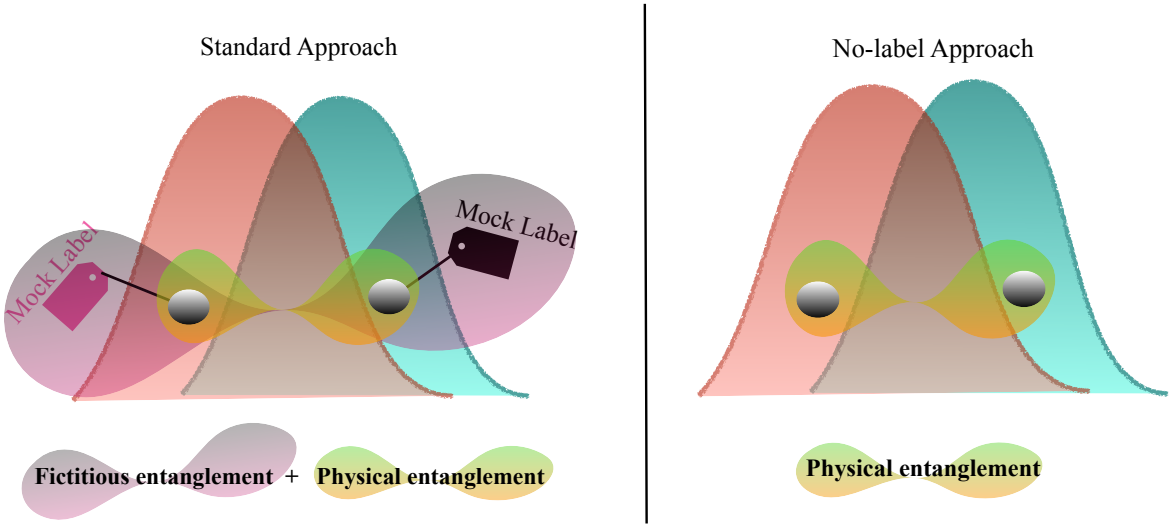

Figure 2.2: **Comparison between SA and no-label approach to IP**. System of two entangled spatially overlapping IP. **Left**: Using the SA it is not clear how to separate the fictitious entanglement, coming from the symmetrization postulate with respect to mock labels, from the true physical entanglement. **Right**: The absence of labels in the no-label approach implies the absence of the fictitious entanglement appearing in the SA.

wave functions: $\Psi_{0^+}(x_{\rm E}, x_{\rm A}) = \psi^{(1)}_{\rm He}(x_{\rm E})\psi^{(2)}_{\rm He}(x_{\rm A}) + \psi^{(2)}_{\rm He}(x_{\rm E})\psi^{(1)}_{\rm He}(x_{\rm A})$, where $(x_{\rm E}, x_{\rm A})$ indicate the positions of the two helium atoms on Earth and Andromeda, respectively. This approach requires to accept the notion, for instance, that the nonrelativistic helium atom generated at $t = 0^+$ in A, because of the identical particle in E, instantaneously develops a nonzero amplitude of being there, although the events $(0^+_{\rm E}, 0^+_{\rm A})$ are spacelike separated.

"The underlying idea is that the particles are energy quanta without individuality." [57]

"To avoid the problems which arise when particles are identical,
we shall assume that they are not."[15]

Therefore, it seems that the origin of the difficulties in the descriptions of IP comes from the first step of the SA, in which one assumes they are not identical [14, 15] and gives them "individuality", marking them with *unobservable*[1] labels. The SA to IP systems is the only case in quantum mechanics where "unobservable" (as a contrast to Dirac's observable) unphysical (mock) labels are introduced, being instead quantum states defined by complete sets of commuting observables.

Recently a different state-based approach has been proposed [58, 34, 59, 60, 61, 62] which describes the quantum states of IP without exploiting mock labels. This no-label approach,

[1] In quantum mechanics, physical quantities associated to a system are called "observables" and they are essential in defining the state of a system. No "unobservables" are required.

initially presented for two IP [58], exhibits conceptual and practical advantages, linked in particular to the treatment of quantum correlations. In fact, from the beginning it completely avoids the existence of the mock entanglement (Figure 2.2). It exploits furthermore, for quantifying the entanglement in these systems, the same well-established notions, tools and criteria commonly employed for NIP systems, such as Schmidt decomposition (showing that it is universally valid both for NIP and IP) [35] and von Neumann entropy. This without the physical ambiguities present in the approaches treated in Chapter 1.

In the following I will reconsider the no-label approach from a fundamental perspective and generalise it to a system of many IP, starting by first principles [39].

2.2 No-label theory

2.2.1 The foundations of the N-particle formalism

Let us take a 1-particle state $|\{\alpha\}\rangle$ characterised by a complete set of commuting observables $\{\alpha\}$. The state of two identical particles can be written, without involving unobservable labels, as a list of the 1-particle states $|\{\alpha_1\},\{\alpha_2\}\rangle$, that I write in a short hand notation as $|\{\alpha_1\},\{\alpha_2\}\rangle := |1,2\rangle$ and that is an overall symbol which cannot be decomposed as tensor products of 1-particle vector states. The sets 1 and 2 may coincide, in this way giving $|\{\alpha_1\},\{\alpha_1\}\rangle = |1,1\rangle$. Generalising to the case of N identical particles, the global quantum state $|\phi^{(N)}\rangle$ is simply a list of the 1-particle kets [39]

$$|\phi^{(N)}\rangle := |1,2,...,N\rangle, \tag{2.1}$$

which does not involve unobservable labels and where more indices may coincide. I remark that, in general, each index in equation (2.1) does not indicate the position of the corresponding 1-particle state in the N particle ket.

In the example illustrated in Fig. 2.1, being the single-particle states at $t = 0^+$ given by $|\mathrm{He_E}\rangle$ and $|\mathrm{He_A}\rangle$, using (2.1) the global final state is $|\mathrm{He_E},\mathrm{He_A}\rangle$. This means that one helium atom is localised in E and one in A. Unphysical labels simply do not appear and the question whether the two identical atoms are entangled is not even needed to be posed.

In order to predict the behavior of a quantum system, probabilities to occupy certain configurations have to be calculated [15]. For one particle, the relevant quantities to get probabilities are the transition amplitudes $\langle k'|k\rangle$ to find the particle in the state $|k'\rangle$ if it is initially prepared in the state $|k\rangle$. Being the state of equation (2.1) not separable in terms of tensor products of 1-particle states, how can the N-particle transition amplitude from it to the state $|1',...,N'\rangle$, namely $\langle 1',...,N'|1,...,N\rangle$, can be written in the no-label approach?

As a starting point, let us require that it can be expressed in terms of the 1-particle prob-

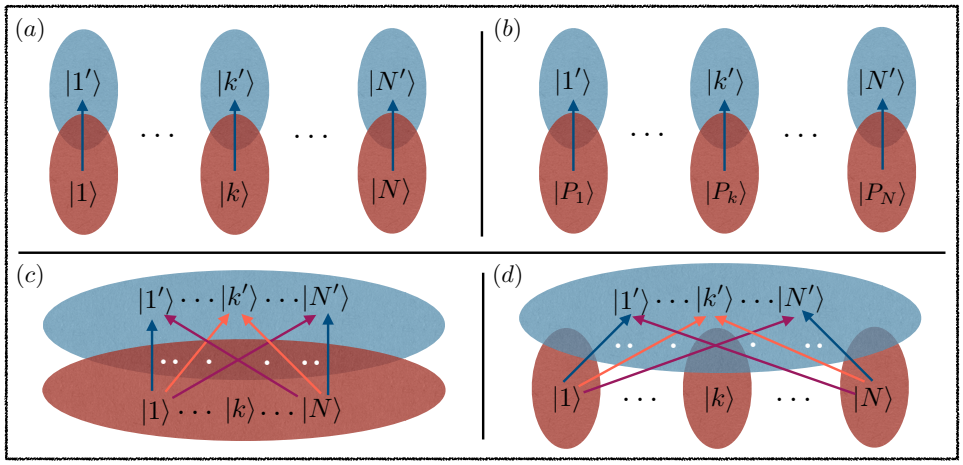

Figure 2.3: (a) and (b): Cluster decomposition principle. The set $\{P_1, ..., P_N\}$ represents the $N!$ permutations of the 1-particle states $|1\rangle, ..., |N\rangle$. (c) General case where there is spatial overlap among the entry 1-particle states in which the global system is prepared (red cloud) and among the exit ones on which the system is measured (blue cloud). (d) Particular situation where only all the entry 1-particle states do not overlap (red clouds). The coloured clouds represent the spatial regions occupied by the states written within them. The arrows show the transition of each $|k\rangle$ state ($k = 1, ..., N$) towards one or more $|k'\rangle$ states ($k' = 1', ..., N'$).

ability amplitudes. When each 1-particle state in the ket (bra) in the transition amplitude is localised in a region far away from the others in the ket (bra) (see Fig. 2.3(a) and (b)), the cluster decomposition principle, stating that distant experiments provide independent outcomes [14], allows us to express the total transition amplitude as the product of the 1-particle ones. In the specific case in which i-th state overlap with the i'-th one, it can be expressed as $\langle 1', 2', ..., N'|1, 2, ..., N\rangle = \langle 1'|1\rangle\langle 2'|2\rangle...\langle N'|N\rangle$ (see Fig.2.3(a)). In general, the contribution to the transition amplitude can come from a generic permutation of the 1-particle states in $|1, 2, ..., N\rangle$, as follows

$$\langle 1', 2', ..., N'|1, 2, ..., N\rangle = \langle 1'|P_1\rangle\langle 2'|P_2\rangle...\langle N'|P_N\rangle, \tag{2.2}$$

where the set $P_1, P_2, ..., P_N$ indicates one of the $N!$ permutations of the 1-particle states $|1\rangle...|N\rangle$ and it represents the case in which the state $|P_k\rangle$ occupies the k-th region (see Fig. 2.3(b)). The transition amplitude (2.2) is linear in each of the 1-particle states.

When both the entry (ket) and exit (bra) 1-particle states are localised in overlapping spatial regions (see Fig. 2.3(c)), to maintain the property of linearity, the N-particle probability amplitude can be expressed as a linear combination of $N!$ terms of the form (2.2)

$$\langle 1', 2', ..., N'|1, 2, ..., N\rangle = \sum_P \alpha_P \langle 1'|P_1\rangle\langle 2'|P_2\rangle...\langle N'|P_N\rangle, \tag{2.3}$$

where $P = \{P_1, P_2, ..., P_N\}$ runs over all the 1-particle state permutations. Taking into account that

$$\langle 1', 2', ..., N'|1, 2, ..., N\rangle^* = \langle 1, 2, ..., N|1', 2', ..., N'\rangle, \tag{2.4}$$

let us take the complex conjugate of Eq. (2.3),

$$\langle 1', ..., N'|1, ..., N\rangle^* = \sum_P \alpha_P^* \langle P_1|1'\rangle ... \langle P_N|N'\rangle. \tag{2.5}$$

From Eq. (2.3), I have

$$\langle 1, ..., N|1', ..., N'\rangle = \sum_Q \alpha_Q \langle 1|Q_1'\rangle ... \langle N|Q_N'\rangle = \sum_Q \alpha_Q \langle Q_1^{-1}|1'\rangle ... \langle Q_N^{-1}|N'\rangle, \tag{2.6}$$

where, considering Eq. (2.4), I have reordered $Q_1', ..., Q_N'$ such that $(Q_1', ..., Q_N') \longrightarrow (1', ..., N')$ and thus $(1, ..., N) \longrightarrow (Q_1^{-1}, ..., Q_N^{-1})$, in which Q^{-1} is the inverse permutation of Q. Comparing Eqs. (2.5) and (2.6), I find that $Q = P^{-1}$ and $\alpha_P^* = \alpha_{P^{-1}}$.

We now consider the simplest case of 2 identical particles, for which any α_P is real and the 2-particle probability amplitude, using (2.3), is

$$\langle 1', 2'|1, 2\rangle = a\langle 1'|1\rangle\langle 2'|2\rangle + b\langle 1'|2\rangle\langle 2'|1\rangle. \tag{2.7}$$

The equation (2.7) associates the order of the states in the 2-particle probability amplitude on the left with the order of the products of the 1-particle probability amplitudes on the right. Swapping the single-particle states in the 2-particle state vector exchanges the weights of the single-particle products. However, this swapping cannot modify the 2-particle amplitude implying that amplitudes may differ only for a global phase factor, that is

$$\begin{aligned} \langle 1', 2'|2, 1\rangle &= e^{i\zeta}\langle 1', 2'|1, 2\rangle = e^{i\zeta} a\langle 1'|1\rangle\langle 2'|2\rangle + e^{i\zeta} b\langle 1'|2\rangle\langle 2'|1\rangle \\ &= a\langle 1'|2\rangle\langle 2'|1\rangle + b\langle 1'|1\rangle\langle 2'|2\rangle \end{aligned}. \tag{2.8}$$

We find that $e^{i\zeta}b = a$ and $e^{i\zeta}a = b$, so $|a| = |b|$ and $(e^{i\zeta})^2 := \eta^2 = 1$ from which $\eta = \pm 1$. In this way, taking $a = 1$ in the linear combination of equation (2.7), $b = \eta$. So, the inner product of two "holistic" state vectors is

$$\langle 1', 2'|1, 2\rangle_\eta := \langle 1'|1\rangle\langle 2'|2\rangle + \eta\langle 1'|2\rangle\langle 2'|1\rangle, \tag{2.9}$$

where the subscript η indicates that it is a symmetrized product. The previous expression represents the core of our approach and includes the particle spin-statistics principle. In fact, according to the Pauli exclusion principle, the probability amplitude of finding two fermions in the same state is zero, so $\langle 1', 1'|1, 2\rangle_\eta = (1 + \eta)\langle 1'|1\rangle\langle 1'|2\rangle$ requires that η is -1. The choice

$\eta = +1$ gives the maximum amplitude of finding two particles in the same state and corresponds to the case of bosons.

As it can be argued from Eq. (2.9), *in the no-label approach, the information about the IP statistics is restated in the language of transition amplitudes, instead of approaching it at the level quantum states. In other words, the fundamental statistics-dependent unit is not the quantum state, but the transition amplitude*.

Generalising the expression (2.9) to an arbitrary number N of identical particles, I can write

$$\langle 1', 2', ..., N'|1, 2, ..., N\rangle_\eta := \sum_P \eta^P \langle 1'|P_1\rangle\langle 2'|P_2\rangle ...\langle N'|P_N\rangle, \tag{2.10}$$

where, in analogy with the 2-particle case, for bosons η^P (P being the parity of the permutation) is always 1 and for fermions it is 1 (-1) for even (odd) permutations. In the following I shall omit, except where necessary, the subscript η in the bra-ket product. Equation (2.10) induces the symmetrization property of the N-system state space: $|1, 2, ..., j, ..., k, ..., N\rangle = \eta|1, 2, ..., k, ..., j, ..., N\rangle$, for $j, k = 1, ..., N$. Linearity of the N-system state vector with respect to each 1-particle state immediately follows from the linearity of the 1-particle amplitudes and the N-particle state vectors thus span the physical symmetric state space $\mathcal{H}_\eta^{(N)}$. I have thus derived, by first principles, the 2-particle probability amplitude [58] and generalised it to the N-particle case.

We remark that in the situations represented by Fig. 2.3(b) and only in this case one can write $\langle 1', ..., N'|P_1, ..., P_N\rangle := (\langle 1'| \otimes ... \otimes \langle N'|)(|P_1\rangle \otimes ... \otimes |P_N\rangle)$. Therefore, for calculation purposes $|1, ..., N\rangle \simeq |1\rangle \otimes ... \otimes |N\rangle$. This is not true if there is overlap either among the 1-particle entry states or among the exit ones (see Fig.2.3(c) and (d)). In this sense probability amplitudes are more fundamental than quantum states.

An arbitrary elementary normalised N-identical particle state is defined as

$$|\Phi^{(N)}\rangle := \frac{1}{\mathcal{N}}|\phi^{(N)}\rangle := \frac{1}{\mathcal{N}}|1, 2, ..., N\rangle, \tag{2.11}$$

where $\mathcal{N} = \sqrt{\langle 1, 2, ..., N|1, 2, ..., N\rangle}$. $|\Phi^{(N)}\rangle$ is expressed in terms of single-particle states as a single state vector, which is to be compared with the $N!$ product state vector in the SA approach: $|\Theta^{(N)}\rangle = \frac{1}{\mathcal{N}} \sum_P \eta^P |1_{P_1}\rangle \otimes |2_{P_2}\rangle \otimes ... \otimes |N_{P_N}\rangle$.

The next step is to define the action of operators in the no-label approach. I limit ourselves to an arbitrary 1-particle operator $A^{(1)}$ that acts on each 1-particle state at a time: $A^{(1)}|k\rangle := |A^{(1)}k\rangle$. Its action on N-particle states is naturally defined as

$$A^{(1)}|1, 2, ..., N\rangle := \sum_k |1, ..., A^{(1)}k, ..., N\rangle. \tag{2.12}$$

2.2.2 Partial trace and von Neumann entropy

I now show that in the no-label formalism, the ambiguities inherent in the operation of partial trace in the SA, due to the lack of IP "individuality" [57], are absent.

To calculate the M-particle partial trace of an N-particle state $\mathrm{Tr}^{(M)}\,|\Phi^{(N)}\rangle\,\langle\Phi^{(N)}|^2$, I have to define a product operation between bra and ket of different number of particles.

I start considering the simplest case of $M=1$. Given a 1-particle orthonormal basis $\{|k'\rangle\}$ and the 1-particle operator $A^{(1)}=|j'\rangle\langle k'|$ and using equation (2.12), its action on a N-particle state $|1,...,N\rangle$ can be written as

$$\begin{aligned} A^{(1)}|1,...,N\rangle &:= \sum_k |1,2,...,j'\langle k'|k\rangle,...,N\rangle \\ &= \sum_k \eta^{k-1}\langle k'|k\rangle|j',1,2,...,\not{k},...,N\rangle, \end{aligned} \tag{2.13}$$

where, in the second line, I have taken out of the N-particle ket the complex number $\langle k'|k\rangle$ and shifted the state $|j'\rangle$ from the k-th site to the first one ($\not{k}$ indicate the lack of k-th state!). Introducing with the symbol $\wedge$ a non-separable symmetric external product between different kets that I call *wedge* product (for fermions this product is the Penrose's wedge product defined in terms of labelled states [63]), the elementary N-particle states can be written as the wedge product of N single particle states, i.e. $|1,2,...,N\rangle := |1\rangle\wedge|2\rangle\wedge...\wedge|N\rangle$ and $(|1,2,...,N\rangle)^\dagger := \langle N|\wedge...\wedge\langle 2|\wedge\langle 1|$. Moreover, $|P_1\rangle\wedge|P_2\rangle\wedge...\wedge|P_N\rangle = \eta^P|1\rangle\wedge|2\rangle\wedge...\wedge|N\rangle$. The wedge product coincides with the multiplication operation of the exterior algebra associated to the N-particle symmetric Hilbert space $\mathcal{H}_\eta^{(N)}$. Therefore, equation (2.13) can be written as

$$A^{(1)}|1,...,N\rangle := |j'\rangle\wedge\sum_k \eta^{k-1}\langle k'|k\rangle|1,2,...,\not{k},...,N\rangle \tag{2.14}$$

and it suggests the introduction of a generalised *dot* product operation between a 1-particle bra and and N-particle ket, defined as

$$\langle k'|\cdot|1,2,...,N\rangle := \sum_{k=1}^{N}\eta^{k-1}\langle k'|k\rangle|1,...,\not{k},...,N\rangle. \tag{2.15}$$

Expressing the N-particles state in terms of wedge products, the dot product is distributive with respect to the wedge. The operation in Eq. (2.15) gives an (unnormalised) $(N-1)$-particle state. The corresponding normalised reduced $(N-1)$-particles pure state $|\Phi_{k'}^{(N-1)}\rangle$ is

$$|\Phi_{k'}^{(N-1)}\rangle = \frac{\langle k'|\cdot|\Phi^{(N)}\rangle}{\sqrt{\langle\Pi_{k'}^{(1)}\rangle_{\Phi^{(N)}}}}, \quad \text{with} \quad \Pi_{k'}^{(1)}=|k'\rangle\langle k'|. \tag{2.16}$$

[2]This operation corresponds to measure the states of M IP without registering the outcomes.

Specifically the normalised 1-particle partial trace of an N-particle state is

$$\rho^{(N-1)} := \frac{1}{\langle \mathbb{I}^{(1)} \rangle_{\Phi^{(N)}}} \mathrm{Tr}^{(1)} |\Phi^{(N)}\rangle\langle\Phi^{(N)}| = \sum_{k'} p_{k'} |\Phi^{(N-1)}_{k'}\rangle\langle\Phi^{(N-1)}_{k'}|, \tag{2.17}$$

where the action of the 1-particle identity operator $\mathbb{I}^{(1)} = \sum_{k'} \Pi^{(1)}_{k'}$ on a N-particles state is $\mathbb{I}^{(1)}|1,...,N\rangle = N|1,...,N\rangle$ and $p_{k'} = \frac{\langle \Pi^{(1)}_{k'} \rangle_{\Phi^{(N)}}}{\langle \mathbb{I}^{(1)} \rangle_{\Phi^{(N)}}}$. It is important to remark that this 1-particle partial trace and the resulting $(N-1)$-reduced density matrix are not affected by the ambiguities of the analogous quantities obtained in the SA, since there is no pretence of establish "which" is the traced out particle and to "which" particles the reduced state is associated.

Consider now the case $M = 2$. The relevant dot product is

$$\langle l', m'| \cdot |1,...,N\rangle = \sum_{k=1}^{N} \eta^{k-1} \langle l'|k\rangle \left[\sum_{j<k} \eta^{j-1} \langle m'|j\rangle |\not{j}, \not{k}\rangle + \sum_{j>k} \eta^{j-2} \langle m'|j\rangle |\not{k}, \not{j}\rangle \right], \tag{2.18}$$

where $|\not{j}, \not{k}\rangle \equiv |1,...,\not{j},...,\not{k},...,N\rangle$. If $N = 2$ equation (2.18) coincide with the 2-particle probability amplitude given by Eq. (2.9). The 2-particle identity operator is $\mathbb{I}^{(2)} = (1/2!) \sum_{\tilde{k}'} \Pi^{(2)}_{\tilde{k}'}$, where $\Pi^{(2)}_{k'} = |\tilde{k}'\rangle\langle\tilde{k}'|$ is the 2-particle projection operator and $\{|\tilde{k}'\rangle := |k'_1, k'_2\rangle / \mathcal{N}_{k'}\}$ ($\mathcal{N}_{k'}$ being a normalisation constant). The $(N-2)$-particle reduced density matrix is

$$\rho^{(N-2)} := \frac{1}{2! \langle \mathbb{I}^{(2)} \rangle_{\Phi^{(N)}}} \mathrm{Tr}^{(2)} |\Phi^{(N)}\rangle\langle\Phi^{(N)}| = \sum_{\tilde{k}'} p_{\tilde{k}'} |\Phi^{(N-2)}_{\tilde{k}'}\rangle\langle\Phi^{(N-2)}_{\tilde{k}'}|, \tag{2.19}$$

where $p_{\tilde{k}'} = \frac{1}{2!} \frac{\langle \Pi^{(2)}_{\tilde{k}'} \rangle_{\Phi^{(N)}}}{\langle \mathbb{I}^{(2)} \rangle_{\Phi^{(N)}}}$ and $|\Phi^{(N-2)}_{\tilde{k}'}\rangle = \frac{\langle \tilde{k}'| \cdot |\Phi^{(N)}\rangle}{\sqrt{\langle \Pi^{(2)}_{\tilde{k}'} \rangle_{\Phi^{(N)}}}}$ is the normalised reduced $(N-2)$-particles pure state.
When required, the generalisation of equation (2.18) to the case of any M is straightforward.

Once the reduced density matrix is obtained, the entanglement between the bipartition of M and $(N-M)$ particles can be measured by the von Neumann entropy

$$S(\rho^{(N-M)}) = -\mathrm{Tr}(\rho^{(N-M)} \log_2 \rho^{(N-M)}). \tag{2.20}$$

Moreover, knowledge of the reduced density matrices of all the possible bipartitions of the system allows the qualitative assessment of the genuine multipartite entanglement of the pure state of N IP, as usually done for NIP [64]. Notice that, since the identical particles entanglement intrinsically depends on both global state structure and observation measurements [65, 34], one has to specify the partial trace and the reduced density matrix corresponding to a desired operational framework [34]. *This result differs from what is obtained in the SA where the partial trace is meaningless [44].*

2.2.3 IP-Schmidt decomposition

In Chapter 1, it is shown that by means of the SA the direct application to IP of the Schmidt decomposition known for NIP gives unphysical results, implying that IP are always entangled, even if they are independently prepared and spatially separated. Moreover, it does not give a criterion to understand which is the role of mock labels in the emergence of the entangled structure of the IP quantum states, when particles spatially overlap. As a result, by analogy with NIP, the Slater decomposition [24, 23, 25] has been introduced for both bosons and fermions, with the attempt to take into account the effect of the symmetrization postulate in the characterization of entanglement. However, the Slater rank, i.e. the number of nonzero coefficients in the decomposition, is not an entanglement witness (in contrast to what appends with the Schmidt rank for NIP). Moreover it gives results which are in contrast with some experimental evidences about IP quantum correlations.

In this section I will recall the generalization of the Schmidt decomposition to the case of two IP, developed by using the no-label approach [35].

Consider two d-level IP in the pure state $|\Psi\rangle$ and choose an orthonormal 2-particle basis $\{|i,j\rangle\}$ in the linear symmetric 2-particle Hilbert space $\mathcal{H}_\eta^{(2)}$. The state $|\Psi\rangle$ can be expressed in the chosen basis, as

$$|\Psi\rangle = \frac{1}{2}\sum_{ij} |i,j\rangle \langle i,j|\Psi\rangle \tag{2.21}$$

and defining the state $|\bar{i}\rangle = \sum_j \langle i,j|\Psi\rangle |j\rangle$, it follows that

$$|\Psi\rangle = \frac{1}{2}\sum_{i} |i,\bar{i}\rangle \,. \tag{2.22}$$

There exists a basis $\{|\bar{i}\rangle\}$ where $\langle\bar{i}'|\bar{i}\rangle \propto \delta_{ii'}$. In fact, considering that $\langle\bar{i}'|\bar{i}\rangle = 2\langle i|\rho^{(1)}|i'\rangle$, where the single-particle partial trace $\rho^{(1)} = \frac{1}{2}\sum_j \langle j|\cdot|\Psi\rangle\langle\Psi|\cdot|j\rangle$ has been used, it is evident that when the states $\{|i\rangle\}$ are the eigenstates of $\rho^{(1)}$ with eigenvalues $\{\lambda_i\}$. The state $\{|\bar{i}\rangle\}$ are orthogonal and in particular $\langle\bar{i}|\bar{i}'\rangle = 2\lambda_i\delta_{ii'}$. As a result, the set of states

$$|\tilde{i}\rangle = \frac{1}{\sqrt{2\lambda_i}}|\bar{i}\rangle = \frac{1}{\sqrt{2}}\frac{1}{\sqrt{\lambda_i}}\sum_j \langle i,j|\Psi\rangle |j\rangle \tag{2.23}$$

is orthonormal. Both $|i\rangle$ and $|\tilde{i}\rangle$ are eigenstates of $\rho^{(1)}$ with the same eigenvalues [35] and substituting $|\bar{i}\rangle = \sqrt{2\lambda_i}|\tilde{i}\rangle$ in $|\Psi\rangle$, we obtain

$$|\Psi\rangle = \frac{1}{\sqrt{2}}\sum_i \sqrt{\lambda_i}\,|i,\tilde{i}\rangle\,, \tag{2.24}$$

with $\lambda_i > 0$ and $\sum_i \lambda_i = 1$. Eq. (2.24) constitutes the sought IP-Schmidt decomposition for

two d-level IP, where the "Schmidt coefficients" $\sqrt{\lambda_i}$ are the square roots of the eigenvalues of the reduced 1-particle density matrix $\rho^{(1)}$ and the states $\{|i\rangle\}$ its eigenstates. The states $|\tilde{i}\rangle$ belongs to the basis $\{|i\rangle\}$ and $\{|i,\tilde{i}\rangle\}$ is the symmetric Schmidt basis.

As for NIP, the positive integer "IP-Schmidt number" s of terms appearing in the IP-Schmidt decomposition, that is the number of nonzero eigenvalues of $\rho^{(1)}$, is an entanglement witness: in fact $s = 1$, indicates that $\rho^{(1)}$ is pure and so $|\Psi\rangle$ is nonentangled. If $s > 1$, $\rho^{(1)}$ is mixed and $|\Psi\rangle$ is entangled. The IP-Schmidt coefficients are directly linked to an entanglement quantifier, that is to the von Neumann entropy of $\rho^{(1)}$: $S(\rho^{(1)}) = -\sum_i \lambda_i \log_2 \lambda_i$.

2.2.4 Connection of the no-label formalism with second quantization

Above I have introduced relations between states differing in the number of particles. This suggests a relationship between the no-label approach to IP and second quantization. However, while in the second quantization particles are elementary excitations of fields, our approach applies to any system of identical quantum objects. Moreover, while in second quantization, creation and annihilation operators connect states differing only by one particle, in the no-label approach, the dot product connect states differing for a generic number of particles. Finally, in the second quantization the fundamental role is played by the commutation rules, while in our approach it is played by the symmetry of probability amplitudes.

To show the connection between the two approaches, I notice that Eq. (2.15) suggests the introduction of a 1-particle annihilation operator

$$a(k)|1,...,N\rangle := \langle k| \cdot |1,...,N\rangle \tag{2.25}$$

and its the adjoint is

$$a^\dagger(k)|1,...,N\rangle := |k\rangle \wedge |1,...,N\rangle. \tag{2.26}$$

Analogously, Eq. (2.18) directly suggests the introduction of 2-particle annihilation and creation operators defined as

$$a(j,k)|1,...,N\rangle := \langle j,k| \cdot |1,...,N\rangle, \tag{2.27}$$

$$a^\dagger(j,k)|1,...,N\rangle := |j,k\rangle \wedge |1,...,N\rangle \tag{2.28}$$

which, in terms of the wedge product can be written as follows

$$a(j,k)|1,...,N\rangle = (\langle k| \wedge \langle j|) \cdot |1,...,N\rangle = \langle k| \cdot (\langle j| \cdot |1,...,N\rangle), \tag{2.29}$$

$$a^\dagger(j,k)|1,...,N\rangle = |j\rangle \wedge |k\rangle \wedge |1,...,N\rangle. \tag{2.30}$$

From the symmetry properties of the states, it is simple to obtain the a's commutation rules. For the 1-particle creation and annihilation operators of equations (2.25) and (2.26) I obtain

$$\begin{aligned} [a(j), a^\dagger(k)]_\eta &= \langle j|k\rangle \\ [a^\dagger(j), a^\dagger(k)]_\eta &= [a(j), a(k)]_\eta = 0, \end{aligned} \tag{2.31}$$

where $[a(j), a^\dagger(k)]_\eta = a(j)a^\dagger(k) - \eta a^\dagger(k)a(j)$ is the commutator for bosons and the anticommutator for fermions. Using Eq. (2.18), Eq. (2.31) generalises, for the 2-particle creation and annihilation operators, to (see Appendix A)

$$\begin{aligned} [a(j,k), a^\dagger(m,n)] &= \langle j,k|m,n\rangle_\eta, \\ [a^\dagger(j,k), a^\dagger(m,n)] &= [a(j,k), a(m,n)] = 0. \end{aligned} \tag{2.32}$$

In the first equation of (2.32) the η in right hand side keeps the memory of the bosonic or fermionic nature of the particles.

2.3 Applications

2.3.1 Spin exchanged states

We consider the well-known W entangled state of nonidentical particles, which constitutes an important resource state for several quantum information tasks [66, 36]. I explicitly describe a single-particle state with the spatial mode ϕ_i ($i = 1, \ldots, N$) and the pseudospin $\uparrow, \downarrow$. The W state has the structure

$$|W\rangle = |\phi_1 \uparrow, \phi_2 \downarrow, ..., \phi_N \downarrow\rangle + |\phi_1 \downarrow, \phi_2 \uparrow, ..., \phi_N \downarrow\rangle + ... + |\phi_1 \downarrow, ..., \phi_{N-1} \downarrow, \phi_N \uparrow\rangle, \tag{2.33}$$

where for nonidentical particles each term of the superposition is a tensor product of single-particle states. The very same structure is considered to hold also for identical particles in separated locations. In this case, is this structure valid under any circumstance? To analyse this aspect, I choose 3 fermions localised in three separated spatial modes A, B and C, so that the state of equation (2.33) is $|W_3\rangle = |A \uparrow, B \downarrow, C \downarrow\rangle + |A \downarrow, B \uparrow, C \downarrow\rangle + |A \downarrow, B \downarrow, C \uparrow\rangle$. When two fermions are in the same spatial mode, for instance $A = B$, this state becomes

$$|\bar{W}_3\rangle = |A \uparrow, A \downarrow, C \downarrow\rangle + |A \downarrow, A \uparrow, C \downarrow\rangle, \tag{2.34}$$

where the state $|A \downarrow, A \downarrow, C \uparrow\rangle$ does not appear because of the Pauli exclusion principle (its norm tends to zero). Using the symmetry properties of the elementary states, $|A \downarrow, A \uparrow, C \downarrow\rangle = -|A \uparrow, A \downarrow, C \downarrow\rangle$, one gets $|\bar{W}_3\rangle = 0$, while one expects no restriction arising from

particle statistics, considering that the two fermions in A have opposite spins. The same problem is thus expected to arise even when the particles are spatially nonoverlapping but non-local measurements are performed. Hence, the form of the W state of equation (2.33) for identical particles does not work in general.

We define a spin exchanged state (SPES) as a suitable linear combination of (unnormalized) elementary states where only particle pseudospins are exchanged, that is

$$|\text{SPES}\rangle := \frac{1}{\mathcal{N}} \sum_{P} \eta^{P} |\phi_1\, \sigma_{P_1}, ..., \phi_N\, \sigma_{P_N}\rangle, \tag{2.35}$$

where P are here the cyclic permutations of pseudospins σ_{P_i} and $\mathcal{N}$ is the global normalisation constant. When $\sigma_1 = \uparrow$ and $\sigma_2 = \ldots = \sigma_N = \downarrow$, the SPES represents a generalisation of the W state for identical particles valid bosons and fermions under any circumstances. Other states of interest are obtained from (2.35) for different pseudospin conditions; for instance, assuming a ring configuration of the N particle and taking $\sigma_1 = \ldots = \sigma_M = \uparrow$ and $\sigma_{(M+1)} = \ldots = \sigma_N = \downarrow$ such states can represent a linear combination of spin block systems in the ring chain.

2.3.2 Separability of spatial and spin degrees of freedom

For any elementary state of NIP, the spatial and spin degrees of freedom, being associated to the individual particle, are independent and separable [67]. This is not the case for elementary states of IP.

As mentioned above, the essence of the no-label approach is the absence of labels and the consequent holistic form of the states that are not separable in tensor products of single-particle states. For a single particle, I have $|\varphi\, \sigma\rangle \equiv |\varphi\rangle \otimes |\sigma\rangle$, i.e. the spatial part of the state can be treated separately from the pseudospin one. Instead, for two IP, when $\varphi_1 \neq \varphi_2$ and $\sigma_1 \neq \sigma_2$, it is $|\varphi_1\, \sigma_1, \varphi_2\, \sigma_2\rangle \neq |\varphi_1, \varphi_2\rangle \otimes |\sigma_1, \sigma_2\rangle$, so measures of position and pseudospin operators may be not independent. One may ask which structure a state of IP must have in order that spatial and pseudospin degrees of freedom are independent from each other.
To fix our ideas, let me take the 2-particle state

$$|\phi^{(2)}\rangle = \alpha|\varphi_1\, \sigma, \varphi_2\, \tau\rangle + \beta|\varphi_1\, \tau, \varphi_2\, \sigma\rangle, \tag{2.36}$$

with $\varphi_1 \neq \varphi_2$, $\tau \neq \sigma$. Let me calculate the probability amplitude of finding a particle with a wave function φ_1' and pseudospin σ' and the other one with wave function φ_2' and pseudospin τ', that is the probability amplitude to find in any elementary 2-particle state $|\phi'^{(2)}\rangle = |\varphi_1'\, \sigma', \varphi_2'\, \tau'\rangle$ the system prepared in $|\phi^{(2)}\rangle$ of Eq. (2.36),

$$\langle\phi'^{(2)}|\phi^{(2)}\rangle = \langle\varphi_1'\, \sigma', \varphi_2'\, \tau'|\{\alpha|\varphi_1\, \sigma, \varphi_2\, \tau\rangle + \beta|\varphi_1\, \tau, \varphi_2\, \sigma\rangle\}. \tag{2.37}$$

Using the expression (2.9), I find that, given $\alpha = 1$, *only when* $\beta = \pm 1$ equation (2.37) can be written as

$$\langle \phi'^{(2)} | \phi^{(2)} \rangle = \langle \varphi'_1 \varphi'_2 | \varphi_1 \varphi_2 \rangle_{\eta\beta} \langle \sigma' \tau' | \sigma \tau \rangle_\beta, \tag{2.38}$$

where $\langle \mu' \ \nu' | \mu \ \nu \rangle_\gamma$ indicates the probability amplitude of the form of equation (2.9) with η substituted by γ. Thus, the well known attitude of separating the spatial and spin part of the IP state in the SA [67], is here restated in the language of transition amplitudes. Since the obtained result is independent of the structure of the elementary bra in the LHS of Eq. (2.38), I can say that in the entangled states of the form $|\phi^{(2)}_\pm\rangle = |\varphi_1 \, \sigma, \varphi_2 \, \tau\rangle \pm |\varphi_1 \, \tau, \varphi_2 \, \sigma\rangle$ the physical behaviour of the spatial part is independent of the spin part. As a result, the actions of two generic spatial and spin operators respectively A_Ψ and A_Σ, (where the subscripts Ψ and Σ indicate the spatial and spin degrees of freedom, respectively) on this state can be expressed as

$$\begin{aligned} A_\Psi \, |\phi^{(2)}_\pm\rangle &:= (A_\Psi |\varphi_1, \varphi_2\rangle_{\eta\pm}) \otimes |\sigma, \tau\rangle_\pm, \\ A_\Sigma \, |\phi^{(2)}_\pm\rangle &:= |\varphi_1, \varphi_2\rangle_{\eta\pm} \otimes (A_\Sigma |\sigma, \tau\rangle_\pm), \end{aligned} \tag{2.39}$$

where the kets' subscripts indicate the symmetry of the state: $|\kappa, \chi\rangle_\gamma = \gamma |\chi, \kappa\rangle_\gamma$. When $\sigma = \uparrow$ and $\tau = \downarrow$, $|\phi^{(2)}_\pm\rangle$ are two (unnormalized) Bell states for a generic value of the IP spatial overlap. It is moreover immediate to show that, analogously, an entangled state of the form $|\psi^{(2)}_\pm\rangle = |\varphi_1 \, \sigma, \varphi_2 \, \sigma\rangle \pm |\varphi_1 \, \tau, \varphi_2 \, \tau\rangle$ always gives

$$\begin{aligned} A_\Psi \, |\psi^{(2)}_\pm\rangle &:= (A_\Psi |\varphi_1, \varphi_2\rangle_\eta) \otimes (|\sigma, \sigma\rangle \pm |\tau, \tau\rangle), \\ A_\Sigma \, |\psi^{(2)}_\pm\rangle &:= |\varphi_1, \varphi_2\rangle_\eta \otimes (A_\Sigma (|\sigma, \sigma\rangle \pm |\tau, \tau\rangle)). \end{aligned} \tag{2.40}$$

Finally, one can separately write in the no-label formalism the actions on the entangled Bell states of spatial and spin operators.

2.3.3 Effects of indistinguishability in a system of three identical qubits

Consider three identical qubits, each in the state $|\varphi_k \ \sigma_k\rangle \equiv |\varphi_k\rangle \otimes |\sigma_k\rangle$ ($k = 1, 2, 3$), where φ_k is the k-th spatial wavefunction and σ_k is the corresponding pseudospin $\uparrow$, $\downarrow$. The 3-qubit elementary state is $|\Phi^{(3)}\rangle = \dfrac{1}{\mathcal{N}} |\varphi_1 \, \sigma_1, \varphi_2 \, \sigma_2, \varphi_3 \, \sigma_3\rangle$, where $\mathcal{N}$ is the normalization constant.

We start taking the total system in the pure state

$$|\Phi^{(3)}\rangle = |\mathrm{A} \downarrow, \mathrm{B} \downarrow, \mathrm{C} \uparrow\rangle, \tag{2.41}$$

where the three spatial wavefunctions have support in the three corresponding separated spatial regions A, B and C, as depicted in Fig. 2.4(a). Considering all the possible bipartitions (AB)-C, (CA)-B, (BC)-A of the three-particle system, by performing localized projective

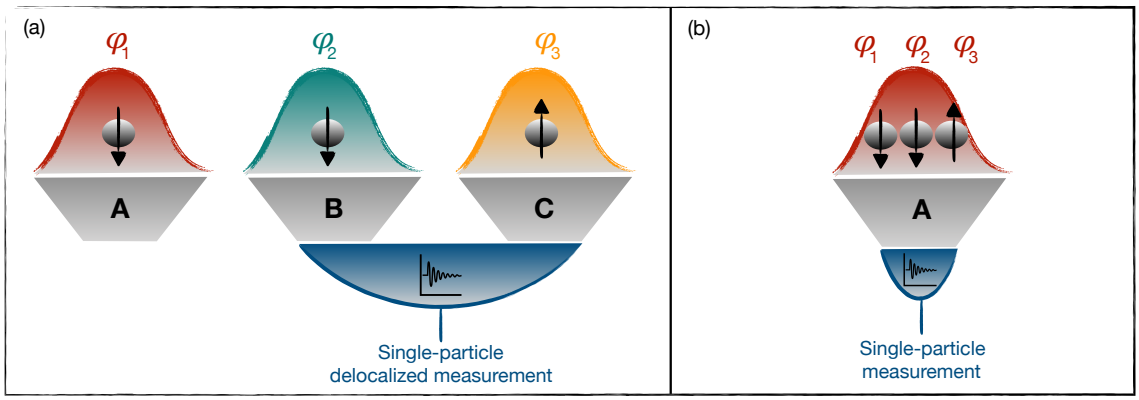

Figure 2.4: (a) Configuration associated to the state $|\Phi^{(3)}\rangle$ when particles are in separate spatial regions (grey zones). (b) Complete spatial overlap of three qubits in the spatial region A.

measurements and partial traces [39] one finds that all the three bipartitions give pure one-particle and two-particle reduced density matrices. Following conventional wisdom this state is, as expected, fully uncorrelated [64]. Thus, separated identical particles, addressed by spatially localized measurements, behave analogously to distinguishable particles. However, in contrast with the case of distinguishable particles which are individually addressable, quantum correlations between identical particles depend on the region where measurements are performed. In fact, if partial traces of an identical particle state are made onto non-local basis, a "measurement-induced" entanglement [58] is obtained. For example, by making on our system of Fig. 2.4(a) in the state $\rho^{(3)} = |\Phi^{(3)}\rangle\langle\Phi^{(3)}|$ a non-local one-particle trace onto the delocalized basis $\left\{\frac{1}{\sqrt{2}}|(\mathrm{B}+\mathrm{C})\ \downarrow\rangle, \frac{1}{\sqrt{2}}|(\mathrm{B}+\mathrm{C})\ \uparrow\rangle\right\}$, I obtain the two-particle mixed state $\rho^{(2)} = \frac{1}{2}(|\mathrm{A}\downarrow,\mathrm{C}\uparrow\rangle\langle\mathrm{A}\downarrow,\mathrm{C}\uparrow| + |\mathrm{A}\downarrow,\mathrm{B}\downarrow\rangle\langle\mathrm{A}\downarrow,\mathrm{B}\downarrow|)$. This shows how entanglement of spatially separated identical particles is affected by the non-local nature of measurements.

I now compare the above results with the analogous case of nonidentical qubits. The global state can be written as the tensor product of single-particle labeled states, namely

$$|\Phi_{\mathrm{d}}^{(3)}\rangle = |\mathrm{A}\downarrow\rangle_1 \otimes |\mathrm{B}\downarrow\rangle_2 \otimes |\mathrm{C}\uparrow\rangle_3 \tag{2.42}$$

(where labels 1, 2, and 3 are physical labels making particles different). This state is manifestly separable and so unentangled [64]. Moreover, if I make partial traces over a non-local basis (e.g., $\mathcal{B}_k = \left\{\frac{1}{\sqrt{2}}|(\mathrm{A}+\mathrm{B})\downarrow\rangle, \frac{1}{\sqrt{2}}|(\mathrm{A}+\mathrm{B})\uparrow\rangle\right\}_k$), due to the fact that now measurements are made on an individual particle, pure reduced density matrices are obtained: the particles thus remain fully uncorrelated. This result does not change even when the three distinguishable qubits completely spatially overlap (A=B=C). This aspect highlights the difference on the entanglement properties of independently-prepared identical and non-identical particles.

To have entanglement of three spatially separated qubits by local measurements, linear

combinations of elementary states [39] are necessary. In particular, I take a superposition of two three-qubit states corresponding to the well-known GHZ state of distinguishable particles [64, 68], $|\Lambda^{(3)}_{\rm GHZ}\rangle = \frac{1}{\sqrt{2}}(|{\rm A}\downarrow, {\rm B}\downarrow, {\rm C}\downarrow\rangle + |{\rm A}\uparrow, {\rm B}\uparrow, {\rm C}\uparrow\rangle)$. All the distinct bipartitions, by means of local partial traces, are easily seen to produce totally mixed reduced density matrices: therefore, the state is maximally three-partite entangled. A further advantage of the no-label formalism here emerges because, when the $|\Lambda^{(3)}_{\rm GHZ}\rangle$ is expressed in terms of unphysical labels, it consists of a linear combination of twelve different product states of three one-particle state vectors. This would make the analysis technically cumbersome and would hinder the identification of physical entanglement from the unphysical one associated to labels.

To evidence the role of the spatial overlap, I now consider the state of three boson qubits condensed in the same spatial mode A, as illustrated in Fig. 2.4(b). This state has the form $|\Psi^{(3)}\rangle = \frac{1}{\sqrt{2}}|{\rm A}\downarrow, {\rm A}\downarrow, {\rm A}\uparrow\rangle$ and admits only one bipartition (two particles)-(one particle). By performing partial traces onto this bipartition, one obtains the one-particle and two-particle reduced density matrices

$$\rho^{(1)} = \frac{1}{\tilde{\mathcal{N}}}{\rm Tr}^{(2)}|\Psi^{(3)}\rangle\langle\Psi^{(3)}| = \frac{2}{3}|{\rm A}\downarrow\rangle\langle{\rm A}\downarrow| + \frac{1}{3}|{\rm A}\uparrow\rangle\langle{\rm A}\uparrow|, \tag{2.43}$$

$$\rho^{(2)} = \frac{1}{\mathcal{N}}{\rm Tr}^{(1)}|\Psi^{(3)}\rangle\langle\Psi^{(3)}| = \frac{2}{3}|{\rm A}\uparrow, {\rm A}\downarrow\rangle\langle{\rm A}\uparrow, {\rm A}\downarrow| + \frac{1}{3}\frac{|{\rm A}\uparrow, {\rm A}\uparrow\rangle}{\sqrt{2}}\frac{\langle{\rm A}\uparrow, {\rm A}\uparrow|}{\sqrt{2}}. \tag{2.44}$$

These density matrices are manifestly mixed and give the same von Neumann entropy $S(\rho^{(1)}) = S(\rho^{(2)}) = -\frac{1}{3}\log_2\frac{1}{3} - \frac{2}{3}\log_2\frac{2}{3}$. This result, differently from the uncorrelated state $|\Phi^{(3)}\rangle$, witnesses that $|\Psi^{(3)}\rangle$ is three-partite entangled [64].

2.4 Discussions

In conclusion, the foundations of a formalism, named no-label formalism, alternative to the particle-based SA, to treat a generic number N of IP have been presented. The novelty of this approach is the absence of unobservable labels addressing particles, in this way avoiding al the difficulties and inconsistencies, due to mock labels, present in the SA to IP quantum states and entanglement. Elementary quantum states of N IP are thus defined as lists of N single-particle states and must not be expressed as tensor products of the latters.

The crucial element of this approach, that is the probability amplitude between N-particle states, has derived by first principles, i.e. the cluster decomposition and the linearity with respect to 1-particle states. In this approach, the fundamental quantities are the probability amplitudes, not the states. Thus this approach translates in the language of probability amplitudes the properties of IP statistics (bosonic and fermionic), which in the SA are contained at the level of quantum states.

The no-label formalism allows us to evaluate, without the ambiguities present in the SA, the entanglement between bipartitions of N IP, not only by treating fermions and bosons on the same footing but also by exploiting the same tools known for NIP, i.e. the $(N-M)$- particles partial trace (which here regains the physical meaning lost in the SA), the von Neumann entropy of the $(N-M)$-particles reduced density matrix and the Schmidt decomposition.

Generalized products between IP states of different dimensions have been defined, showing that the corresponding vector spaces can be connected by generalized multi-particle creation and annihilation operators. This gave the possibility to connect the no-label approach into second quantization, showing that the commutation rules between N-particles creation and annihilation operators are established by the N-particles properties of probability amplitudes.

Some applications have been presented: a new class of states, called spin-exchanged states (SPES) has been introduced, which are the generalization of the W state to spatially overlapping IP. Finally, the effects of spatial overlap on the entanglement of three identical qubits have been treated. It has also been shown that IP quantum correlations are not an intrinsic property of the quantum state alone but also depend on the performed measurements. We have then shown for a system of three bosonic qubits in the same site that spatial overlap constitutes an entangling mechanism.

Chapter 3

Spatially localized operations and classical communication (sLOCC)

3.1 Introduction

In Chapter 2, it has been shown that entanglement between a bipartition M and $(N-M)$ of N identical particles (IP) can be measured by the von Neumann entropy of the reduced density matrix, obtained by the M-particle (or $N-M$) partial trace for IP (see Section 2.2.2).

Entanglement is especially relevant to carry out quantum information tasks in a Bell-like scenario (i.e. between spatially separated locations). However, it is easy to show that, in general, the two reduced density matrices of M and $N-M$ particles can still spatially overlap, if at the beginning overlap among the N particles is present. This depends on the basis chosen to perform the partial trace. Therefore, the entanglement measured by von Neumann entropy in this case may not be directly exploitable in a Bell-like setup.

In this Chapter, I will introduce an operational framework based on *spatially localised operations and classical communication* (sLOCC) to quantify, as function of the spatial overlap of a number N of IP, the entanglement operationally exploitable for quantum information processes between separate laboratories.

Then, I will define the sLOCC-based concurrence of a generic state of 2 IP [69], to characterize their entanglement analogously to the case of nonidentical particles (NIP).

Finally, a measure of the spatial indistinguishability of IP will beintroduced [69].

3.2 Operational framework

The identification, manipulation and exploitation of purely quantum resources is essential to implement quantum information processes [70]. Usually identical particles are the elementary

building blocks of quantum networks [71, 72, 73, 74, 75]: as a result, the interest for the role played by particle indistinguishability is increasing. However, while for NIP an operational framework to exploit in practice their properties is well established by individual (local) operations on each particle and classical communication (LOCC) [64], for IP, which are individually unaddressable [76, 24, 58, 39], the concept of "particle locality" residing in LOCC is meaningless. The problem of their direct utilization remained open for a long time, in particular when they spatially overlap, since the quantum correlations are primarily usefull to implement quantum information tasks between separate locations. In this respect, a new framework based on *spatially* localized operations and classical communication (sLOCC) has been recently introduced for systems of 2 IP [34]. I now introduce its generalization to the case of a generic number N of IP and, in the rest of the chapter, I show how it allowed us to clearly highlight the role of spatial overlap of IP, and so of spatial indistinguishability, in the emergence of operationally exploitable entanglement.

Consider a system of N independently prepared IP. The i-th single-particle state ($i = 1, 2, ..., N$) is characterized by a spatial wave function ψ_i and in general particles can spatially overlap (Fig.3.1). A local one-particle measurement for systems of IP is the measurement of a property of one particle performed on a localized region of space $\mathcal{R}$ [33].

The sLOCC framework is based on the choice of N spatial regions $\mathcal{R}_i$ in which to perform single-particle measurements, satisfying the following Properties:

1. $\mathcal{R}_i$ have to be spatially separated,

2. the probability of finding at least one particle in each region has to be different from zero.

In this case, analogously to what happens for NIP in which I individually (locally) address

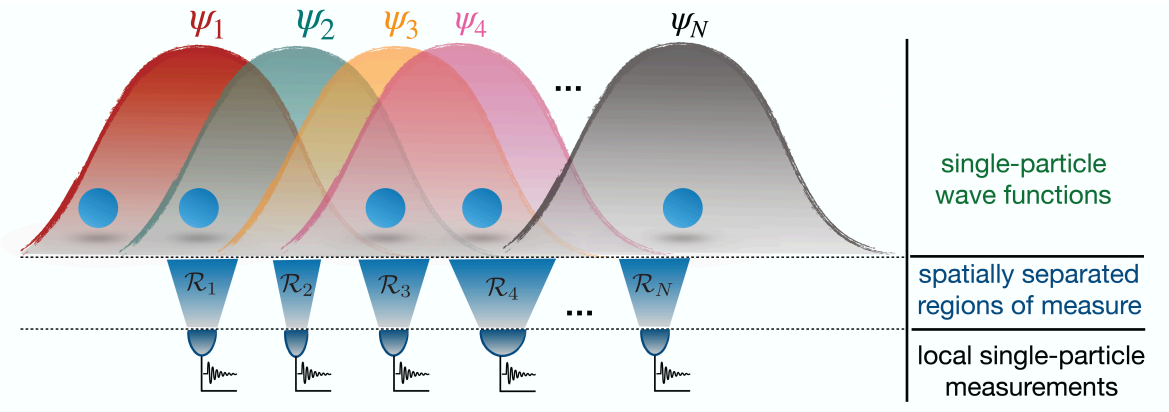

Figure 3.1: Illustration of different single-particle spatial wave functions ψ_i ($i = 1, \ldots, N$) associated to N identical particles in a generic spatial configuration. The sLOCC framework is based on local single-particle measurements, each performed in one of N separate spatial regions $\mathcal{R}_i$ [69].

particles independently from their spatial configurations (LOCC framework), I here address separate spatial regions. This concept is closer to the spirit of quantum field theory, which exploits "space locality" instead of "particle locality". This configuration is particularly useful to exclude correlations between the distant regions induced by the measurement process [24] and, as I are going to show, it gives us the possibility to make it emerge in a quantitative way not only the role played by the spatial indistinguishability of particles in their quantum correlations and features [34, 61, 62, 69], but also to introduce an entropic indistinguishability measure as an information resource [69].

3.3 Entanglement of a pure state of 2 identical particles: von Neumann entropy

Let us consider two independently prepared NIP, A and B. Particle A is prepared with the wave function ψ and pseudospin $\uparrow$ and particle B with the wave function ψ' and pseudospin $\downarrow$. The global state is $|\Psi\rangle_{\mathrm{AB}} = |\psi\uparrow\rangle_{\mathrm{A}} \otimes |\psi'\downarrow\rangle_{\mathrm{B}}$ and under LOCC it is separable, independently on the spatial configuration of ψ and ψ'. On the other hand, if particles are identical the global state in the no-label approach is

$$|\Psi\rangle = |\psi\uparrow, \psi'\downarrow\rangle . \tag{3.1}$$

Do particles in the state of Eq. (3.1) present correlations? In order to establish under LOCC correlations between single-particle measurements for NIP pure states, von Neumann entropy of the reduced density matrices associated to the different particles is used. Ananlogously, under sLOCC correlations between single-particle measurements on IP in two separated spatial regions can be quantified by knowing the reduced density matrices localized in the two regions. Let us choose two separate spatial regions, called $\mathcal{L}$ and $\mathcal{R}$ (Fig.3.2). By performing the partial trace of $|\Psi\rangle\langle\Psi|$, as an example, onto the one-particle basis $\{|\mathrm{L}\downarrow\rangle, |\mathrm{L}\uparrow\rangle\}$, where $|\mathrm{L}\rangle$ is a specific state localized in $\mathcal{L}$, and by projecting onto the subspace spanned by $\{|\mathrm{R}\downarrow\rangle, |\mathrm{R}\uparrow\rangle\}$, where $|\mathrm{R}\rangle$ is a specific state localized in $\mathcal{R}$, one obtains the following 1-particle reduced density matrix in $\mathcal{R}$

$$\rho_{\mathrm{R}}^{(1)} = \frac{1}{P_L P'_R + P'_L P_R}(P_L P'_R\,|\mathrm{R}\downarrow\rangle\langle\mathrm{R}\downarrow| + P'_L P_R\,|\mathrm{R}\uparrow\rangle\langle\mathrm{R}\uparrow|), \tag{3.2}$$

where $P_{\mathrm{X}} = |x|^2 = |\langle \mathrm{X}|\psi\rangle|^2$ and $P'_X = |x'|^2 = |\langle \mathrm{X}|\psi'\rangle|^2$ ($\mathrm{X} = \mathrm{L}, \mathrm{R}$ and $x = l, r$) are the probabilities of finding a particle in $|\mathrm{X}\rangle$.

The von Neumann entropy $S(\rho_{\mathrm{R}}) = -\mathrm{Tr}(\rho_{\mathrm{R}}^{(1)} \log_2 \rho_{\mathrm{R}}^{(1)})$[1] quantifies the entanglement $E_{\mathrm{LR}}(\Psi)$

[1] We remark that, by performing the partial trace in the basis $\{|\mathrm{R}\downarrow\rangle, |\mathrm{R}\uparrow\rangle\}$ and projecting onto the subspace spanned by $\{|\mathrm{L}\downarrow\rangle, |\mathrm{L}\uparrow\rangle\}$, I obtain $\rho_{\mathrm{L}}^{(1)}$ and $S(\rho_{\mathrm{L}}^{(1)}) = S(\rho_{\mathrm{R}}^{(1)})$.

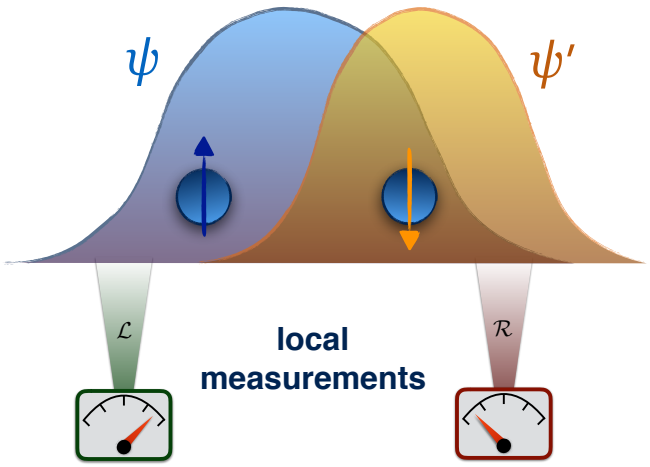

Figure 3.2: System composed by two IP, with opposite pseudospins and spatially overlapping single-particle wave functions ψ and ψ'. Their entanglement is quantified by performing in the sLOCC framework single-particle measurements localized in separate spatial regions $\mathcal{L}$ and $\mathcal{R}$ [34].

between the pseudospins in the separate spatial regions, [34] thai is

$$E_{\mathrm{LR}}(\Psi) = -\frac{P_L P'_R}{P_L P'_R + P'_L P_R} \log_2 \frac{P_L P'_R}{P_L P'_R + P'_L P_R} - \frac{P'_L P_R}{P_L P'_R + P'_L P_R} \log_2 \frac{P'_L P_R}{P_L P'_R + P'_L P_R}. \quad (3.3)$$

It can be shown that it coincides with the entanglement of formation of the state (see Supp. Mat. of [34])

$$|\Psi_{\mathrm{LR}}\rangle = \frac{lr' \,|\mathrm{L}\uparrow, \mathrm{R}\downarrow\rangle + \eta r l' \,|\mathrm{L}\downarrow \mathrm{R}\uparrow\rangle}{\sqrt{|lr'|^2 + |rl'|^2}}, \quad (3.4)$$

where η is 1 for bosons and -1 for fermions, conditionally obtained projecting $|\Psi\rangle$ in the subspace spanned by the basis $\mathcal{B}_{LR} = \{|\mathrm{L}\sigma, \mathrm{R}\tau\rangle\,; \sigma, \tau = \downarrow, \uparrow\}$. This state is the distributed resource state between $\mathcal{L}$ and $\mathcal{R}$[2]. The entanglement coming from Eq.(3.3) has been analysed in function of the spatial overlap of the two wave functions ψ and ψ'. If their square moduli do not share a common region of space (no spatial overlap), $E_{\mathrm{L}\mathcal{R}}(\Psi) = 0$. As an example consider the case in which ψ is localized in $\mathcal{L}$ and ψ' in $\mathcal{R}$: thus $P'_{\mathrm{L}} = P_{\mathrm{R}} = 0$ and the resource state of Eq. (3.4) becomes $|\Psi_{\mathrm{LR}}\rangle = |\mathrm{L}\uparrow, \mathrm{R}\downarrow\rangle$, that under the chosen framework can be written as a separable state $|\Psi_{\mathrm{LR}}\rangle = |\mathrm{L}\uparrow\rangle \otimes |\mathrm{R}\downarrow\rangle$, since particles are spatially addressable and so distinguishable (like NIP).

If ψ and ψ' partially overlap and one or both the spatial regions $\mathcal{L}$ and $\mathcal{R}$ are outside the overlap region, the framework does not allow to make it emerge the effects due to the spatial indistinguishability of particles and the result is analogous to the case of no spatial overlap.

[2]If the two particles have the same pseudospin and so $|\Psi\rangle = |\psi\sigma, \psi'\sigma\rangle$, the state obtained after the projection onto the chosen operational subspace is always unentangled, in fact it is $|\Psi_{\mathrm{LR}}\rangle = |\mathrm{L}\sigma, \mathrm{R}\tau\rangle$, even if particles completely spatially overlap.

On the other hand, if $\mathcal{L}$ and $\mathcal{R}$ are both in the overlap region, a certain amount of entanglement associated to the state of Eq. (3.4) and quantified by Eq. (3.3) is conditionally obtained with a probability $P_{\rm LR} = |lr'|^2 + |rl'|^2$.

Finally, if ψ and ψ' completely overlap, i.e. when the spatial region in which the two particles can be found with nonzero probabilities is the same, it is evident from Eq. (3.3) that there is always a certain amount of entanglement. The latter reachs the maximum value $E_{\rm LR}(\Psi) = 1$ when $P_L = P'_L$ and $P_R = P'_R$, with a probability $P_{\rm LR} = 2P_{\rm L}P_{\rm R}$. This probability is maximum ($P_{\rm LR} = 1/2$) when $P_{\rm L} = P_{\rm R} = 1/2$.

The entanglement quantified by Eq. (3.3), as I have shown, is strictly due to the particle indistinguishability coming from the spatial overlap of single-particle wave functions. The sLOCC operational framework naturally suggests the introduction, from an experimental perspective, of a figure of merit for the exploitable entanglement of identical particles given by $E_{\rm exp} := E_{LR}P_{LR}$.

We now use the pseudospin observable $\mathcal{O}_S := \mathbf{O}_S \cdot \boldsymbol{\sigma}_S$ ($S = L, R$) with eigenvalues ± 1, where $\mathbf{O}_S$ is the unit vector in an arbitrary direction in the spin space and $\boldsymbol{\sigma}_S = (\sigma_x^S, \sigma_y^S, \sigma_z^S)$ is the Pauli matrices vector. The CHSH-Bell inequality [77] in this context is

$$\mathcal{B}(\rho_{LR}) = |\langle \mathcal{O}_L \mathcal{O}_R \rangle + \langle \mathcal{O}_L \mathcal{O}'_R \rangle + \langle \mathcal{O}'_L \mathcal{O}_R \rangle - \langle \mathcal{O}'_L \mathcal{O}'_R \rangle| \leq 2, \tag{3.5}$$

where $\mathcal{B}(\rho_{LR})$ is the Bell function expressed in terms of the correlation functions of the pseudospin observables and $\mathcal{O}'_S$ indicates the measurement in a direction different from that of $\mathcal{O}_S$ [33]. The maximum value of the Bell function $\mathcal{B}_{\rm max}$ in terms of the concurrence (entanglement) [78, 64] of the state $|\Psi_{\rm LR}\rangle$ is [39]

$$\mathcal{B}_{\rm max} = 2\sqrt{1 + C(\Psi_{LR})^2} = 2\sqrt{1 + \left(\frac{2|lr'l'r|}{P_{LR}}\right)^2}, \tag{3.6}$$

where I have used the explicit expression of $C(\Psi_{LR})$. We have obtained $\mathcal{B}_{\rm max}(\rho_{LR}) > 2$ when $C(\Psi_{LR}) > 0$, i.e. whenever there is spatial overlap between ψ and ψ' and the local measurements are performed inside the overlap region (that is, all the four probability amplitudes l, l', r, r' are nonzero). The violation of the CHSH-Bell inequality identifies the presence of nonlocal correlations between the pseudospin outcomes in the regions $\mathcal{L}$ and $\mathcal{R}$.

Therefore, spatial overlap between wave functions associated to independently prepared IP can generate nonlocality effects which can be tested in quantum optical scenarios [79].

In the next Chapters, I will show that this correlations and nonlocal effects are physical, in the sense that they can be used to operationally implement both theoretically and experimentally quantum information tasks.

3.4 Concurrence of a mixed state of two identical particles

In Section 3.3 I have shown how the sLOCC framework gives us the possibility to quantify the entanglement of two independently prepared IP in a pure state. I now generalize our treatment to the case of a generic mixed state of two IP.

The entanglement of formation known for NIP [80] can be straightforwardly redefined to the case of IP, thanks to the same sLOCC framework presented in Section 3.3.

Consider, as before, two identical qubits, with spatial wave functions $\psi = \psi_1$ and $\psi' = \psi_2$, for which one desires to characterize the entanglement between the pseudospins. The density matrix of an arbitrary state of the two identical qubits can be written as

$$\rho = \sum_{\sigma_1,\sigma_2,\sigma_1',\sigma_2'=\downarrow,\uparrow} p_{\sigma_1\sigma_2}^{\sigma_1',\sigma_2'} \left|\psi_1\sigma_1, \psi_2\sigma_2\right\rangle \left\langle\psi_1\sigma_1', \psi_2\sigma_2'\right| / \mathcal{N}, \tag{3.7}$$

where $\mathcal{N}$ is a normalization constant. Projecting ρ onto the (operational) subspace spanned by the computational basis $\mathcal{B}_{\mathrm{LR}} = \{|\mathrm{L}\uparrow, \mathrm{R}\uparrow\rangle, |\mathrm{L}\uparrow, \mathrm{R}\downarrow\rangle, |\mathrm{L}\downarrow, \mathrm{R}\uparrow\rangle, |\mathrm{L}\downarrow, \mathrm{R}\downarrow\rangle\}$ by the projector

$$\Pi_{\mathrm{LR}}^{(2)} = \sum_{\tau_1,\tau_2=\uparrow,\downarrow} |\mathrm{L}\tau_1, \mathrm{R}\tau_2\rangle \langle \mathrm{L}\tau_1, \mathrm{R}\tau_2|, \tag{3.8}$$

one gets the distributed resource state

$$\rho_{\mathrm{LR}} = \Pi_{\mathrm{LR}}^{(2)} \rho \Pi_{\mathrm{LR}}^{(2)} / \mathrm{Tr}(\Pi_{\mathrm{LR}}^{(2)} \rho), \tag{3.9}$$

with probability $P_{\mathrm{LR}} = \mathrm{Tr}(\Pi_{\mathrm{LR}}^{(2)}\rho)$. The trace operation must clearly be performed in the LR-subspace. The state ρ_{LR}, containing one particle in $|\mathrm{L}\rangle$ and one particle in $|\mathrm{R}\rangle$, is the exploitable distributed resource state for quantum information tasks and can be diagonalized as $\rho_{\mathrm{LR}} = \sum_i p_i |\Psi_i^{\mathrm{LR}}\rangle \langle\Psi_i^{\mathrm{LR}}|$, where p_i is the weight of each pure state $|\Psi_i^{\mathrm{LR}}\rangle$ which is in general unseparable. Entanglement of formation of ρ_{LR} is as usual [81] $E_f(\rho_{\mathrm{LR}}) = \min \sum_i p_i E(|\Psi_i^{\mathrm{LR}}\rangle)$, where minimization occurs over all the decompositions of ρ_{LR} and $E(\Psi_i^{\mathrm{LR}})$ is the entanglement of the pure state $|\Psi_i^{\mathrm{LR}}\rangle$. We thus define the operational entanglement $E_{\mathrm{LR}}(\rho)$ of the original state ρ obtained by sLOCC as the entanglement of formation of ρ_{LR}, that is

$$E_{\mathrm{LR}}(\rho) := E_f(\rho_{\mathrm{LR}}). \tag{3.10}$$

We can conveniently quantify the entanglement of formation $E_f(\rho_{\mathrm{LR}})$ by the concurrence $C(\rho_{\mathrm{LR}})$, according to the well-known relation $E_f = h[(1 + \sqrt{1 - C^2})/2]$ [82, 80], in which $h(x) = -x \log_2 x - (1 - x) \log_2(1 - x)$. The IP-concurrence $C_{\mathrm{LR}}(\rho)$ in the sLOCC framework can be

easily introduced by

$$C_{\mathrm{LR}}(\rho) := C(\rho_{\mathrm{LR}}) = \max\{0, \sqrt{\lambda_4} - \sqrt{\lambda_3} - \sqrt{\lambda_2} - \sqrt{\lambda_1}\}, \tag{3.11}$$

where λ_i are the eigenvalues, in decreasing order, of the non-Hermitian matrix $R = \rho_{\mathrm{LR}}\tilde{\rho}_{\mathrm{LR}}$, being $\tilde{\rho}_{\mathrm{LR}} = \sigma_y^{\mathrm{L}} \otimes \sigma_y^{\mathrm{R}} \rho_{\mathrm{LR}}^* \sigma_y^{\mathrm{L}} \otimes \sigma_y^{\mathrm{R}}$ with localized Pauli matrices $\sigma_y^{\mathrm{L}} = |\mathrm{L}\rangle\langle\mathrm{L}| \otimes \sigma_y$, $\sigma_y^{\mathrm{R}} = |\mathrm{R}\rangle\langle\mathrm{R}| \otimes \sigma_y$. I remark that the tensor product in $\sigma_y^{\mathrm{L}} \otimes \sigma_y^{\mathrm{R}}$ is allowed by the chosen framework in which $|\mathrm{L}\rangle$ and $|\mathrm{R}\rangle$ are two spatially separated states, thus the procedure to obtain the non-Hermitian matrix R is analogous to the one for NIP [83]. The entanglement quantifier of ρ so obtained contains all the information about spatial indistinguishability, due to the spatial overlap, and statistics (bosons or fermions) of the particles.

As I have shown in this section and in the previous one, entanglement of IP is strictly linked to the spatial overlap of the single-particle wave functions and so to the spatial indistinguishability with respect to specific set of measurements. In order to bring our results to a more fundamental level, a measure of the degree of spatial indistinguishability has been introduced and I will present it in the following section [69].

3.5 Entropic measure of spatial indistinguishability

Identity of particles is a yes or not property both in classical and quantum mechanics. In the literature the terms "identical" and "indistinguishable" are generally used as synonymous [84, 26, 43]. However, as I have shown, IP can be distinguishable under certain measurements, behaving like NIP. In other words, quantum mechanically, to IP it can be attributed the further property of indistinguishability, associated to a specific set of quantum measurements, differently from identity that is an intrinsic property of the system. And it is to indistinguishability, not to identity by itself, that the effects of bosonic and fermionic statistics is attributed. In fact, as an example, no bosonic behavior is associated to two independently prepared and spatially separated identical photons, although identical, under sLOCC (distinguishable photons).

With respect to the set of measurements, it seems natural to define a continuous degree of indistinguishability, quantifying how much the measurement process can distinguish the particles. In this section, I deal with this aspect that has been developed within sLOCC. For simplicity, the treatment shall be presented for pure states, but it is also valid for mixed states.

Consider a N IP elementary pure state $|\Psi^{(N)}\rangle = |\chi_1, \chi_2, ..., \chi_N\rangle$, where $|\chi_i\rangle$ is the i-th single-particle state. Each $|\chi_i\rangle$ is characterized by the set of values $\chi_i = \chi_i^a, \chi_i^b, \ldots, \chi_i^n$ corresponding to a complete set of commuting observables $\hat{a}, \hat{b}, \ldots, \hat{n}$. For example, if $\hat{a}$ describes the spatial distribution of the single-particle states, χ_i^a is a spatial wavefunction ψ_i. The N-particle degree of indistinguishability is expected to depend both on their quantum state and the

measurement performed on the system. To define a suitable class of measurements, I take the N-particle state

$$|\alpha\beta\rangle_N := |\alpha_1\beta_1, \alpha_2\beta_2, \ldots, \alpha_N\beta_N\rangle\,, \tag{3.12}$$

where the i-th single-particle state $|\alpha_i\beta_i\rangle$ is characterized by a subset $\hat{a}, \hat{b}, \ldots, \hat{j}$ of the $\hat{a}, \hat{b}, \ldots, \hat{n}$ commuting observables with eigenvalues $\alpha_i = \alpha_i^a, \alpha_i^b, \ldots, \alpha_i^j$, and by the remaining observables $\hat{k}, \ldots, \hat{n}$ with eigenvalues $\beta_i = \beta_i^k, \ldots, \beta_i^n$. In the first member of Eq. (3.12) I have set $\alpha = \{\alpha_1, ..., \alpha_N\}$ and $\beta = \{\beta_1, ..., \beta_N\}$. The N-particle projector on outcomes (α, β) of the complete set of observables is $\Pi_{\alpha\beta}^{(N)} = |\alpha\beta\rangle_N \langle\alpha\beta|$, while the projector on outcomes α of the partial set of observables is

$$\Pi_\alpha^{(N)} = \sum_\beta \Pi_{\alpha\beta}^{(N)}. \tag{3.13}$$

Within the sLOCC framework, I can quantify to which extent particles in the state $|\Psi^{(N)}\rangle$ can be distinguished by knowing the results α of the local measurements described by $\Pi_\alpha^{(N)}$ of Eq. (3.13), considering that single-particle spatial wave functions $\{\psi_i\}$ can overlap (Fig. 3.1). The (sLOCC) measurements have to satisfy the following properties: 1) the N single-particle states $\{|\alpha_i\beta_i\rangle\}$ are peaked in separated spatial regions $\{\mathcal{R}_i\}$ (Fig. 3.1); 2) $\langle\Psi^{(N)}|\Pi_\alpha^{(N)}|\Psi^{(N)}\rangle \neq 0$, i.e. the probability of obtaining the projected state must be different from zero.
I indicate with $P_{\alpha_i\chi_j}$ the single-particle probability that the result α_i comes from the state $|\chi_j\rangle$. I then define the joint probability $P_{\alpha\mathcal{P}} := P_{\alpha_1\chi_{p_1}} P_{\alpha_2\chi_{p_2}} \cdots P_{\alpha_N\chi_{p_N}}$, where $\mathcal{P} = \{p_1, p_2, ..., p_N\}$ is one of the $N!$ permutations of the N single-particle states $\{|\chi_i\rangle\}$. Notice that $P_{\alpha\mathcal{P}}$ can be nonzero for each of the $N!$ permutations, since in general the outcome α_i can come from any of the single-particle state $|\chi_j\rangle$. The quantity $\mathcal{Z} = \sum_\mathcal{P} P_{\alpha\mathcal{P}}$ thus accounts for this no which-way effect concerning the probabilities. The amount of the no-which way information, emerging from the outcomes α of the measurement $\Pi_\alpha^{(N)}$, is a measure of the indistinguishability of the particles in the state $|\Psi^{(N)}\rangle$. Using $P_{\alpha\mathcal{P}}$ and $\mathcal{Z}$, that enclose the essence of this lack of information, the following entropic measure of the indistinguishability degree has been introduced

$$\mathcal{I}_\alpha := -\sum_\mathcal{P} \frac{P_{\alpha\mathcal{P}}}{\mathcal{Z}} \log_2 \frac{P_{\alpha\mathcal{P}}}{\mathcal{Z}}. \tag{3.14}$$

This quantity depends on measurements performed on the state. If the particles are initially all spatially separated, each in a different measurement region, only one permutation remains and $\mathcal{I}_\alpha = 0$: I have complete knowledge on the single-particle state $|\chi_j\rangle$ which gives the outcome α_i, meaning that the particles are distinguishable with respect to the measurement $\Pi_\alpha^{(N)}$. On the other hand, if for each pair $p_i \in \mathcal{P}$ and $p_i' \in \mathcal{P}' \neq \mathcal{P}$ one has $P_{\alpha_i\chi_{p_i}} = P_{\alpha_i\chi_{p_i'}}$, indistinguishability is maximum and reaches the value $\mathcal{I}_\alpha = \log_2 N!$. We now apply the previous theory to a two-particle system.
Consider the state of two identical qubits $|\Psi^{(2)}\rangle = |\chi_1, \chi_2\rangle = |\psi_1\sigma_1, \psi_2\sigma_2\rangle$, where ψ_i $(i = 1, 2)$

is the spatial degree of freedom (wave function) and σ_i is the internal degree of freedom (pseudospin, basis $\{\uparrow, \downarrow\}$). In general, $|\psi_1\rangle$ and $|\psi_2\rangle$ can spatially overlap. To quantify the degree of spatial indistinguishability, I perform a measurement of the form of Eq. (3.13), where α are only the spatial degrees of freedom. I choose two spatial regions $\mathcal{L}$ and $\mathcal{R}$ satisfying the Properties 1. and 2. presented in Section 3.2. So, spatially localized measurements are performed by the projector $\Pi^{(2)}_{\mathrm{LR}}$ of Eq. (3.8). Calling $P_{\mathrm{X}\psi_{\mathrm{i}}} = |\langle \mathrm{X}|\psi_i\rangle|^2$ ($\mathrm{X} = \mathrm{L}, \mathrm{R}$ and $i = 1, 2$) the probability of finding in $|X\rangle$ the particle coming from $|\psi_i\rangle$, the measure of the spatial indistinguishability of the particles is quantified, from Eq.(3.14), as

$$\begin{aligned}\mathcal{I}_{\mathrm{LR}} = &- \frac{P_{\mathrm{L}\psi_1} P_{\mathrm{R}\psi_2}}{\mathcal{Z}} \log_2 \frac{P_{\mathrm{L}\psi_1} P_{\mathrm{R}\psi_2}}{\mathcal{Z}} \\ &- \frac{P_{\mathrm{L}\psi_2} P_{\mathrm{R}\psi_1}}{\mathcal{Z}} \log_2 \frac{P_{\mathrm{L}\psi_2} P_{\mathrm{R}\psi_1}}{\mathcal{Z}},\end{aligned} \tag{3.15}$$

where $\mathcal{Z} = P_{\mathrm{L}\psi_1} P_{\mathrm{R}\psi_2} + P_{\mathrm{L}\psi_2} P_{\mathrm{R}\psi_1}$. In general, $0 \leq \mathcal{I}_{\mathrm{LR}} \leq 1$. If particles do not spatially overlap, I have maximal information and $\mathcal{I}_{\mathrm{LR}} = 0$. It's the same if particles spatially overlap but one of the two spatial regions, for example $\mathcal{L}$, of the chosen framework is out of the overlap region: in this case, performing a measurement in $\mathcal{L}$ only one of the two particles has nonzero probability to be detected and it is so spatially distinguishable from the other. $\mathcal{I}$ attains 1 when $P_{\mathrm{L}\psi_2} = P_{\mathrm{L}\psi_1}$ and $P_{\mathrm{R}\psi_2} = P_{\mathrm{R}\psi_1}$: there is no information about the origin of the two particles found in $\mathcal{L}$ and $\mathcal{R}$.

3.6 Discussions

In this Chapter, the generalization to a number N of IP of the well known LOCC-framework for NIP has been introduced. This substitutes, because of the unaddressability of IP, the concept of particle-locality (as used in LOCC) with the one of space-locality (in the same spirit of quantum field theory). In fact, within sLOCC single-particle measurements address spatial regions occupied by IP, contrary to what happens for NIP in which are the particles which are addressed. This gives the possibility of identifying and quantifying the effect played by IP spatial overlap in the emergence of the operationally exploitable entanglement in a Bell-like scenario. Concurrence and entanglement of formation have been defined for an arbitrary pure or mixed state of two identical qubits, generalizing the methods known for NIP by means of the sLOCC framework and showing explicitly that entanglement depends on spatial overlap between single-particle wave functions.

In this Chapter I have introduced the difference between *identity* and *indistinguishability* of IP in quantum mechanics, in contrast to what happens in the standard quantum mechanical approach where they are considered synonyms. Not having realized this difference is what causes, in the label-based standard approach, some of the formal mock effects of particle statistics in

systems of physically distinguishable IP (e.g. when they are independently prepared and space-like separated). I have defined the continuous degree of spatial indistinguishability of IP by an entropic measure of information, showing that it is not an intrinsic property of IP systems (contrary to identity), but a measurement-dependent one. This achievement entails a continuous quantitative identification of indistinguishability as an informational resource. Hence, one can evaluate the amount of operational entanglement exploitable by sLOCC under general conditions of indistinguishability and state mixedness.

Part II

Consequences of indistinguishability: concepts and applications

Chapter 4

Quantum teleportation activated by experimentally tailored indistinguishability

4.1 Introduction

In this Chapter, I will present a conceptual setup to control the degree of spatial indistinguishability (Chapter 3) of two identical particles (IP) in the framework of spatially localized operations and classical communication (sLOCC). Then I will show the experiment implemented in order to achieve the following goals: (i) tune the indistinguishability of two initially uncorrelated photons by the tailoring their spatial overlap, (ii) activation of a nonlocal entanglement, in two well separated regions of space, only by spatial indistinguishability and (iii) implementation of the teleportation of the state of a third photon, distinguishable from the others, exploiting the entanglement due to indistinguishability.

4.2 Theory

4.2.1 Preparation of the system

Consider a system of two identical qubits with opposite pseudospins in the state

$$|\Psi\rangle = |\psi \uparrow, \psi' \downarrow\rangle \,. \tag{4.1}$$

In order to verify the presence of indistinguishability-enabled correlations within a Bell-like scenario of separate locations, consider the specific case in which the wave function of each particle is a superposition of two specific bound states, $|\mathrm{L}\rangle$ and $|\mathrm{R}\rangle$, peaked in correspondence

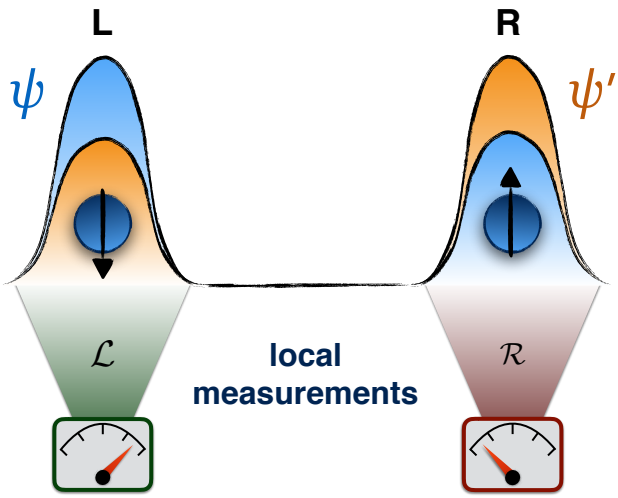

Figure 4.1: System of two completely overlapping identical particles, one with wave function ψ and pseudospin $\uparrow$, the other with wave function ψ' and pseudospin $\downarrow$ [34].

of two separated spatial regions $\mathcal{L}$ and $\mathcal{R}$ (Fig.4.1), respectively, that is

$$\begin{aligned} |\psi\rangle &= l\,|\mathrm{L}\rangle + r\,|\mathrm{R}\rangle\,, \\ |\psi'\rangle &= l'\,|\mathrm{L}\rangle + r'\,|\mathrm{R}\rangle\,, \end{aligned} \tag{4.2}$$

with $|l|^2 + |r|^2 = |l'|^2 + |r'|^2 = 1$. Using Eq.(4.2), the global state $|\Psi\rangle$ of Eq. (4.1) can be expanded as

$$|\Psi\rangle = ll'\,|\mathrm{L}\uparrow, \mathrm{L}\downarrow\rangle + rr'\,|\mathrm{R}\uparrow, \mathrm{R}\downarrow\rangle + \sqrt{P_{\mathrm{LR}}}\,|\Psi_{\mathrm{LR}}\rangle\,, \tag{4.3}$$

where $|\Psi_{\mathrm{LR}}\rangle$ is the distributed resource state of Eq.(3.4), whose explicit expression is

$$|\Psi_{\mathrm{LR}}\rangle = \frac{lr'\,|\mathrm{L}\uparrow, \mathrm{R}\downarrow\rangle + \eta rl'\,|\mathrm{L}\downarrow, \mathrm{R}\uparrow\rangle}{\sqrt{|lr'|^2 + |rl'|^2}}, \tag{4.4}$$

in which η is 1 for bosons and -1 for fermions. As I have shown in Section 3.3, the spatial overlap of the two particles, depending on the probabilities with which they occupy the same spatial regions, directly influences their entanglement [34]. Operating in the sLOCC framework, by choosing the two spatial regions $\mathcal{L}$ and $\mathcal{R}$ to perform single-particle local measurements, the state $|\Psi_{\mathrm{LR}}\rangle$ can be obtained from $|\Psi\rangle$ with a probability $P_{\mathrm{LR}} = |lr'|^2 + |l'r|^2$. In order to exploit the effects of particle indistinguishability in the chosen framework, each region has to be occupied by at least one particle (second property of the sLOCC framework, presented in Section 3.2), so the cases $l = l' = 1$ ($|\Psi\rangle = |\mathrm{L}\uparrow, \mathrm{L}\downarrow\rangle$) and $l = l' = 0$ ($|\Psi\rangle = |\mathrm{R}\uparrow, \mathrm{R}\downarrow\rangle$) are excluded. I here recall the indistinguishability degree introduced in Eq. (3.15) of Section (3.5)

$$\mathcal{I} = -\sum_{i}^{2} p_{\mathrm{LR}}^{(i)} \log_2 p_{\mathrm{LR}}^{(i)}, \tag{4.5}$$

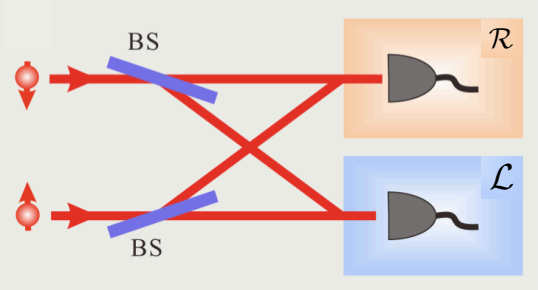

Figure 4.2: The simplest setup thought to produce entanglement by sLOCC due to spatial indistinguishability.

where $p_{\rm LR}^{(1)} = |lr'|^2/(|lr'|^2 + |l'r|^2)$ and $p_{\rm LR}^{(2)} = 1 - p_{\rm LR}^{(1)}$. This measure differs from zero only when the two wave functions spatially overlap in both measurement regions ($0 < |l|, |l'| < 1$), reaching the maximum ($\mathcal{I} = 1$) for complete overlap ($|l|^2 = |l'|^2$, which implies $|r|^2 = |r'|^2$).

To implement this theoretical scenario, we have proposed a neat conceptual scheme with polarized photons illustrated in Figure 4.2. Two initially-uncorrelated photons are created, one with polarization $\uparrow$ and one with $\downarrow$. Each photon is then spread in a controllable manner by a beam-splitter (BS) towards two separated locations $\mathcal{L}$ and $\mathcal{R}$, where single-photon measurements are simultaneously performed by sLOCC. This scheme can be seen as a modified version of the Hanbury Brown and Twiss (HBT) experiment [40, 85]: the relevant difference consists in initially polarizing the photons and in controlling their spatial wave functions. It allows us to establish the direct connection between the amount of entanglement and the degree of photon spatial indistinguishability.

In the next section, I will show that the indistinguishability-enabled entanglement present in the distributed resource state $|\Psi_{\rm LR}\rangle$ has a physical operational role, since it can be used to implement quantum teleportation.

4.2.2 Teleportation by means of indistinguishability-enabled entanglement

In order to implement a quantum teleportation protocol [20, 86], it is useful to exploit the maximal operational entanglement achievable from the state of Eq.(4.3) with the highest probability. For instance, by choosing $|\psi\rangle = |\psi'\rangle = (|{\rm L}\rangle + |{\rm R}\rangle)/\sqrt{2}$, the distributed resource state, available with probability $P_{\rm LR}^{\rm max} = 1/2$, is the maximally entangled Bell state

$$|\Psi_{\rm LR}^{\rm max}\rangle = (|{\rm L}\uparrow, {\rm R}\downarrow\rangle + \eta\,|{\rm L}\downarrow, {\rm R}\uparrow\rangle)/\sqrt{2}. \tag{4.6}$$

In the same laboratory where the site $\mathcal{L}$ is, a third particle is prepared with an arbitrary pseudospin. This third particle is distinguishable from the others for being either of a different species, independently from its spatial overlap with them, or identical but spatially separated

from the other particles and its state can be written as $|\varphi\rangle_{\rm d} = a\,|{\rm L}'\uparrow\rangle_{\rm d} + b\,|{\rm L}'\downarrow\rangle_{\rm d}$, where $|{\rm L}'\rangle$ is localized in a site accessible together with $\mathcal{L}$ yet separated from the latter and the subscript "d" stands for "distinguishable". After having obtained the state $|\Psi_{\rm LR}^{\rm max}\rangle$ of Eq. (4.6), the global state of the three particles can be written as

$$\frac{1}{2}\left[|1_{\rm L'L}^{(\eta)}\rangle\,\mathbb{1}_{\rm R} + |1_{\rm L'L}^{(-\eta)}\rangle\,\sigma_z^{\rm R} + |2_{\rm L'L}^{(\eta)}\rangle\,\sigma_x^{\rm R} + |2_{\rm L'L}^{(-\eta)}\rangle\,(-i)\sigma_y^{\rm R}\right]|\varphi_{\rm R}\rangle\,, \tag{4.7}$$

where

$$\begin{aligned} |1_{\rm L'L}^{(\eta)}\rangle &= (|{\rm L}'\uparrow\rangle_{\rm d}\,|{\rm L}\downarrow\rangle + \eta\,|{\rm L}'\downarrow\rangle_{\rm d}\,|{\rm L}\uparrow\rangle)/\sqrt{2}, \\ |2_{\rm L'L}^{(\eta)}\rangle &= (|{\rm L}'\uparrow\rangle_{\rm d}\,|{\rm L}\uparrow\rangle + \eta\,|{\rm L}'\downarrow\rangle_{\rm d}\,|{\rm L}\downarrow\rangle)/\sqrt{2}, \end{aligned} \tag{4.8}$$

are the Bell states between the particle "d" and one of the two IP (1 and 2 in the kets indicate the number of excited spins in the Bell states), $\mathbb{1}_{\rm R}$ is the identity operator in $\mathcal{R}$, $\sigma_i^{\rm R}$ $(i = x, y, z)$ are the Pauli matrices and $|\varphi\rangle_{\rm R} = a\,|{\rm R}\uparrow\rangle + b\,|{\rm R}\downarrow\rangle$ is the target state teleported in the region $\mathcal{R}$. Eq.(4.7) has the structure of the standard teleportation protocol [20]. The implementation of the latter, starting from the initial state $|\Psi\rangle$ and exploiting the resource state $|\Psi_{\rm LR}^{\rm max}\rangle$, succeeds with probability $P_{\rm LR}^{\rm max}$ and follows the standard recipe [20]: (i) Luna in the laboratory containing $\mathcal{L}'$ and $\mathcal{L}$ performs the Bell measurements and (ii) communicates the outcomes to Rudy placed in $\mathcal{R}$ who (iii) performs a given operation. If Luna counts either zero or two particles in $\mathcal{L}$, she tells Rudy to reject the procedure; in the other cases, Luna communicates the outcome ($|\Psi_{\rm L'L}^{(\eta)}\rangle$, $|\Phi_{\rm L'L}^{(\eta)}\rangle$, $|\Phi_{\rm L'L}^{(-\eta)}\rangle$, $|\Psi_{\rm L'L}^{(-\eta)}\rangle$) to Rudy who makes a corresponding operation ($\mathbb{1}_{\rm R}$, $\sigma_x^{\rm R}$, $\sigma_y^{\rm R}$, $\sigma_z^{\rm R}$) to transform the state of its particle into the desired one. This teleportation protocol, although conditional, is purely quantum since it beats the classical teleportation fidelity threshold $2/3$ [64]. *The teleportation mechanism here described basically differs from previous ones using identical particles, based on entangled particle number states* [30, 87].

4.3 Experiment

4.3.1 Preparation of the system: experimental setup

An experiment proving that two initially independent photons become entangled only to their spatial indistinguishability has been implemented in an all-optical setup (Fig.4.3(a)) at the CAS Key Laboratory of Quantum Information of Hefei (China) by the group of Guang-Can Guo, reproducing the theoretical scheme presented in Fig.4.2 and quantitatively showing the dependence of entanglement on the spatial indistinguishability degree of Eq. (4.5).

The first purpose is the preparation of the state $|\Psi_{\rm prep}\rangle = |\psi H, \psi' V\rangle$, where H ($\uparrow$) and V($\downarrow$) denote, respectively, the horizontal and vertical polarization of photons. I now present the setup.

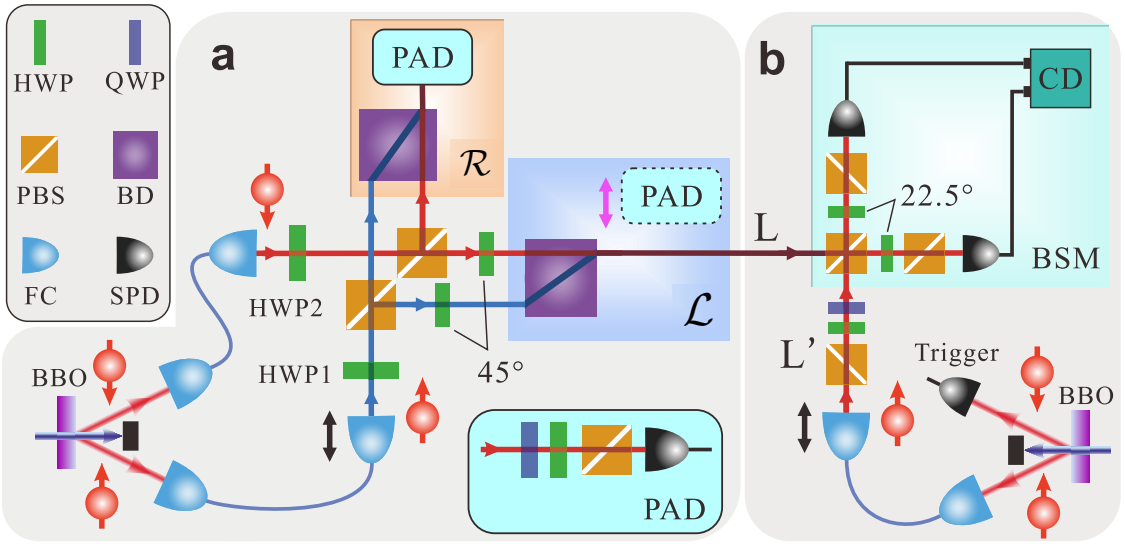

Figure 4.3: **Experimental setup.** (**a.**) **State preparation**. Two initially-uncorrelated photons from a BBO crystal with polarization H ($\uparrow$) and V ($\downarrow$), respectively, are collected separately by two single-mode fibers via fiber couplers (FCs). A BS for each photon is realized by the sequence of a half-wave plate (HWP1, HWP2), a polarization beam splitter (PBS) and a final HWP at $45°$ placed before $\mathcal{L}$, which leaves the initial polarization of each photon unchanged. The spatial degrees of freedom ψ and ψ' in which the photons share the same wavelength are marked as the blue and red colors, respectively, to differentiate. In each region $\mathcal{L}$ and $\mathcal{R}$, one beam displacer (BD) is used to combine two paths of photons. The inset displays the unit of polarization analysis detection (PAD) at the final detection placed in $\mathcal{L}$ and $\mathcal{R}$, consisting of a quarter-wave plate (QWP), a HWP and a PBS before the single photon detector (SPD). (**b.**) **Experimental illustration of quantum teleportation**. The photons in $\mathcal{L}$ are sent to perform the Bell state measurement (BSM) and meanwhile the PAD here which is marked by the dashed frame is removed. One of the photon pair generated by pumping another BBO is prepared as the state to be teleported, while the other photon detected directly is treated as the trigger signal. BSM is implemented with a PBS followed by two HWPs at $22.5°$ and PBSs. The signals from two SPDs are processed by a CD to coincide with the signals from $\mathcal{R}$ and trigger.

Pumping by pulsed ultraviolet light at 400 nm a BBO (beta-barium borate) crystal, two photons are emitted (with wavelength 800 nm) via type II spontaneous parametric down conversion (SPDC) with initial polarization H and V, respectively, and then collected into single-mode fibers.

At first, their identity has been characterized by performing the two-photon interference and using the visibility of the Hong Ou-Mandel (HOM) dip (the set up for the HOM experiment and the dip are shown in Fig. 4.4(a) and (b), respectively). Here one obtained a visibility $\nu = 97.7\%$, clearly revealing the indistinguishability of the employed operational photons.

Moreover it has been verified with a very high fidelity of $(99.9 \pm 0.1)\%$ that photons are initially completely uncorrelated in the product state $|H\rangle \otimes |V\rangle$ (Fig. 4.4(c)).

The state $|\Psi_{\text{prep}}\rangle$ is prepared by adjusting the spatial degrees of freedom $|\psi\rangle$ and $|\psi'\rangle$ by a sequence of a half-wave plate (HWP), a polarizing beam-splitter (PBS) and a final HWP at $45°$ before the location $\mathcal{L}$. Notice that the setup is devised in such a way that all the optical elements independently act on a single photon (Fig 4.3(a)). The operation of HWP on photon polarization with an angle θ compared with the optical axis could be written as $\begin{pmatrix} \cos 2\theta & \sin 2\theta \\ \sin 2\theta & -\cos 2\theta \end{pmatrix}$. By setting HWP1 at $(\pi/2 - \alpha)/2$, the photon in $|\psi\rangle$ with polarization $|H\rangle$ ($\uparrow$) changes to $\sin\alpha\ |H\rangle + \cos\alpha\ |V\rangle$. As the PBS transmits $|H\rangle$ polarization and reflects $|V\rangle$ polarization, I have $|V\rangle$ before $\mathcal{L}$ which should be $|H\rangle$. Thus, here, a HWP at $45°$ is used to flip $|V\rangle$ to $|H\rangle$. Now, $|\psi, H\rangle$ is prepared to be $|\psi, H\rangle = \cos\alpha\ |\mathrm{L}H\rangle + \sin\alpha\ |\mathrm{R}H\rangle$. Following the same

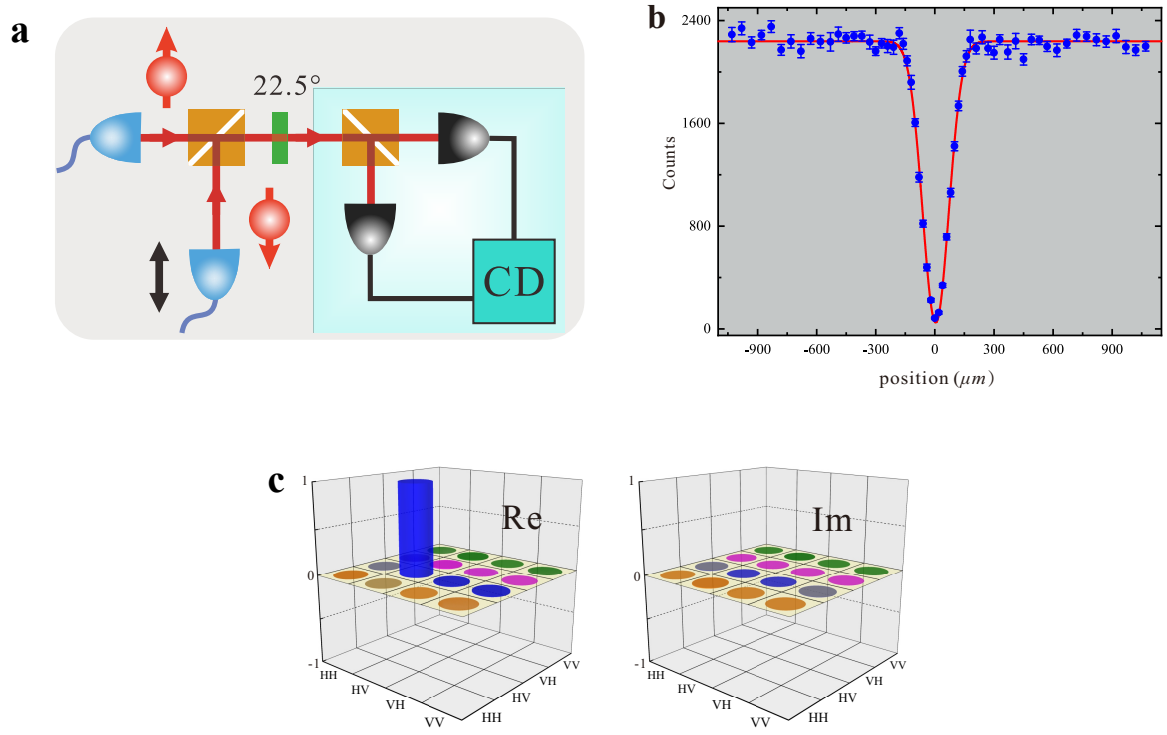

Figure 4.4: (**a**) **Experimental illustration of HOM measurement**. The first polarization beam splitter (PBS) combines two photons which are in the polarization H ($\uparrow$) and V ($\downarrow$), respectively. One photon is placed on a movable stage to scan the position. The photons are detected by two single photon detectors (SPD) after a half-wave plate (HWP) at $22.5°$ and a second PBS. The coincidence device analyzes the signals from two SPDs and outputs the coincidence counting. (**b**) **The HOM dip of the two-photon interference.** The counts are obtained in 5 seconds with the pumping power 30 mW. The blue dots are the experimental results. The red curve represents the fitting Gaussian function $G_x = a(1 - d\ e^{-b(x-c)^2})$ (parameters $a,\ b,\ c$ and d are determined from the fit) and the visibility of HOM dip is defined as $\nu = (G_{max} - G_{min})/G_{max}$. (**c**) **Experimental tomography of the initial state** $|H\rangle \otimes |V\rangle$ of the two photons from BBO crystal with a high fidelity $(99.9 \pm 0.1)\%$. Two subgraphs show the real and imaginary parts of the density matrix, respectively.

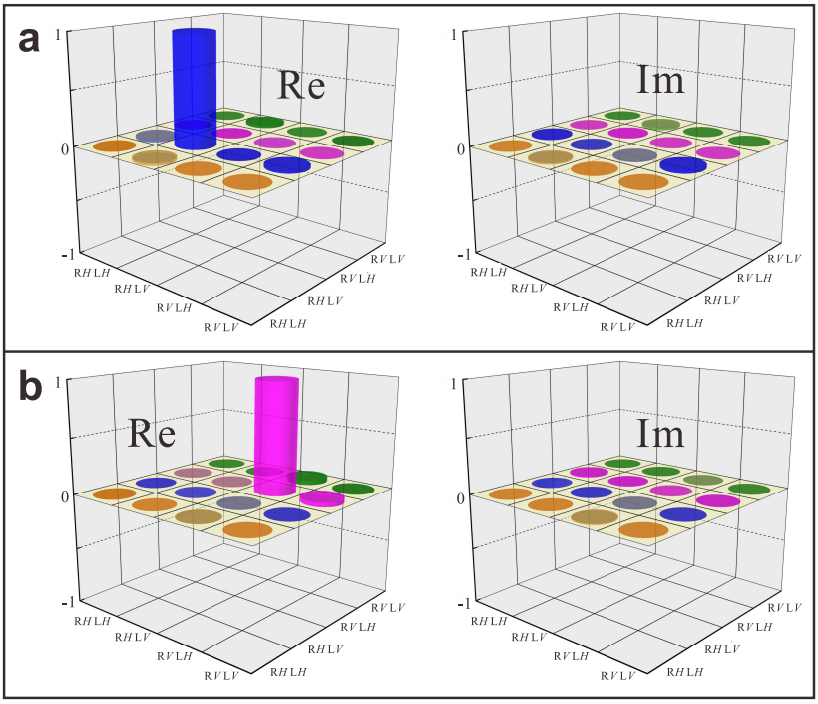

Figure 4.5: (a) and (b): **No overlap cases**. Two subgraphs in (a) correspond to the real and imaginary part of $|\Psi_{\mathrm{LR}}\rangle$ with $\alpha = \beta = \pi/2$, respectively. And the fidelity is $(99.8 \pm 0.1)\%$. The results of $\alpha = \beta = 0$ are presented in (b) and a fidelity $(99.4 \pm 0.1)\%$ is obtained.

method with HWP2 at $-\beta/2$, I prepare the other photon in $|\psi'\rangle$ with $|V\rangle$ ($\downarrow$) to be $|\psi', V\rangle = \sin\beta\ |\mathrm{L}V\rangle + \cos\beta\ |\mathrm{R}V\rangle$. In other words, by rotating HWP1 and HWP2, characterized by the angles $(\pi/2 - \alpha)/2$ and $-\beta/2$, respectively, one can conveniently control the weights of each spatial wave function on the two final measurement locations, while the PBSs separate the different polarizations of the photons. The final HWPs at 45° have the role of maintaining the initial polarization of each photon unvaried before detection. By suitably setting α and β, I can prepare a series of $|\Psi_{\mathrm{prep}}\rangle$ for different configurations of the wave functions and thus of the degree of spatial indistinguishability $\mathcal{I}$.

The unit of polarization analysis detection (PAD), consisting of a quarter-wave plate (QWP), a HWP and a PBS, is placed on both sides of $\mathcal{L}$ and $\mathcal{R}$ to implement the spatially localized operations and measurements (see inset of Fig. 4.3(a)). Classical communication is realized with the help of a coincidence device which deals with the electrical signals of single-photon detectors (SPDs) and outputs the coincidence counting on the two locations $\mathcal{L}$ and $\mathcal{R}$. An interference filter whose full width at half maximum is 3 nm is placed before each SPD. The sLOCC framework is so achieved at the measurement stage.

4.3.2 Entanglement from experimentally tunable indistinguishability

The experimental setup of Fig.4.3(a), after the sLOCC measurements are performed (which formally means projecting onto the two-particle operational subspace spanned by the basis $\mathcal{B}_{\rm LR} = \{|{\rm L}\sigma, {\rm R}\tau\rangle\ ,\ \sigma, \tau = H, V\}$) [34], produces the two-photon state

$$|\Psi_{\rm LR}\rangle = \frac{\cos\alpha\cos\beta\ |{\rm L}H,\ {\rm R}V\rangle + \sin\alpha\sin\beta\ |{\rm L}V,\ {\rm R}H\rangle}{\sqrt{\cos^2\alpha\ \cos^2\beta + \sin^2\beta\ \sin^2\alpha}}, \tag{4.9}$$

obtained with probability $P_{\rm LR} = \cos^2\alpha\ \cos^2\beta + \sin^2\beta\ \sin^2\alpha$. This distributed resource state, conditionally obtained, is in general an entangled state contained in the prepared state $|\Psi_{\rm prep}\rangle$ (see Eq.(4.3)). Looking at the experimental scheme, its origin can be exclusively attributed to the spatial indistinguishability of the photons. We are now able to experimentally verify the amount of entanglement for different spatial configurations of the two wave functions $|\psi\rangle$ and $|\psi'\rangle$ on the two measurement regions $\mathcal{L}$ and $\mathcal{R}$.

As a first point, no entanglement is found when the two wave functions do not spatially overlap. In fact, in this case $\mathcal{I} = 0$ since the two photons can be distinguished by their spatial locations. This situation is retrieved when $\alpha = \beta = 0\ (\pi/2)$ (Fig.4.5(a) and (b)), which gives $|\psi\rangle = |{\rm L}\rangle$ ($|{\rm R}\rangle$) and $|\psi'\rangle = |{\rm R}\rangle$ ($|{\rm L}\rangle$). The final state of the experiment reduces to the product state $|\Psi_{\rm LR}\rangle = |{\rm L}H,\ {\rm R}V\rangle$ ($|{\rm L}V,\ {\rm R}H\rangle$).

Entanglement is then produced both for partial and complete overlap of the wave functions. Under partial overlap, ψ and ψ' do not exhibit the same probabilities to find the particle in regions $\mathcal{L}$ and $\mathcal{R}$. The degree of indistinguishability is $0 < \mathcal{I} < 1$, which in turn provides a given amount of entanglement lower than 1. From Eq. (4.9), one then observes that the maximally entangled (Bell) states $|\Psi^{\pm}_{\rm LR}\rangle = (|{\rm L}H,\ {\rm R}V\rangle \pm |{\rm L}V,\ {\rm R}H\rangle)/\sqrt{2}$ are obtained for $\alpha \pm \beta = \pi/2$ (with $\alpha \neq 0, \pi/2$), which corresponds to complete overlap of the two wave functions and thus to $\mathcal{I} = 1$.

To experimentally prove the different amounts of entanglement for various spatial configurations of the wave functions, one conveniently fix $\alpha = \pi/4$, for which $|\psi\rangle = (|{\rm L}\rangle + |{\rm R}\rangle)/\sqrt{2}$ and

$$|\Psi_{\rm LR}\rangle = \cos\beta\ |{\rm L}H,\ {\rm R}V\rangle + \sin\beta\ |{\rm L}V,\ {\rm R}H\rangle\,. \tag{4.10}$$

The concurrence [83] of this state, here used to quantify the shared entanglement between photon polarizations in $\mathcal{L}$ and $\mathcal{R}$, is given by $C(\Psi_{\rm LR}) = \sin 2\beta$. The degree of spatial indistinguishability of Eq. (4.5) becomes $\mathcal{I} = -\cos^2\beta\ \log_2(\cos^2\beta) - \sin^2\beta\ \log_2(\sin^2\beta)$ which happens to coincide with the entanglement of formation $E_f(\Psi_{\rm LR})$ of the state $|\Psi_{\rm LR}\rangle$ [34]. *Therefore, a monotonic relation $C(\Psi_{\rm LR}) = f(\mathcal{I})$ exists between the concurrence and the indistinguishability of the photons.* Furthermore, the experimental test of Bell inequalities on the various distributed resource states $|\Psi_{\rm LR}\rangle$ under sLOCC is performed to obtain a direct verifica-

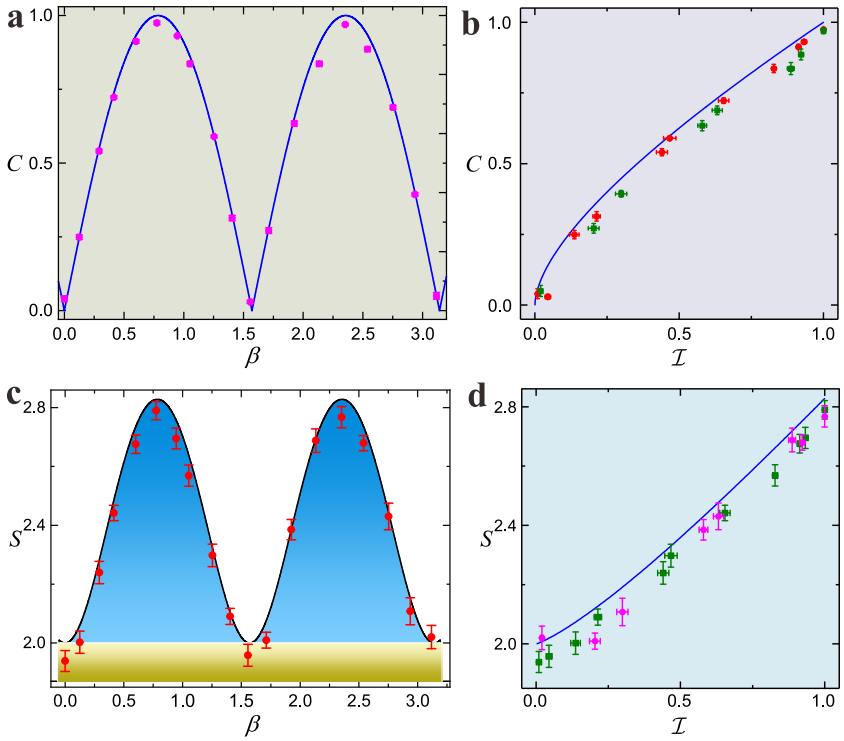

Figure 4.6: **Entanglement versus indistinguishability. a, b.** Concurrence $C(\Psi_{\rm LR})$ of the distributed resource state $|\Psi_{\rm LR}\rangle$ for $\alpha = \pi/4$ as a function of β and spatial indistinguishability $\mathcal{I}$, respectively. The blue line is the theoretical prediction. The pink dots with the error bars in **a** are the experimental results. The red and green dots in **b** denote the experimental results for $\beta \in [0, \pi/2]$ and $\beta \in (\pi/2, \pi]$, respectively. **c, d.** Behaviour of the Bell function S in the CHSH test for $\alpha = \pi/4$ versus β and $\mathcal{I}$. The black curve and red points with error bars in **c** represent the quantum prediction and experimental results, respectively. The blue line in **d** is the theoretical prediction while the pink and green dots are the experimental results for $\beta \in [0, \pi/2]$ and $\beta \in (\pi/2, \pi]$, respectively. All error bars here are estimated as the standard deviation from the statistical variation of the photon counts, which is assumed to follow a Poisson distribution.

tion of the (nonlocal) entanglement between the photon polarizations [88]. Here, the Bell function S is employed to perform a Clauser-Horne-Shimony-Holt (CHSH) test [89]. For the pure two-qubit state of Eq. (4.10) theoretically predicted, I get $S = 2\sqrt{1+C^2} = 2\sqrt{1+\sin^2 2\beta}$ [17, 90]. Bell inequality is violated when $S > 2$, witnessing the presence of quantum correlations which are not reproducible by any classical local model.

The experimental results of $C(\Psi_{\rm LR})$ as a function of both β and $\mathcal{I}$ are shown in Fig. 4.6 (a)-(b) respectively, obtained after state reconstruction. While the experimental results of Bell function S versus β and $\mathcal{I}$ are displayed in Fig. 4.6(c)-(d), respectively. The results for S of most of the generated states are above the classical threshold 2, while some others do not pass the CHSH test because of the imperfect behaviour of experimental elements. Results clearly demonstrate that most of generated states are Bell nonlocal (entangled) states. For $\beta = \pi/4$, $|\Psi_{\rm LR}\rangle$ in Eq. 4.10 is expected to be maximally entangled. In the experiment, in correspon-

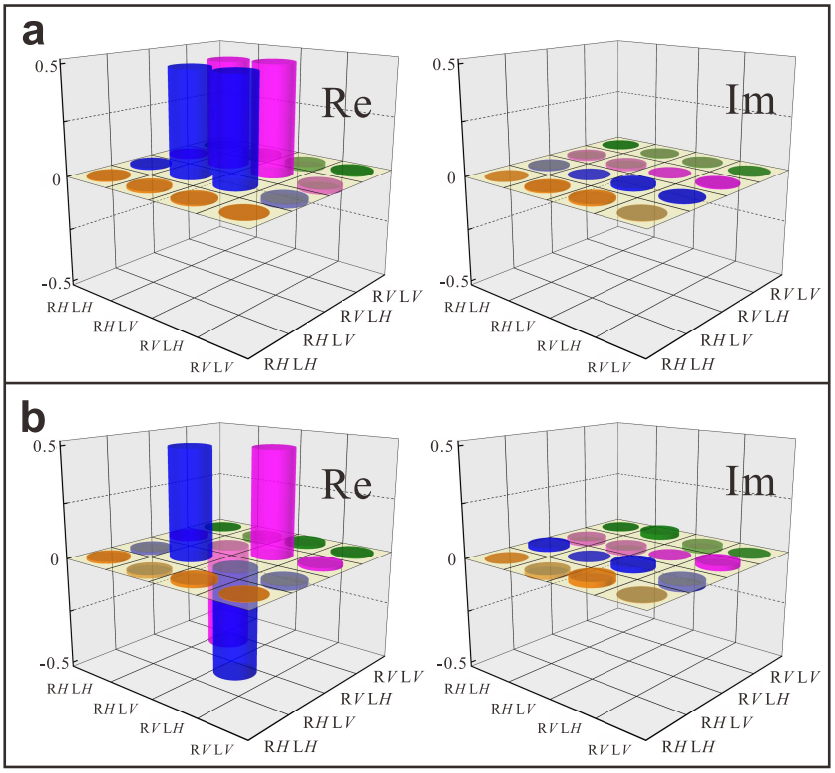

Figure 4.7: **Maximally entangled state generation.** Experimental results of the generated maximally entangled states in correspondence to complete spatial overlap of the wave functions ($\mathcal{I} = 1$). Panel **a** shows the real part and imaginary part of the reconstructed density matrix for $\alpha = \pi/4$ and $\beta = 0.776 \pm 0.006$, for which the expected state is $|\Psi^+_{\mathrm{LR}}\rangle$. Panel **b** shows the real part and imaginary part of the reconstructed density matrix for $\alpha = \pi/4$ and $\beta = 2.352 \pm 0.004$, the expected state being $|\Psi^-_{\mathrm{LR}}\rangle$.

dence of $\beta = 0.776 \pm 0.006$ I achieve $S = 2.79 \pm 0.03$, which violates the Bell inequality by 26 standard deviations. The generated state holds a fidelity of $(98.6 \pm 0.2)\%$ compared to the expected maximally entangled state $|\Psi^+_{\mathrm{LR}}\rangle$, whose reconstructed density matrix is presented in Fig. 4.7(a). Moreover, when $\beta = 3\pi/4$, that is when $|\psi'\rangle = (|\mathrm{L}\rangle - |\mathrm{R}\rangle)/\sqrt{2}$ and $|\psi\rangle$ are orthogonal yet completely overlapping, the maximally entangled state $|\Psi^-_{\mathrm{LR}}\rangle$ should be retrieved. In the experiment, such a state is generated with fidelity $(98.0 \pm 0.8)\%$ in correspondence to $\beta = 2.352 \pm 0.004$, as shown in Fig. 4.7(b). All the results provide strong experimental evidence that entanglement is effectively generated by spatial indistinguishability of photons.

4.3.3 Results of the teleportation

We have verified the generation of polarization entangled states exploiting only different degrees of spatial indistinguishability of two independently prepared initially uncorrelated photons. I now show that the maximal amount of the indistinguishability-enabled entanglement is high enough to implement the quantum teleportation process shown in Section 4.2.2. The detailed

state	$\|H\rangle$	$\|V\rangle$	$\|+\rangle$	$\|-\rangle$	$\|\phi_-\rangle$	$\|\phi_+\rangle$
$F_{\rm exp}(\%)$	90.0 ± 2.0	84.7 ± 1.9	83.1 ± 2.0	82.2 ± 1.9	84.3 ± 1.7	86.3 ± 2.2

Table 4.1: Fidelities of the six states $\rho_{\rm exp}$ with respect to the initially prepared state in the quantum teleportation process.

setup is presented in Fig. 4.3(b). A heralded single photon is generated by pumping a second BBO crystal. One photon is used as the trigger signal while the other photon is sent to the side of L$'$ as the target to be teleported. The combination of a HWP and a QWP is used to prepare the photon into an arbitrary state $|\phi\rangle = a\,|H\rangle + b\,|V\rangle$ with $|a|^2 + |b|^2 = 1$. To teleport the information of $|\phi\rangle$ to the photon located in $\mathcal{R}$, a Bell-state measurement (BSM) is performed between L and L$'$. Here, the Bell state $|\Phi_{\rm LL'}\rangle = (|{\rm L}H,\ {\rm L}'H\rangle + |{\rm L}V,\ {\rm L}'V\rangle)/\sqrt{2}$ is performed by exploiting a PBS and setting the two HWPs at 22.5° [91, 92]. Correspondingly, the single-particle operation in $\mathcal{R}$ rotating the state of its photon to the desired one is $\sigma_x = |H\rangle\langle V| + |V\rangle\langle H|$ which is implemented with a HWP at 45°. Performing the quantum tomography of single-qubit state in R, one can obtain the teleportation information. Quantum teleportation is here realized exploiting the distributed maximally entangled state $|\Psi^+_{\rm LR}\rangle$ above, generated by complete spatial indistinguishability ($\mathcal{I} = 1$) of the original two photons. The value $\alpha = \beta = \pi/4$ is chosen which implies that $|\Psi^+_{\rm LR}\rangle$ is obtained with maximum probability ($P_{\rm succ} = 50\%$). The results of the tomography give a visibility of $87,9\%$. The eigenvectors of σ_i $(i = x,\ y,\ z)$ are prepared as the additional photon states $|\phi\rangle$ in L$'$ to be teleported. This implies $|\phi_{\rm ideal}\rangle \in \{|H\rangle,\ |V\rangle,\ |+\rangle = (|H\rangle + |V\rangle)/\sqrt{2},\ |-\rangle = (|H\rangle - |V\rangle)/\sqrt{2},\ |\phi_-\rangle = (|H\rangle - i|V\rangle)/\sqrt{2}\},\ |\phi_+\rangle = (|H\rangle + i|V\rangle)/\sqrt{2}\}$. First, one perform the tomography of the effectively prepared $\rho_{\rm prep} = |\phi_{\rm prep}\rangle\langle\phi^*_{\rm prep}|$ in L$'$. Comparing it with $|\phi_{\rm ideal}\rangle$, the fidelity of $\rho_{\rm prep}$ is $F = \langle\phi_{\rm ideal}|\rho_{\rm prep}|\phi_{\rm ideal}\rangle$. In this experiment, the average fidelity of prepared $\rho_{\rm prep}$ is about 99.8%. With tomographic measurements performed in $\mathcal{R}$, the experimental states of quantum teleportation $\rho_{\rm exp}$ have been reconstructed.

The state fidelity $F_{\rm exp}$ with respect to the initially prepared state $\rho_{\rm prep}$ is then introduced as a figure of merit for the teleported state $\rho_{\rm exp}$. For the six initial states listed above, without the background subtraction, the corresponding fidelities are measured and shown in Table 4.1 which are clearly higher than the classical fidelity limit of $2/3$ [93]. Furthermore, the quantum process matrix χ of quantum teleportation [94] is reconstructed by means of a tomographic analysis by comparing $\rho_{\rm prep}$ and $\rho_{\rm exp}$. The matrix χ is defined with $\rho_{\rm exp} = \Sigma^4_{i,\,j=1}\,\chi_{ij}\,\sigma_i \cdot \rho_{\rm prep} \cdot \sigma_j$ where $\sigma_1 = I$ and $\sigma_{2,\,3,\,4} = \sigma_{x,\,y,\,z}$, which in the ideal case gives $\chi_{11} = 1$ with all the other elements equal to 0 [95]. By assuming χ with several unknown parameters and employing the experimental results of $\rho_{\rm prep}$ and $\rho_{\rm exp}$, I can calculate the elements of χ. The experimental results are shown in Fig.4.8 with a fidelity $F_\chi = (79.4 \pm 1.6)\%$. All error bars in this work are estimated as the standard deviation from the statistical variation of the photon counts, which is assumed to follow a Poisson distribution.

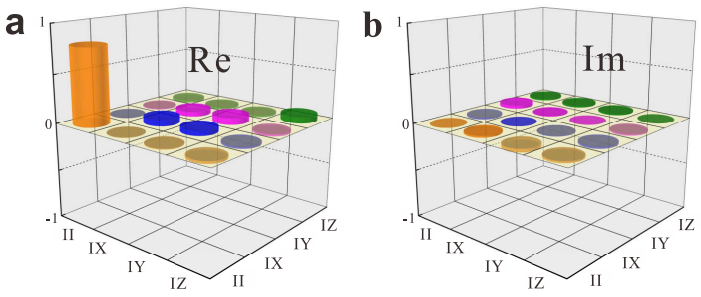

Figure 4.8: The quantum process matrix of quantum teleportation. Experimental reconstruction of quantum process matrix χ for the teleportation protocol. **a, b** show the real and imaginary parts of χ, respectively. Here, I is identity matrix σ_1 and $X,\ Y,\ Z$ correspond to $\sigma_x,\ \sigma_y,\ \sigma_z$, respectively.

4.4 Discussions

In this Chapter, I have presented an experiment realized in an all-optical setup, in which the spatial indistinguishability of two initially uncorrelated photons has been directly tailored by controlling their spatial degrees of freedom, in such a way that they are led to partially or totally overlap in two separated regions. The fact that photons were initially not entangled has been verified with a very high fidelity $(99.9 \pm 0.1)\%$. In order to study the effect of indistinguishability on the emergence of entanglement between photons, single-particle measurements have been performed for different values of spatial overlap within sLOCC. The result is that the amount of entanglement increases with the degree of photon spatial indistinguishabiliy. The Clauser-Horne-Shimony-Holt (CHSH) test has been also performed, showing that the generated entanglement is nonlocal. Moreover, it is useful to remark that the realization of the sLOCC framework excludes any possible measurement-induced entanglement on the initial state, as may instead happen in optical interferometry with spread detection.

Notice that if the setup was run by two initially uncorrelated nonidentical particles, no entanglement would be generated.

The results of the experiment have shown that spatial indistinguishability is a fundamental catalyst of nonlocal entanglement and this is high enough to enable conditional teleportation with fidelities above the classical threshold (82-90$\%$).

Chapter 5

Transfer of entanglement in a quantum network by means of indistinguishability

5.1 Introduction

Usual state transfer procedures [96] uses identical particles (IP) and exploit their entanglement. However, no effect associated to the statistical nature of particles typically shows up, since in these processes they are always distinguishable. One may wonder if, in general, employing IP may lead to new features in the context of quantum communication, when their indistinguishability can be exploited as a direct resource. Indistinguishability has been already shown to be useful for some quantum information protocols [97, 98, 99, 100, 101, 58, 35, 36, 39, 34] and for quantum metrology [2, 75, 61]. In this context, one of the problems which remains to investigate is the role played by the quantum statistical nature of IP into the mechanisms of entanglement transfer within large-scale networks.

In this Chapter, I will present a new process of entanglement transfer for fermions in a many-node quantum network, exploiting their indistinguishability by means of sLOCC. Although the idea of using IP indistinguishability to generate entanglement is not a new one, the present process shows that remote entanglement among two distant sites can be generated by only locally counting particles in the sites and classical communication. These characteristics constitute the key achievement of this project. I will compare this process to that with indistinguishable bosons in the same network and to that with IP (both bosons and fermions) in a network with the number of nodes equal to the number of particles, whose essential ingredients recall, although partially, the standard process of entanglement swapping.

5.2 Entanglement swapping in a nutshell

I concentrate the attention on the entanglement swapping (ES), which is a key process in the context of large-scale distribution of quantum information [102, 103, 104, 105], to build quantum relays and quantum repeaters [106, 96] and is subject of intense experimental interest [107, 108, 109, 110, 111, 112]. ES is an intrinsically quantum phenomenon which permits to entangle two particles not sharing a common past, each particle being outside the light cone of the other. So far, in all the implementations, essential ingredients are

1. preparation of entangled pairs,

2. Bell measurements [113].

In particular, in the standard ES process [114], two pairs of entangled particles are initially prepared (particles in each pair are not independently prepared) and a Bell measurement is successively performed on two particles of the different pairs. As a result, the other two particles become entangled even if they never interacted [115, 116]. ES has been experimentally realized using identical but distinguishable particles (photons) by applying the usual operational framework for NIP, based on particle addressability (local operations and classical communication (LOCC)) [64]. The initial entangled pairs of photons are typically created by spontaneous parametric down conversion (SPDC) [107, 108, 111, 109, 110]. To exclude the possibility of initial classical correlations, some experiments have adopted two synchronized independent SPDC sources [109, 110]. Recently, ES has been successfully achieved in a quantum network, entangling two photons over a distance of 100 km [112]. and, moreover, multiple ES has been theoretically proposed and experimentally realized by extension of the standard protocol [117, 118, 119, 120]. However, the overall success of the process is influenced by the low creation rate of photon pairs in SPDC [121, 122, 123] and by the inefficiency in the realization of Bell measurements [113, 109, 124, 125, 126, 127, 128, 129].

5.3 Network with coincident intermediate nodes

5.3.1 Fermions

Experimental techniques to control fermions in quantum networks have been recently developed [130, 131, 132, 133, 134, 135, 136]. In the following I focus on unveiling remarkable aspects introduced by both fermionic statistics and spatial overlap in the process of remote entanglement distribution.

To this aim, I first describe the basic process which serves as the elementary step for the extension to a many-node quantum network. As displayed in Fig. 5.1, I take four identical

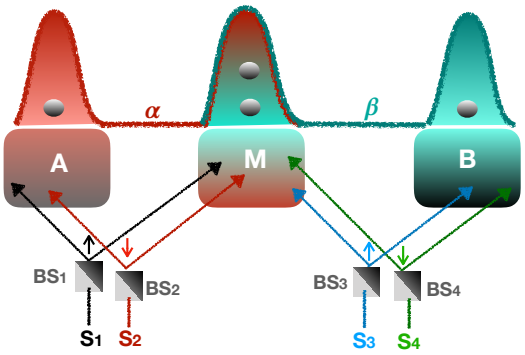

Figure 5.1: **Basic network.** Scheme for the entanglement transfer by four independently-prepared indistinguishable fermions, with a shared intermediate node M. The delocalized spatial modes α and β partially overlap in correspondence of the intermediate node M. Post-selection by sLOCC leaves two fermions with opposite pseudospins in the central node M and two entangled fermions in the extreme nodes, A and B.

fermions (two pairs), prepared by four independent (space-like separated) sources $\{\mathrm{S}_i,\ i = 1, ..., 4\}$. Each particle is sent to the corresponding beam splitter BS_i. The two sources S_1 and S_2 independently prepare two fermions with opposite pseudospin. Each beam splitter sends the particle with the same amplitude into two separated spatial nodes (sites) A and M, so that each particle is in the same delocalized spatial mode $|\alpha\rangle = (|\mathrm{A}\rangle + |\mathrm{M}\rangle)/\sqrt{2}$. Similarly, sources S_3 and S_4 generate the fermions of the second pair with opposite pseudospin in the delocalized spatial mode $|\beta\rangle = (|\mathrm{M}\rangle + |\mathrm{B}\rangle)/\sqrt{2}$ (right side of Fig. 5.1). The modes $|\alpha\rangle$ and $|\beta\rangle$ partially overlap in the shared intermediate node M and the I-th node (I = A, M, B) is chosen such that only the localized bound state $|\mathrm{I}\rangle$ is present. The condition that particles are in the chosen localized bound states can be assured by keeping only the cases when local detectors do not measure particles elsewhere and by classically communicating the results. The initially prepared four-fermion state $|\Psi_{\mathrm{f}}^{(4)}\rangle$ (Appendix B.1) can be then formally obtained from $|\alpha\downarrow, \alpha\uparrow, \beta\downarrow, \beta\uparrow\rangle$ by dropping, because of the Pauli exclusion principle, the terms with the same pseudospins in the central node (same spatial state $|\mathrm{M}\rangle$)[137]. The ultimate scope is to generate entanglement between particles in the far nodes A and B. This can be achieved by using sLOCC [34], which here consist in a post-selection locally counting only one particle of the first pair in A and one particle of the second pair in B and using classical communication among these sites (this counting implies that in the central node M there are two particles). The classical communication allows sites A and B to know when an entangled pair is obtained. Notice that the local counting operation is a free operation with respect to entanglement [138]. Such a post-selection can be implemented utilizing, for instance, absorbtionless particle-counting detectors in A and B, which do not disturb the pseudospin state [139, 140, 141, 101]. Similar non-demolition measurements are applied in the other post-selections by sLOCC used in this Chapter.

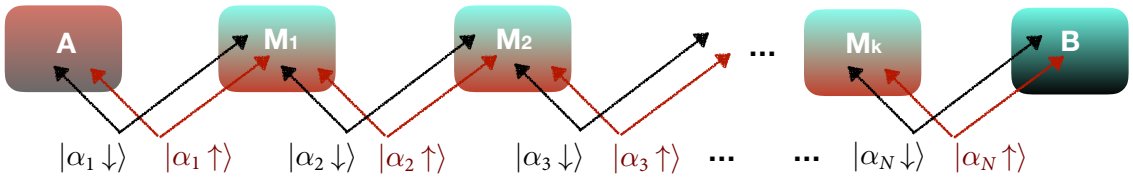

Figure 5.2: **Many-node quantum network.** Scheme for remote entanglement distribution between distant nodes A and B by n independently-prepared indistinguishable particles with $k = N - 1$ shared intermediate nodes, being $N = n/2$ the number of involved particle pairs. This process is the straightforward generalization of the scheme of Fig. 5.1.

One then gets the post-selected global state (see Appendix B.1)

$$|\Psi^{(4)}_{\mathrm{f,PS}}\rangle = |\Psi_{\mathrm{M}}, 1^{-}_{\mathrm{AB}}\rangle, \tag{5.1}$$

where

$$|\Psi_{\mathrm{M}}\rangle = |\mathrm{M}\uparrow, \mathrm{M}\downarrow\rangle\,, \; |1^{-}_{\mathrm{AB}}\rangle = \frac{|\mathrm{A}\downarrow, \mathrm{B}\uparrow\rangle - |\mathrm{A}\uparrow, \mathrm{B}\downarrow\rangle}{\sqrt{2}} \tag{5.2}$$

in which 1 in the ket indicates the number of excited spins in the state. Therefore, it has been obtained a maximally entangled state over the distant nodes A and B, despite the latter are always independent and the particles do not share any common past. I stress that if the four particles are not identical, the same post-selection procedure does not give rise to an entangled state. The probability with which the state of Eq. (5.1) is obtained is shown in Appendix B.1. I remark that this entanglement distribution is reached without entanglement-inducing Bell measurements on the central particles, but just exploiting the indistinguishability of non-interacting fermions in M. In fact, the spatial overlap of fermions in the shared intermediate site M plays the key role of an entanglement-transfer gate. Schemes for entanglement swapping without Bell measurements have been proposed in contexts where interaction is essential (e.g., cavity QED) [125, 142, 126, 143].

The basic scheme of Fig. 5.1 can be straightforwardly iterated to create a remote entanglement transfer in a many-node quantum network. This is achieved by means of n identical fermions and $k = N - 1$ shared intermediate nodes M_i ($i = 1, \ldots, k$), where $N = n/2$ is the number of particle pairs. As displayed in Fig. 5.2, each j-th pair ($j = 1, \ldots, N$) has opposite pseudospins and spatial mode $|\alpha_j\rangle$, with $|\alpha_1\rangle = (|\mathrm{A}\rangle + |\mathrm{M}_1\rangle)/\sqrt{2}$, $|\alpha_N\rangle = (|\mathrm{M}_k\rangle + |\mathrm{B}\rangle)/\sqrt{2}$ and $|\alpha_j\rangle = (|\mathrm{M}_{j-1}\rangle + |\mathrm{M}_j\rangle)/\sqrt{2}$ for $j = 2, \ldots, k$. The aim is to activate entanglement of particles in the remote far nodes A and B of the network. The modes $|\alpha_i\rangle$ and $|\alpha_{i+1}\rangle$ partially overlap in the shared intermediate node M_i and the I-th node (I = A, M_i, B) is taken, as already mentioned above, such that only the localized bound state $|\mathrm{I}\rangle$ is present. Once again the initial n-fermion state $|\Psi^{(n)}_{\mathrm{f}}\rangle$ can be formally determined starting from the state $|\alpha_1\downarrow, \alpha_1\uparrow, \ldots, \alpha_N\downarrow, \alpha_N\uparrow\rangle$

simply by dropping, because of the Pauli exclusion principle, the terms having the same pseudospins in each intermediate node. After that, by counting one particle in A and one in B (this entails that each node $\mathrm{M_i}$ contains two particles) and allowing for classical communication as before, the post-selected global state is

$$|\Psi_{\mathrm{f,PS}}^{(n)}\rangle = |\Psi_{\mathrm{M}_1}, \Psi_{\mathrm{M}_2}, \ldots, \Psi_{\mathrm{M}_k}, 1_{\mathrm{AB}}^{-}\rangle, \tag{5.3}$$

obtained with a probability $P_{\mathrm{f}}(n) = |\langle\Psi_{\mathrm{f,PS}}^{(n)}|\Psi_{\mathrm{f}}^{(n)}\rangle|^2$ explicitly shown in Appendix B.1 and where $|1_{\mathrm{M}_i}\rangle = |\mathrm{M}_i\uparrow, \mathrm{M}_i\downarrow\rangle$ and $|1_{\mathrm{AB}}^{-}\rangle$ is the maximally entangled (Bell) state of Eq. (5.2). Thus, it has been generated entanglement of particle pseudospins between the independent distant locations A and B of the many-node network, starting with independently-prepared identical fermions, with no Bell measurements and only using local counting operations. I remark that all these features make the remote entanglement activation based on identical fermions deeply different from the standard processes of entanglement transfer, such as ES (Section 5.2).

5.3.2 Bosons

The basic setup of Fig. 5.1 can be also thought to be run with identical bosons. I shall show that, in this case, a Bell measurement onto the intermediate site M is eventually required for achieving the desired entanglement transfer, similarly to a standard protocol of ES. The sLOCC framework is now realized by locally counting two particles in the intermediate node M and only one particle in each of the far nodes A and B, also allowing for classical communication among the different sites. From the initial (unnormalized) state $|\alpha\downarrow, \alpha\uparrow, \beta\downarrow, \beta\uparrow\rangle$, one gets the four-boson post-selected state (see Appendix B.2)

$$|\Psi_{\mathrm{b,PS}}^{(4)}\rangle = \frac{|\Psi_{\mathrm{M}}, 1_{\mathrm{AB}}^{+}\rangle + |\Phi_{\mathrm{M}}^{+}, 2_{\mathrm{AB}}^{+}\rangle - |\Phi_{\mathrm{M}}^{-}, 2_{\mathrm{AB}}^{-}\rangle}{\sqrt{3}}, \tag{5.4}$$

where $|\Phi_{\mathrm{M}}^{\pm}\rangle = (|\mathrm{M}\downarrow, \mathrm{M}\downarrow\rangle \pm |\mathrm{M}\uparrow, \mathrm{M}\uparrow\rangle)/2$, $|\Psi_{\mathrm{M}}\rangle$ is given in Eq. (5.2), while the distant sites A and B share the Bell states

$$\begin{aligned} |1_{\mathrm{AB}}^{+}\rangle &= \frac{1}{\sqrt{2}}(|\mathrm{A}\downarrow, \mathrm{B}\uparrow\rangle + |\mathrm{A}\uparrow, \mathrm{B}\downarrow\rangle), \\ |2_{\mathrm{AB}}^{\pm}\rangle &= \frac{1}{\sqrt{2}}(|\mathrm{A}\downarrow, \mathrm{B}\downarrow\rangle \pm |\mathrm{A}\uparrow, \mathrm{B}\uparrow\rangle). \end{aligned} \tag{5.5}$$

I remark that in Eqs. (5.4) and (5.5), 1 and 2 in the kets indicate the number of excited spins in the Bell states. The presence of these three Bell states is a consequence of the fact that bosonic systems admit two-particle states with the same pseudospins in M. As in the standard ES procedure, a joint (Bell) measurement in the shared intermediate node M determines the entangled state in which the first and the last boson of the network collapse, each outcome occurring with

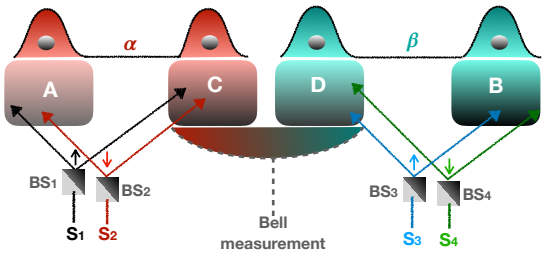

Figure 5.3: Four-node scheme for the entanglement swapping by indistinguishable particles (bosons or fermions). Four independent single-particle sources S_i ($i = 1, ..., 4$) send each particle to the corresponding beam splitter (BS_i). α and β are the (delocalized) spatial modes peaked in correspondence of the separated spatial nodes A-C and D-B, respectively. Post-selection by sLOCC leaves only one particle in each node and Bell measurements are finally performed.

probability $p = 1/3$, as seen from Eq. (5.4). Since each of the three Bell-state outcomes from the joint measurement in M realizes the desired entanglement transfer over A and B, the success probability of the process coincides with the probability of obtaining the post-selected state of Eq. (5.4) (Appendix B.2). This bosonic protocol can be then extended, analogously to the standard multiple ES, by a cascaded procedure [118]. The scheme remains that of Fig. 5.2 with n independently-prepared identical bosons and $k = N - 1$ intermediate nodes ($N = n/2$). The sLOCC framework again consists in counting two particles in each intermediate node and one in the distant nodes A and B, also allowing for classical communication of the counting outcomes. One gets the post-selected state $|\Psi^{(n)}_{\mathrm{b,PS}}\rangle$ and performs Bell measurements step by step on each intermediate node M_i ($i = 1, ..., k$) to transfer entanglement over A and B. The success probability is $P_{\mathrm{b}}(n) = |\langle\Psi^{(n)}_{\mathrm{b,PS}}|\Psi^{(n)}_{\mathrm{b}}\rangle|^2$ (see Appendix B.2).

5.4 Network with separated intermediate nodes

I shall now discuss a procedure, much closer to the standard ES, which can be obtained with indistinguishable particles (bosons or fermions) by employing intermediate separated nodes instead of common intermediate ones.

We take a system made of four IP (either bosons or fermions), prepared by four independent (space-like separated) sources $\{\mathrm{S}_i,\ i = 1, ..., 4\}$. Each particle is sent to the corresponding beam splitter BS_i, as depicted in Fig. 5.3. The two sources S_1 and S_2 independently prepare two particles with opposite pseudospin. Each beam splitter sends the particle with the same amplitude into two separated sites A and C, so that each particle is in the same delocalized spatial mode $|\alpha\rangle = (|\mathrm{A}\rangle + |\mathrm{C}\rangle)/\sqrt{2}$. Similarly, sources S_3 and S_4 generate the particles of the second pair with opposite pseudospin in the delocalized spatial mode $|\beta\rangle = (|\mathrm{D}\rangle + |\mathrm{B}\rangle)/\sqrt{2}$ (right side of Fig. 5.3). All the nodes are spatially separated (the modes $|\alpha\rangle$ and $|\beta\rangle$ are or-

thogonal) and the I-th node (I = A, B, C, D) is chosen such that only the localized bound state $|\mathrm{I}\rangle$ is present. The condition that particles are in the chosen localized bound states can be assured by keeping only the cases when local detectors do not measure particles elsewhere and by classically communicating the results. The global four-particle quantum state [58] is therefore $|\Psi^{(4)}\rangle = |\alpha\downarrow, \alpha\uparrow, \beta\downarrow, \beta\uparrow\rangle$. From this state it is possible to obtain entanglement in the pseudospin degrees of freedom linked to the spatial overlap of particles in each pair. This is achieved by sLOCC [34], which here consist in a post-selection counting only one particle of the first pair in A and one particle of the second pair in B and classically communicating this outcome to each other. This post-selection can be implemented using, for instance, one absorbtionless particle-counting detector in A and one in B, which do not disturb the pseudospin state [139, 140, 141, 101]. Similar non-demolition measurements are applied in the other post-selections used along the paper. As a result, each node contains one particle and I obtain the state (see Appendix B.3)

$$|\Psi^{(4)}_{\mathrm{PS}}\rangle = |1^{\eta}_{\mathrm{AC}}, 1^{\eta}_{\mathrm{DB}}\rangle\,, \tag{5.6}$$

where $|1^{\eta}_{\mathrm{AC}}\rangle$ and $|1^{\eta}_{\mathrm{DB}}\rangle$ are the two-particle Bell states

$$\begin{aligned} |1^{\eta}_{\mathrm{AC}}\rangle &= \frac{1}{\sqrt{2}}(|\mathrm{A}\downarrow, \mathrm{C}\uparrow\rangle + \eta|\mathrm{A}\uparrow, \mathrm{C}\downarrow\rangle), \\ |1^{\eta}_{\mathrm{DB}}\rangle &= \frac{1}{\sqrt{2}}(|\mathrm{D}\downarrow, \mathrm{B}\uparrow\rangle + \eta|\mathrm{D}\uparrow, \mathrm{B}\downarrow\rangle). \end{aligned} \tag{5.7}$$

Even if the particles have been independently prepared, as a consequence of sLOCC, the state $|\Psi^{(4)}_{\mathrm{PS}}\rangle$ shows that the pair of particles in A and C is maximally entangled in the pseudospin degrees of freedom, as the DB-pair. This state is obtained with probability $P(4) = |\langle\Psi^{(4)}_{\mathrm{PS}}|\Psi^{(4)}\rangle|^2 = 1/4$. At this stage the particles can be distinguished, since they are in spatially separated sites. *I stress that for each pair, if the particles are nonidentical, the same post-selection procedure does not give rise to an entangled state.* The structure of the state of Eq. (5.6) allows to implement the standard protocol of entanglement swapping (ES) [114]: performing a Bell measurement on near central nodes C and D transfers entanglement to the particles in the far nodes A and B. Notice that this procedure does not require, at the preparation stage, two entangled pairs. The present scheme works for both bosons and fermions, also when particles of different pairs are not identical. Moreover, in analogy with the standard ES, it can be naturally iterated by a cascaded procedure [118] to realize multistage entanglement swapping with $n = 2N$ independently-prepared particles, being N the number of involved particle pairs. This is achieved by using a network with $n - 2$ separated central nodes, where each pair of identical particles (either bosons or fermions) is prepared with opposite pseudospins in an equal delocalized spatial mode peaked in correspondence of two separated nodes (as shown for the two pairs in Fig. 5.3). After obtaining a single particle in each central node and performing Bell

measurements step by step onto two central nodes [118], one eventually entangles the particles in the extreme nodes of the network with probability $P(n) = 1/2^N$.

5.5 Discussions

In this Chapter I have presented a new way to obtain entanglement transfer in a large-scale quantum network which is fundamentally activated by IP spatial indistinguishability. The standard ES, that is the renowned process for entanglement transfer with distinguishable particles, necessitates to start from entangled particle pairs and requires final Bell measurements [114]. Our process, when run by identical fermions, enables remote entanglement among distant nodes through the following different mechanisms: (i) no distribution of initial entangled pairs, (ii) without performing Bell measurements. This because IP spatial overlap acts as an entangling gate, therefore, the process only requires local counting of independently-prepared IP.

The key advantage of this process is that it simplifies the task of distributing entanglement, overcoming the drawbacks encountered in the usual entanglement transfer procedures during the initial preparation stage and the final measurement phase. In fact, it skips the necessity of sources of entangled particle pairs, which are for instance generated by SPDC at the very low rate of about 10^{-2} for single laser pulse [122], and also avoids the experimental inefficiency associated to Bell measurements [113, 109, 124, 125, 126, 127, 128, 129].

Our results make it emerge once more [34] that IP spatial indistinguishability is a resource that can be operationally exploited in the framework based on sLOCC.

The proposed fermionic process could be, for instance, realized by using: quantum dots as sources of single electrons that can be initialized in particular spin states [131], emitted on demand [132] and directed to quantum point contacts acting as electronic beam splitters [133, 144]; single electrons, that have been also recently shown to be controlled within atomic circuits [134]; urther setups in quantum optics, simulating fermionic statistics using photons and integrated photonics [135, 136] that could, in principle, represent convenient platforms.

Chapter 6

Robust entanglement preparation against noise by controlling spatial indistinguishability

6.1 Introduction

Entanglement is a form of quantum correlation at the heart of quantum information and quantum computing processes. It is therefore very important to initialize composite quantum systems into highly entangled states. However, the interaction of these systems with the environment tends to wear down entanglement, not only during the dynamics but already in the initial phase of pure state preparation, rendering it mixed. As a result, the protection of entanglement from noise is of great relevance for quantum-enhanced processes. In this Chapter, I will treat this subject by means of a system of two identical particles (IP) in the Werner state, which is an emblematic example of a pure entangled state preparation in presence of white noise. By exploiting the concurrence for identical particles (IP-concurrence) and the entropic measure of indistinguishability (Chapter 3, I will study the possibility to protect nonlocal entanglement from preparation noise.

6.2 Entanglement of formation of the IP-Werner state under sLOCC

Werner state is defined as a mixture of a pure maximally entangled Bell state and of the maximally mixed state (white noise [17, 16]). Assuming to be interested in generating the Bell state $|1^{\pm}_{\rm AB}\rangle = (|\uparrow_{\rm A},\downarrow_{\rm B}\rangle \pm |\downarrow_{\rm A},\uparrow_{\rm B}\rangle)/\sqrt{2}$, where 1 in the ket indicates the number of excited spins in the state, the explicit expression of the Werner state, is $W^{\pm}_{\rm AB} = (1-p)\,|1^{\pm}_{\rm AB}\rangle\,\langle 1^{\pm}_{\rm AB}| + p\mathbb{I}_4/4$, $\mathbb{I}_4$ is

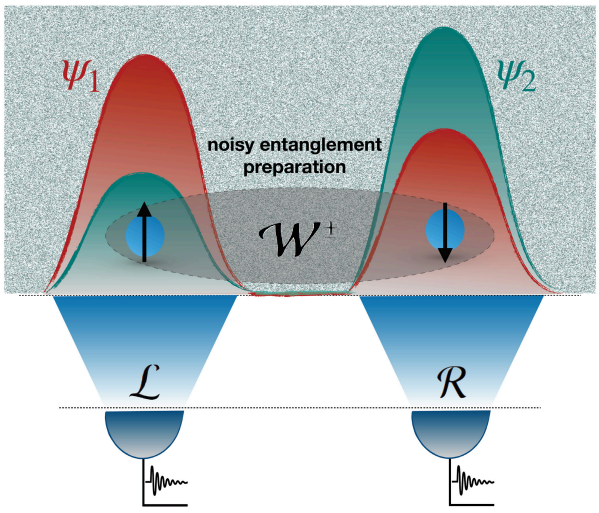

Figure 6.1: **Noisy entanglement preparation with tailored spatial indistinguishability.** Illustration of two controllable spatially overlapping wave functions ψ_1, ψ_2 peaked in the two localized regions of measurement $\mathcal{L}$ and $\mathcal{R}$. The two identical qubits are prepared in an entangled state under noisy conditions, giving $\mathcal{W}^{\pm}$. The degree of spatial indistinguishability can be tuned, being $0 \leq \mathcal{I}_{\rm LR} \leq 1$.

the 4×4 identity matrix and p is the noise probability which accounts for the amount of white noise in the system during the pure state preparation stage. It is known that the concurrence for such state is $C(W^{\pm}_{\rm AB}) = 1 - 3p/2$ when $0 \leq p < 2/3$, being zero otherwise [17].

In perfect analogy, the IP-Werner state with spatial wave functions ψ_1, ψ_2 can be defined by

$$\mathcal{W}^{\pm} = (1-p)\left|1^{\pm}\right\rangle\left\langle 1^{\pm}\right| + p\mathbb{I}_4/4, \tag{6.1}$$

where $\mathbb{I}_4 = \sum_{i=1,2;s=\pm}\left|i^s\right\rangle\left\langle i^s\right|$ is expressed in the orthogonal Bell-state basis $\mathcal{B}_{\{1^{\pm},2^{\pm}\}} = \{\left|1^+\right\rangle, \left|1^-\right\rangle, \left|2^+\right\rangle, \left|2^-\right\rangle\}$ with

$$\begin{aligned}\left|1^{\pm}\right\rangle &:= (\left|\psi_1\uparrow,\psi_2\downarrow\right\rangle \pm \left|\psi_1\downarrow,\psi_2\uparrow\right\rangle)/\sqrt{2},\\ \left|2^{\pm}\right\rangle &:= (\left|\psi_1\uparrow,\psi_2\uparrow\right\rangle) \pm \left|\psi_1\downarrow,\psi_2\downarrow\right\rangle)/\sqrt{2}.\end{aligned} \tag{6.2}$$

where 1 and 2 indicates in the LHS kets indicates the number of excited spins. In Eq. (6.1), $\left|1^{\pm}\right\rangle$ is the target pure state to be prepared and $\mathbb{I}_4/4$ is the noise as mixture of the four Bell states. Notice that the states of Eqs. (6.1) and (6.2) are in general not normalized, this depending on the specific spatial degrees of freedom [39]. Focusing on the observation of entanglement in a Bell scenario of separate locations $\mathcal{L}$ and $\mathcal{R}$, a well-suited configuration for the spatial wave functions is $\left|\psi_1\right\rangle = l\left|\mathrm{L}\right\rangle + r\left|\mathrm{R}\right\rangle$ and $\left|\psi_2\right\rangle = l'\left|\mathrm{L}\right\rangle + r'e^{i\theta}\left|\mathrm{R}\right\rangle$, where l, r, l', r' are non-negative real numbers ($l^2 + r^2 = l'^2 + r'^2 = 1$) and θ is a phase. The wave functions are thus peaked in the two localized measurement regions $\mathcal{L}$ and $\mathcal{R}$, as depicted in Figure 6.1. I here recall the

degree of spatial indistinguishability $\mathcal{I}_{\rm LR}$ of Eq. (3.15) in Chapter 3

$$\begin{aligned}\mathcal{I}_{\rm LR} = &- \frac{P_{{\rm L}\psi_1} P_{{\rm R}\psi_2}}{\mathcal{Z}} \log_2 \frac{P_{{\rm L}\psi_1} P_{{\rm R}\psi_2}}{\mathcal{Z}} \\ &- \frac{P_{{\rm L}\psi_2} P_{{\rm R}\psi_1}}{\mathcal{Z}} \log_2 \frac{P_{{\rm L}\psi_2} P_{{\rm R}\psi_1}}{\mathcal{Z}},\end{aligned} \tag{6.3}$$

where with $P_{{\rm L}\psi_1} = l^2$, $P_{{\rm L}\psi_2} = l'^2$ (implying $P_{{\rm R}\psi_1} = r^2$, $P_{{\rm R}\psi_2} = r'^2$), and $\mathcal{Z} = P_{{\rm L}\psi_1} P_{{\rm R}\psi_2} + P_{{\rm L}\psi_2} P_{{\rm R}\psi_1}$. The degree of spatial indistinguishability is tailored by adjusting the shapes of $|\psi_1\rangle$ and $|\psi_2\rangle$.

Given the configuration of the spatial wave functions and using the sLOCC framework, the amount of operational entanglement contained in $\mathcal{W}^{\pm}$ can be obtained by the IP-concurrence (see Section 3.4 of Chapter 3). Projecting $\mathcal{W}$ onto the subspace spanned by the computational basis $\mathcal{B}_{\rm LR} = \{|{\rm L}\uparrow, {\rm R}\uparrow\rangle, |{\rm L}\uparrow, {\rm R}\downarrow\rangle, |{\rm L}\downarrow, {\rm R}\uparrow\rangle, |{\rm L}\downarrow, {\rm R}\downarrow\rangle\}$ by means of the projector

$$\Pi^{(2)}_{\rm LR} = \sum_{\tau_1, \tau_2 = \uparrow, \downarrow} |{\rm L}\tau_1, {\rm R}\tau_2\rangle \langle {\rm L}\tau_1, {\rm R}\tau_2|, \tag{6.4}$$

the following distributed resource state

$$\mathcal{W}^{\pm}_{\rm LR} = \Pi^{(2)}_{\rm LR} \mathcal{W}^{\pm} \Pi^{(2)}_{\rm LR} / {\rm Tr}(\Pi^{(2)}_{\rm LR} \mathcal{W}^{\pm}), \tag{6.5}$$

is obtained with probability $P_{\rm LR} = {\rm Tr}(\Pi^{(2)}_{\rm LR} \mathcal{W}^{\pm})$. The trace operation is performed in the LR-subspace. The (normalized) state $\mathcal{W}^{\pm}_{\rm LR}$ can be then treated as the state of two distinguishable qubits in separated bound states $|{\rm L}\rangle$, localized in the region $\mathcal{L}$, and $|{\rm R}\rangle$, localized in the region $\mathcal{R}$. Therefore, the sLOCC-based concurrence $C_{\rm LR}(\mathcal{W}^{\pm}) := C(\mathcal{W}^{\pm}_{\rm LR})$ can be calculated by the usual criterion for distinguishable qubits [82, 80] (Chapter 3).

I now report the explicit expressions of $C(\mathcal{W}^{\pm}_{\rm LR})$ for some cases of particular interest. In the following, only the cases $\theta = 0, \pi$ in $|\psi_2\rangle$ will be considered.

- **Werner state $\mathcal{W}^{-}$**

Consider at first in Eq. (6.1) the state $\mathcal{W}^{-}$, by choosing for fermions the value $\theta = 0$ and for bosons $\theta = \pi$. One finds

$$C(\mathcal{W}^{-}_{\rm LR}) = \max\left\{0, \frac{(4-3p)(lr' + l'r)^2 - 3p(lr' - l'r)^2}{4\left(l^2 r'^2 + l'^2 r^2 + lr' rl'(2-3p)\right)}\right\}, \tag{6.6}$$

which is the same for both fermions and bosons, but with a statistically-dependent probability

$$P_{\rm LR} = \frac{2\left(l^2 r'^2 + l'^2 r^2 + lr' rl'(2-3p)\right)}{2 - \eta(2-3p)(ll' - \eta rr')^2}. \tag{6.7}$$

The plot of the concurrence as a function of $\mathcal{I}_{LR}$ and p, fixing $l = r'$, is reported in Figure 6.2(a).

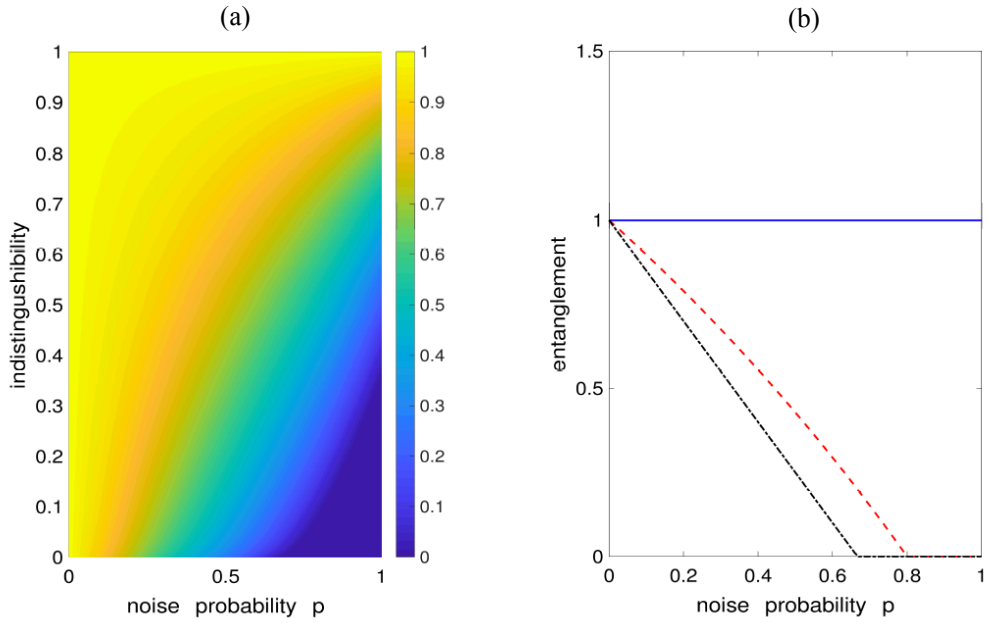

Figure 6.2: **a. Concurrence of the Werner state $\mathcal{W}^-$.** Contour plot of entanglement $C_{\rm LR}(\mathcal{W}^-)$ versus noise probability p and spatial indistinguishability $\mathcal{I}_{\rm LR}$ for target state $|1^-\rangle$, fermions (with $\theta = 0$) or bosons (with $\theta = \pi$), fixing $l = r'$. **b. Concurrence of the Werner states $\mathcal{W}^\pm$ for completely indistinguishable and distinguishable qubits.** Entanglement $C_{\rm LR}(\mathcal{W}^\pm)$ as a function of noise probability p for different degrees of spatial indistinguishability $\mathcal{I}_{\rm LR}$ and system parameters: blue solid line is for target state $|1^-\rangle$, $\mathcal{I}_{\rm LR} = 1$ ($l = l'$), fermions (with $\theta = 0$) or bosons (with $\theta = \pi$); red dashed line is for target state $|1^+\rangle$, $\mathcal{I}_{\rm LR} = 1$ ($l = l'$), fermions (with $\theta = \pi$) or bosons (with $\theta = 0$); black dot-dashed line is for distinguishable qubits ($\mathcal{I}_{\rm LR} = 0$, $l = 1$ and $l' = 0$ or vice versa).

When the indistinguishability degree is maximum, i.e. $\mathcal{I}_{\rm LR} = 1$ ($l = l'$), using in Eq. (6.2) the explicit expressions of the wave functions $|\psi_1\rangle$ and $|\psi_2\rangle$, we obtain by sLOCC the distributed Bell state $\mathcal{W}^-_{\rm LR} = |1^-_{\rm LR}\rangle\langle 1^-_{\rm LR}|$, with $|1^-_{\rm LR}\rangle = (|{\rm L}\uparrow, {\rm R}\downarrow\rangle - |{\rm L}\downarrow, {\rm R}\uparrow\rangle)/\sqrt{2}$. In this case, the concurrence is

$$C(\mathcal{W}^-_{\rm LR}) = 1, \textit{ for any noise probability } p \textit{ and given } \mathcal{I}_{\rm LR} = 1, \tag{6.8}$$

whose behaviour in function of the noise probability p is shown by the blue solid line of Figure 6.2**b**. The probability $P_{\rm LR}$ of Eq. (6.7) is plotted in Figure 6.3(a) as a function of noise probability p for some degrees of the spatial indistinguishability. $P_{\rm LR}$ is maximized when $l = l' = 1/\sqrt{2}$, taking the values $P_{\rm LR} = 1/2$ for fermions and $P_{\rm LR} = 1 - 3p/4$ for bosons.

- **Werner state $\mathcal{W}^+$**

Differently, when in Eq. (6.1) the state $\mathcal{W}^+$ is considered and the values $\theta = \pi$ and $\theta = 0$

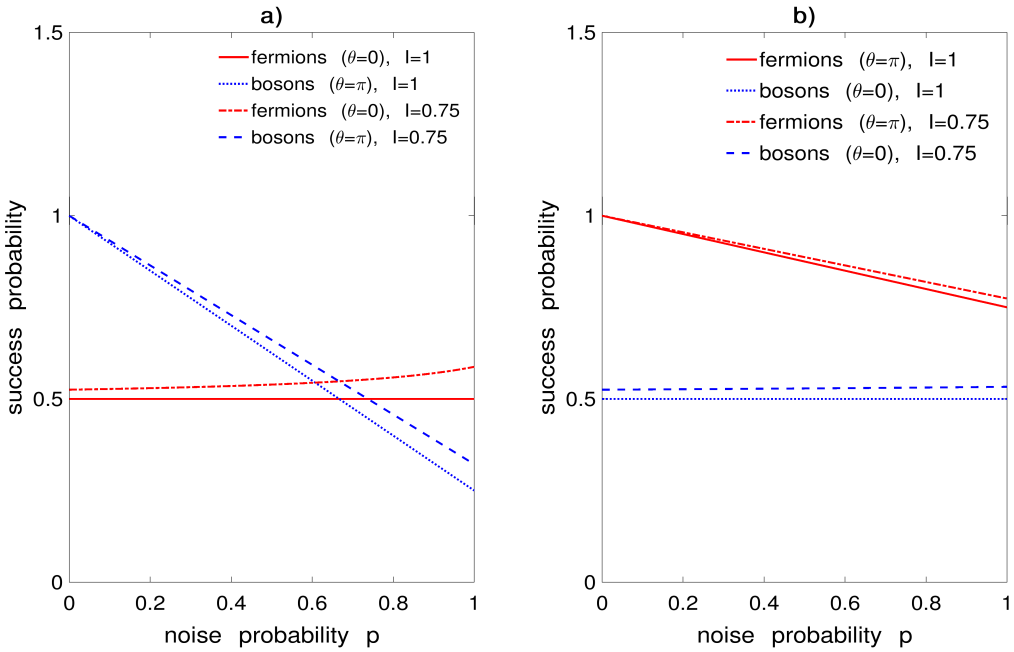

Figure 6.3: **Probabilities**. sLOCC probability $P_{\rm LR}$ as a function of noise probability p for some degrees of spatial indistinguishability $\mathcal{I}_{\rm LR} := \mathrm{I}$ and particle statistics, fixing $l = r'$ in the wave functions $|\psi_1\rangle$ and $|\psi_2\rangle$. **a.** Target pure state $|1^-\rangle$ in Eq. (6.1). **b.** Target pure state $|1^+\rangle$ in Eq. (6.1).

are chosen for fermions and bosons, respectively, one obtains again a statistically-independent concurrence

$$C(\mathcal{W}^+_{\rm LR}) = \max\left\{0, \frac{(4-5p)(lr'+l'r)^2 - p(lr'-l'r)^2}{4\left(l^2r'^2 + l'^2r^2 + lr'rl'(2-p)\right)}\right\}, \tag{6.9}$$

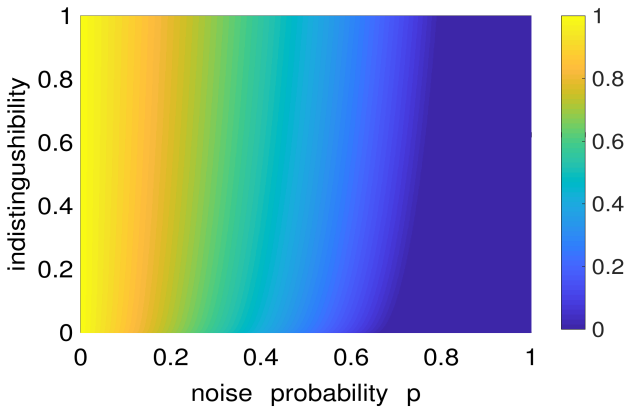

Figure 6.4: **Concurrence of the Werner state** $\mathcal{W}^+$. Contour plot of $C(\mathcal{W}^+)$ versus noise probability p and spatial indistinguishability $\mathcal{I}_{\rm LR}$, for fermions (with $\theta = \pi$) or bosons (with $\theta = 0$), fixing $l = r'$ in the spatial wave functions $|\psi_1\rangle$ and $|\psi_2\rangle$.

with a statistically-dependent probability

$$P_{\rm LR} = \frac{2\left(l^2 r'^2 + l'^2 r^2 + l r' r l'(2-p)\right)}{2 + \eta(2-p)(ll' + \eta r r')^2} \tag{6.10}$$

The concurrence of Eq. (6.9) is given by the contour plot in Fig. 6.4 in terms of both indistinguishability degree $\mathcal{I}_{\rm LR}$ and noise probability p, fixing $l = r'$.

However, differently from the previous case ($\mathcal{W}^-$), when particles are maximally indistinguishable, i.e. $\mathcal{I}_{\rm LR} = 1$ ($l = l'$), one gets a p-dependent concurrence $C(\mathcal{W})^+_{\rm LR}$, with

$$C(\mathcal{W}^+_{\rm LR}) = \begin{cases} (4-5p)/(4-p), & \textit{for } 0 \leq p < 4/5 \\ 0 & elsewhere \end{cases}, \quad \textit{given } \mathcal{I}_{\rm LR} = 1. \tag{6.11}$$

The entanglement now decreases with increasing noise, remaining however larger than the one for nonidentical qubits (red dashed line of Fig. 6.2**b**). The sLOCC probability is maximized when $l = l' = 1/\sqrt{2}$, taking the value $P_{\rm LR} = 1 - p/4$ for fermions and $P_{\rm LR} = 1/2$ for bosons. The probability $P_{\rm LR}$ of Eq. (6.10) is plotted in Fig. 6.3(b) as a function of noise probability p for some degrees of spatial indistinguishability $\mathcal{I}_{\rm LR}$.

The choice of the state to generate (either $|1^-\rangle$ or $|1^+\rangle$) makes a difference relative to noise protection by indistinguishability. However, we remark that identical qubits in the distributed resource state $\mathcal{W}^{\pm}_{\rm LR}$, are individually addressable. Local unitary operations (rotations) in $\mathcal{L}$ and $\mathcal{R}$ can be applied to each qubit to transform the noise-free prepared $|1^{\rm LR}_-\rangle$ into any other Bell state [17]. Moreover, notice that these behaviours are achieved with probabilities $P_{\rm LR}$ high enough to be of experimental relevance.

Since the preparation of $|1^-\rangle$, represented by Eq. (6.1), results to be noise-free for both fermions and bosons when $\mathcal{I}_{\rm LR} = 1$, it is important to know what happens when the degree of spatial indistinguishability realistically not perfectly maximum (between 0.7 and 1). In Fig.6.2**a** we display entanglement as a function of both p and $\mathcal{I}_{\rm LR}$. The plot reveals that entanglement preparation can be efficiently protected against noise also for $\mathcal{I}_{\rm LR} < 1$.

6.3 CHSH-Bell inequality violation for the $\mathcal{W}^{\pm}$ state

For distinguishable particles a given value of entanglement by itself does not guarantee that the correlations cannot be reproduced by a classical local hidden variable model [17, 22]. The Bell inequality violations are therefore utilized to show that a given amount of entanglement of mixed states assures not classically reproducible nonlocal quantum correlations [17]. For two distinguishable qubits in an arbitrary state ρ, the CHSH-Bell inequality can be written as $B(\rho) \leq 2$ [17], where 2 represents the classical threshold. Whenever a quantum state produces

$B(\rho) > 2$, its corresponding entanglement is inherently quantum nonlocal.

These arguments can be straightforwardly generalized to the case of indistinguishable particles. In fact, after sLOCC the identical qubits can be individually addressed and a Bell test can be performed on their global state by spin-like measurements onto the separated bound states $|\mathrm{L}\rangle$, localized in the region $\mathcal{L}$, and $|\mathrm{R}\rangle$, localized in the region $\mathcal{R}$ [34]. The distributed resource state $\mathcal{W}^{\pm}_{\mathrm{LR}}$, stemming from $\mathcal{W}^{\pm}$ of Eq. (6.1) after sLOCC, has an X structure in the computational basis $\mathcal{B}_{\mathrm{LR}} = \{|\mathrm{L}\uparrow, \mathrm{R}\uparrow\rangle, |\mathrm{L}\uparrow, \mathrm{R}\downarrow\rangle, |\mathrm{L}\downarrow, \mathrm{R}\uparrow\rangle, |\mathrm{L}\downarrow, \mathrm{R}\downarrow\rangle\}$. That is, only the diagonal and off-diagonal elements are in general nonzero. According to the Horodecki criterion for the CHSH-Bell inequality violation of a two-qubit density matrix [78], the expression of the optimized Bell function for an X-shape density matrix ρ_X can be written as [145]

$$B(\rho_X) = 2\sqrt{\mathcal{P}^2 + \mathcal{Q}^2}, \tag{6.12}$$

with $\mathcal{P} = \rho_{11} + \rho_{44} - \rho_{22} - \rho_{33}$ and $\mathcal{Q} = 2(|\rho_{14}| + |\rho_{23}|)$, where ρ_{ij} are the density matrix elements in the computational basis. For $\mathcal{W}^{\pm}_{\mathrm{LR}}$, these elements are functions of both the degree of spatial indistinguishability $\mathcal{I}_{\mathrm{LR}}$, through the wave function parameters l and l', and the noise probability p. It is thus possible to look for Bell inequality violations, that is $B_{\mathrm{LR}}(\mathcal{W}^{\pm}) := B(\mathcal{W}^{\pm}_{\mathrm{LR}}) > 2$, for different values of $\mathcal{I}_{\mathrm{LR}}$ and p. Fixing $l = r'$ in the wave functions $|\psi_1\rangle$ and $|\psi_2\rangle$, the degree of spatial indistinguishability can be continuously varied.

As shown in the previous section, entanglement can be protected by noise also for $\mathcal{I}_{\mathrm{LR}} < 1$. What is the minimum degree of $\mathcal{I}_{\mathrm{LR}}$ that guarantees nonlocal protected entanglement in $\mathcal{L}$ and $\mathcal{R}$?

- **Werner state** $\mathcal{W}^{-}$

For both fermions and bosons, the behaviour of the Bell function $B(\mathcal{W}^{-}_{\mathrm{LR}})$ is displayed in Figure 6.5**a**. *When* $0.76 < \mathcal{I}_{\mathrm{LR}} \leq 1$*, that is* $0.56 < C(\mathcal{W}^{-}_{\mathrm{LR}}) \leq 1$*, the Bell inequality is violated independently of noise probability* p*.*
This is basically different from the case of distinguishable qubits A and B where, as known [17], the Werner state $W^{\pm}_{\mathrm{AB}}$ violates Bell inequality only for small white noise probabilities $0 \leq p < 0.29$ (giving $0.68 < C(W^{\pm}_{\mathrm{AB}}) \leq 1$).

- **Werner state** $\mathcal{W}^{+}$

For both fermions and bosons, the behavior of $B(\mathcal{W}^{+}_{\mathrm{LR}})$ is reported in Figure 6.5**b**. When $\mathcal{I}_{\mathrm{LR}} = 1$, *the violation of the Bell inequality depends on the noise probability* p: one has $B(\mathcal{W}^{+}_{\mathrm{LR}}) > 2$ for $0 \leq p < 0.36$, which means $0.6 < C(\mathcal{W}^{+}_{\mathrm{LR}}) \leq 1$.

The main result comes from the case of $\mathcal{W}^{-}$: although significant changes in the shapes of the 1-particle wave functions, the spatial indistinguishability $\mathcal{I}_{\mathrm{LR}}$ anyway remains beyond the threshold (≈ 0.76) which assures noise-free generation of non-local entanglement. We notice

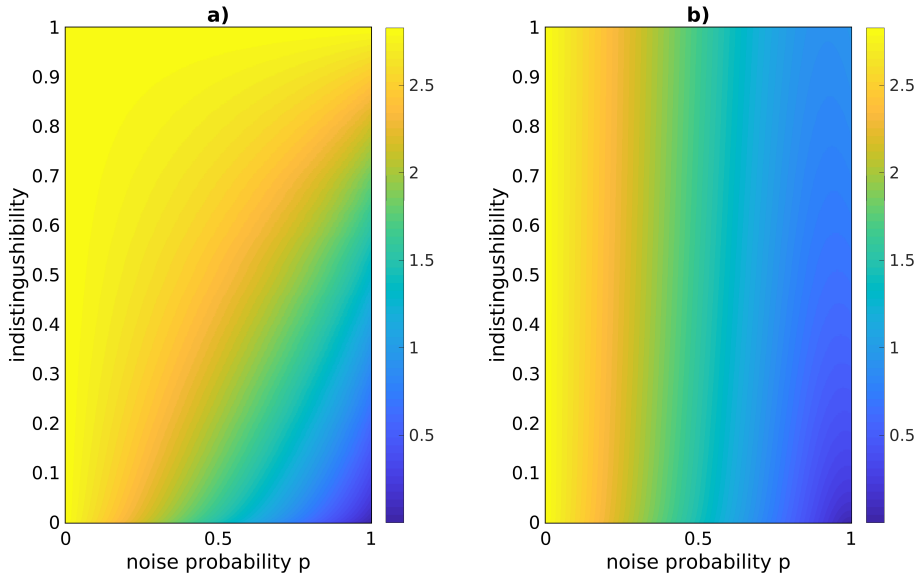

Figure 6.5: **Bell function**. Bell function $B(\mathcal{W}^{\pm}_{\rm LR})$ versus noise probability p and degree of spatial indistinguishability. To vary $\mathcal{I}_{\rm LR}$ we fix $l = r'$ in$|\psi_1\rangle$ and $|\psi_2\rangle$. **a.** Target pure state $|1^-\rangle$ in Eq. (6.1) for both fermions (with $\theta = 0$) and bosons (with $\theta = \pi$). **b.** Target pure state $|1^+\rangle$ in Eq. (6.1) for both fermions (with $\theta = \pi$) and bosons (with $\theta = 0$).

that if the two operational regions $\mathcal{L}$ and $\mathcal{R}$ are two nodes of a quantum network, the protection of entanglement between the two nodes for a fixed value of indistinguishability ($\mathcal{I}$) is invariant with respect to finite changes of the 1-particle spatial wave functions in the nodes. In this sense we may talk about "topological protection" of entanglement

6.4 Discussions

In this Chapter, I have analysed the effect of quantum indistinguishability on entanglement preparation in the generalised IP-Werner state. This IP-state is obtained from the Werner state of two distinguishable (separated) identical qubits after letting them overlapping (see Chapter 8). I have shown that, starting with a noisy Werner state, the sLOCC permit to obtain, when indistinguishability is maximum, a noiseless nonlocal maximally entangled state; this result is independent of particle statistics. Moreover, spatial indistinguishability possesses robustness to variations in the configuration of spatial wave functions. In this sense, the main result of this chapter is that *indistinguishability behaves analogously to a topological resource of quantum networks*.

These results may also provide the explanation of coherence endurance due to particle indistinguishability [146].

Chapter 7

Indistinguishability-enabled coherence

7.1 Introduction

In this Chapter, I will study the coherence of independently prepared identical particles (IP) in function of their spatial indistinguishability, showing how to generalize all the notions of resource theory of quantum coherence [147, 148, 149, 150, 151, 152, 153], known for nonidentical particles (NIP), due to IP. Then, I will investigate whether the IP indistinguishability-enabled coherence plays an operational role in the implementation of quantum information tasks. In particular, I will exploit this coherence in a phase discrimination game [149]. Finally I will examine in a specific case the role played by particle statistics in the protocol.

7.2 Coherence as a resource

The purpose of a quantum resource theory (QRT) is to characterize tools useful for the implementation of quantum-enabled tasks under certain physical constraints. Indeed, it comes from the impossibility to perform certain operations at no cost. The operations to which I have access, in accordance with these constraints (e.g. superselection rules or experimental difficulties), are the so-called *free operations*. Due to the fact that they represent only a certain subgroup of all the possible quantum operations, only certain quantum states can be obtained by means of them and these are the *free states* of the theory.

"*Basic economic principles dictate that*
objects acquire value when they cannot be easily obtained."[138]

As consequence, all the other states are called *resources*, not only since they cannot be obtained for free but also since they allow us to circumvent the physical constraints to implement some tasks unachievable by using only free states and free operations.

Resource theories are useful since it allows us to quantitatively evaluate the advantage used by a quantum state rather than another carrying out a physical processes. All the measures of a resource remain constants or monotonically decrease under the free operations, according to the fact that the resource has a value and no arbitrary amount of it can be created without a cost. Moreover, the resource theory gives the possibility to approach quantum tasks in terms of required free operations and of the consumptions of the resources.

Quantum coherence is a property of quantum systems coming from the possibility to prepare them in quantum states which are superposition of two or more different physical configurations and it is a basis-dependent concept.

Being a purely quantum feature, it represents the core of quantum-enhanced technologies [148, 154] and, as a consequence, a resource theory [138] of coherence for nonidentical particles has been proposed, in order to characterize, quantify and exploit coherence [147, 148, 149, 150, 151, 152, 153]. Chosen a reference basis, diagonal and non diagonal states in that basis are called incoherent (free) states and coherent (resource) states, respectively. The free operations to which I have access are the so-called *incoherent operations* and they cannot create coherence starting from incoherent states. They map the set of incoherent states into itself and all the measures of coherence proposed, such as the relative entropy of coherence, the l_1 norm of coherence [155] and the robustness of coherence [149] are monotones under incoherent operations.

It has been shown that coherence of a quantum state has an operational relevance in the implementation of phase discrimination protocols using distinguishable particles: the robustness of coherence quantifies not only the amount of coherence of a quantum state but also the advantage offered by its presence in a metrology protocol [149, 156]. In the context of quantum thermodynamics, a link between the coherence of a quantum state and the extractable work has been identified [157], and very recently the role of quantum coherence as a resource for the non-equilibrium entropy production has been pinpointed [158].

The resource theory of coherence is well defined for single-particle systems and for systems of multi-distinguishable particles. On the other hand, recently, it has been shown that indistinguishability of identical particles confers on quantum systems original properties that can be used as sources of entanglement to implement quantum information processes, impossible to perform if particles are distinguishable [54, 34, 62, 97, 98, 99, 100, 101].

In the following, I will show how the sLOCC framework gives the possibility to characterize the coherence of identical particles under general conditions of spatial overlap [61]. The aim now is to show how indistinguishability may be a source of operational coherence, highlighting also the role of particle statistics. Clearly, and in contrast to the case of distinguishable particles, to achieve this I must consider at least two (identical) particles.

7.3 Coherence of identical particle states

Let us consider, in the no-label formalism [58, 59, 39], two identical pseudospins (that is particles with a two-level internal state space) in the mixed state

$$\rho^{\mathrm{IP}} = \sum_{\sigma,\tau=\downarrow,\uparrow} p_{\sigma\tau} \left|\psi\sigma, \psi'\tau\right\rangle \left\langle\psi\sigma, \psi'\tau\right| , \tag{7.1}$$

where ψ and ψ' represent the spatial degrees of freedom and σ and τ are the pseudospins. The coefficients $p_{\sigma\tau}$ are such that $\mathrm{Tr}[\rho^{\mathcal{I}}] = 1$. Each term $|\psi\sigma, \psi'\tau\rangle$ in the sum is the state of two IP, one of which is characterised by ψ and σ, the other by ψ' and τ.

To define the coherence of this state, an orthonormal basis has to be chosen. Let us now make some considerations about which "preferred" basis is opportune to choose, depending on the possible operations that can be performed for free on the system. As I have said, a resource theory requires the identification of a physically and operationally meaningful set of free operations, to manipulate resourceful states. Analogously to the case of distinguishable particles, both single-particle and two-particle operations on the system are allowed. Identical particles are physically not addressable individually [159, 50], thus the concept of single-particle operation may seem ill-defined, requiring us to differentiate them. As an example, since the global Hilbert space is not a tensor product of two single-spin spaces, if a CNOT gate[1] (free operation for distinguishable particles [152]) has to operate, it is not possible to differentiate between the control and the target particle.

Following the procedure to identify and quantify the useful entanglement between identical particles [34], in order to characterize the quantum coherence I here adopt a framework based on sLOCC, which consists of the identification of specific separate spatial regions to make single-particle and two-particle local measurements. In particular, I choose the basis $\mathcal{B}^{\mathrm{IP}} = \{|\mathrm{L}\sigma, \mathrm{R}\tau\rangle \,;\ \sigma, \tau = \downarrow, \uparrow\}$, where $|\mathrm{L}\rangle$ and $|\mathrm{R}\rangle$ are two states spatially localized in the separate regions $\mathcal{L}$ and $\mathcal{R}$, respectively. If ρ^{IP} is diagonal in the chosen basis, it is incoherent, otherwise I say that $\rho^{\mathcal{I}}$ is coherent.
For NIP, identified by labels A and B, the state of Eq. (7.1) would correspond to $\rho^{\mathrm{NIP}} = \sum_{\sigma,\tau} p_{\sigma\tau}(|\psi\sigma\rangle \langle\psi\sigma|)_{\mathrm{A}} \otimes (|\psi'\tau\rangle \langle\psi'\tau|)_{\mathrm{B}}$. Being particles addressable, the framework of spatially local operations and classical communication coincides with the LOCC one and the operational basis is $\mathcal{B}^{\mathrm{NIP}} = \{|\mathrm{L}\sigma\rangle_{\mathrm{A}} \otimes |\mathrm{R}\tau\rangle_{\mathrm{B}} \,; \sigma, \tau = \downarrow, \uparrow\}$. Regardless of the spatial overlap of $|\psi\rangle$ and $|\psi'\rangle$,

[1] The CNOT is a quantum logic gate which acts on two qubits. It modifies or not the state of a qubit (target qubit) after having controlled the state of the other qubit (control qubit). It is used as an entangling gate in quantum circuits [16].

ρ^{NIP} is incoherent, in fact

$$\begin{aligned}\rho_{\mathrm{LR}}^{\mathrm{NIP}} =& \frac{1}{\mathcal{N}} \sum_{\sigma\tau} p_{\sigma\tau} \left(\Pi_{\mathrm{L}} \left|\psi\sigma\right\rangle \left\langle\psi\sigma\right| \Pi_{\mathrm{L}}\right)_{\mathrm{A}} \otimes \left(\Pi_{\mathrm{R}} \left|\psi'\tau\right\rangle \left\langle\psi'\tau\right| \Pi_{\mathrm{R}}\right)_{\mathrm{B}} \\ =& \sum_{\sigma\tau} p_{\sigma\tau} (\left|\mathrm{L}\sigma\right\rangle \left\langle\mathrm{L}\sigma\right|)_{\mathrm{A}} \otimes (\left|\mathrm{R}\tau\right\rangle \left\langle\mathrm{R}\tau\right|)_{\mathrm{B}},\end{aligned} \tag{7.2}$$

where $\Pi_{\mathrm{L}} = \sum_{\sigma} (\left|\mathrm{L}\sigma\right\rangle \left\langle\mathrm{L}\sigma\right|)_{\mathrm{A}}$ and $\Pi_{\mathrm{R}} = \sum_{\sigma} (\left|\mathrm{R}\sigma\right\rangle \left\langle\mathrm{R}\sigma\right|)_{\mathrm{B}}$. As a result, the mixed state ρ^{NIP} for two independently prepared NIP, being diagonal in the chosen basis, is incoherent. Projecting, on the other hand, ρ^{IP} of Eq. (7.1) on the chosen subspace spanned by the basis $\mathcal{B}^{\mathrm{IP}}$, I obtain the following state

$$\begin{aligned}\rho_{\mathrm{LR}}^{\mathrm{IP}} = \frac{1}{\mathcal{N}} \sum_{\sigma,\tau=\downarrow,\uparrow} & p_{\sigma\tau}(|l|^2|r'|^2 \left|\mathrm{L}\sigma, \mathrm{R}\tau\right\rangle \left\langle\mathrm{L}\sigma, \mathrm{R}\tau\right| + \eta l r' l'^* r^* \left|\mathrm{L}\sigma, \mathrm{R}\tau\right\rangle \left\langle\mathrm{L}\tau, \mathrm{R}\sigma\right| \\ & + \eta l' r l^* r'^* \left|\mathrm{L}\tau, \mathrm{R}\sigma\right\rangle \left\langle\mathrm{L}\sigma, \mathrm{R}\tau\right| + \eta |l'|^2 |r|^2 \left|\mathrm{L}\tau, \mathrm{R}\sigma\right\rangle \left\langle\mathrm{L}\tau, \mathrm{R}\sigma\right|),\end{aligned} \tag{7.3}$$

where $\mathcal{N}$ is a global normalization factor, $l = \langle L|\psi\rangle$, $r' = \langle R|\psi'\rangle$, $l' = \langle L|\psi'\rangle$ and $r = \langle R|\psi\rangle$ are the probability amplitudes of finding one particle in the two spatially separate states $\left|\mathrm{L}\right\rangle$ and $\left|\mathrm{R}\right\rangle$, and η is 1 for bosons and -1 for fermions. I recall from Section 3.5 of Chapter 3 that the spatial indistinguishability degree is

$$\mathcal{I}_{\mathrm{LR}} = -\sum_{i}^{2} p_{\mathrm{LR}}^{(i)} \log_2 p_{\mathrm{LR}}^{(i)}, \tag{7.4}$$

where $p_{\mathrm{LR}}^{(1)} = |lr'|^2/(|lr'|^2 + |l'r|^2)$ and $p_{\mathrm{LR}}^{(2)} = 1 - p_{\mathrm{LR}}^{(1)}$. Assuming, for instance, $l, r' \neq 0$, the remaining probability amplitudes l' and r are zero if and only if $\left|\psi\right\rangle$ and $\left|\psi'\right\rangle$ do not spatially overlap. If $p_{\downarrow\uparrow} = p_{\uparrow\downarrow} = 0$, the state ρ^{IP} does not contain coherence, regardless of the spatial indistinguishability of particles. Otherwise, the state is coherent if and only if the particles spatially overlap ($\mathcal{I}_{\mathrm{LR}} \neq 0$ from Eq. (8.26)). If they do not overlap ($\mathcal{I}_{\mathrm{LR}} = 0$), the state is incoherent: nonoverlapping identical particles act like nonidentical ones. In the chosen framework, all the monotones introduced to quantify the coherence of nonidentical particles can be used. As an example, all the considerations just done for the coherence $C(\rho^{\mathrm{IP}})$ of the state of Eq. (7.3) are reflected in the l_1-norm of the state $C_{l_1}(\rho_{\mathrm{LR}}^{\mathrm{IP}}) = \sum_{i\neq j} |(\rho_{\mathrm{LR}}^{\mathrm{IP}})_{ij}|$, that is

$$C(\rho^{\mathrm{IP}}) := C_{l_1}(\rho_{\mathrm{LR}}^{\mathrm{IP}}) = \frac{2}{\mathcal{N}}(|p_{\downarrow\uparrow} l r' l'^* r^*| + |p_{\uparrow\downarrow} l' r l^* r'^*|) \tag{7.5}$$

explicitly dependent on the overlap parameters and so on the spatial indistinguishability (Eq. 8.26).

The sLOCC framework has the advantage that, incoherent operations, known for NIP, can

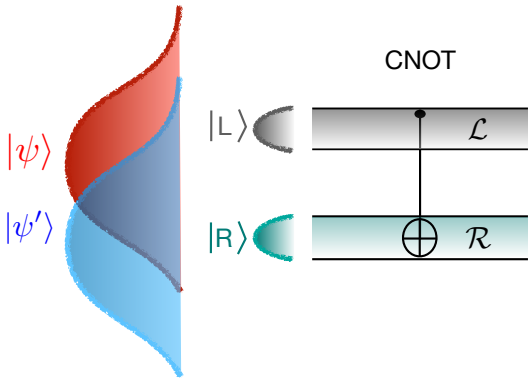

Figure 7.1: **CNOT gate for spatially overlapping IP in the sLOCC framework**. $|\psi\rangle$ and $|\psi'\rangle$ are the 1-particle spatial wave functions. $|\mathrm{L}\rangle$ and $|\mathrm{R}\rangle$ are two specific states localized in two spatially separated spatial regions $\mathcal{L}$ and $\mathcal{R}$, respectively.

be straightforwardly translated in the context of IP systems. Let us consider for example the CNOT gate. In the standard implementation with NIP, there are individually addressed control and target spins. By analogy, for IP one can identify the measurement regions $\mathcal{L}$ and $\mathcal{R}$ as control and target regions, respectively (Fig. 7.1). Applying it to the state of Eq. (7.3) when it is incoherent, it can be easily shown that it gives us an incoherent state. Therefore the CNOT gate remains an incoherent operation which transforms incoherent states of IP into incoherent states.

7.4 Application: phase discrimination protocol

IP have been used for purposes of quantum metrology within the context of particle-number states [160]. Our purpose here is to exploit the contribution to coherence due to the spatial indistinguishability, so determining its operational role in quantum information processing. It is known that within the context of quantum metrology, quantum coherence of states of non-identical particles is a resource for phase discrimination tasks [149, 161]. I now describe an analogous game for indistinguishability-enabled quantum coherence. The state of two independently prepared nonidentical particles A and B, for instance, $|\Psi\rangle_{\mathrm{AB}} = |\psi\downarrow\rangle_{\mathrm{A}} \otimes |\psi'\uparrow\rangle_{\mathrm{B}}$, is manifestly incoherent in the basis $\mathcal{B}^{\mathrm{NIP}} = \{|\mathrm{L}\sigma\rangle_{\mathrm{A}} \otimes |\mathrm{R}\tau\rangle_{\mathrm{B}}\}$, regardless of the spatial overlap of $|\psi\rangle$ and $|\psi'\rangle$. Differently, let us consider the corresponding elementary state for two independently prepared identical particles

$$|\Psi\rangle = |\psi\downarrow, \psi'\uparrow\rangle, \tag{7.6}$$

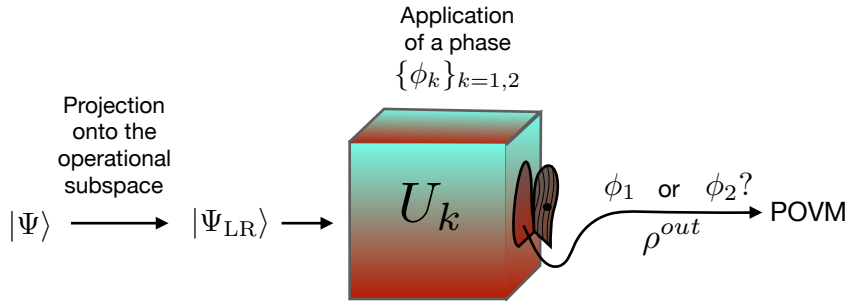

Figure 7.2: **Phase discrimination game**. A 2-particles state $|\Psi\rangle_{\rm LR}$, obtained projecting the state $|\Psi\rangle$ of two IP in the chosen operational subspace, is sent in a box where a unitary operator U_k applies either a phase ϕ_1 or a phase ϕ_2 to the state. The state ρ^{out} coming out of the box is a classical mixture. The optimal POVM is performed in order to guess which phase has been applied.

whose projection in the operational subspace spanned by $\mathcal{B}^{\rm IP}$ is

$$|\Psi_{\rm LR}\rangle = \frac{1}{\mathcal{N}_{\rm LR}}(lr'|{\rm L}\downarrow,{\rm R}\uparrow\rangle + \eta l'r|{\rm L}\uparrow,{\rm R}\downarrow\rangle), \tag{7.7}$$

with the normalization constant $\mathcal{N}_{\rm LR} = \sqrt{|lr'|^2 + |l'r|^2}$. Notice that the resource (coherent) state above is conditionally prepared depending on the spatial overlap of the particles [34]. A non-zero coherence for this state can only stem from indistinguishability ($l'r \neq 0$). Let us send $|\Psi_{\rm LR}\rangle$ in a box where a unitary transformation $U_k = e^{i\hat{G}\phi_k}$ ($\hat{G}$ is the generator of the transformation) applies one of the phases $\{\phi_k\}_{k=1,2}$ with a probability p_k to the state (see Fig. 7.2). The requirement is that U_k is a free (incoherent) operation, so $\hat{G} = \sum_{\sigma\tau}\omega_{\sigma\tau}|{\rm L}\,\sigma,{\rm R}\,\tau\rangle\langle{\rm L}\,\sigma,{\rm R}\,\tau|$. The action of the box is

$$\begin{aligned}|\Psi^k_{\rm LR}\rangle &= U_k|\Psi_{\rm LR}\rangle \\ &= \frac{1}{\mathcal{N}_{\rm LR}}[lr'e^{i\omega_{\downarrow\uparrow}\phi_k}|{\rm L}\downarrow,{\rm R}\uparrow\rangle + \eta l're^{i\omega_{\uparrow\downarrow}\phi_k}|{\rm L}\uparrow,{\rm R}\downarrow\rangle].\end{aligned} \tag{7.8}$$

Due to our ignorance of which of the two phases has been applied, the state coming out of the box is in the following classical mixture

$$\rho^{out} = \sum_{k=1,2} p_k|\Psi^k_{\rm LR}\rangle\langle\Psi^k_{\rm LR}|. \tag{7.9}$$

Physically, the effect of the box can be realized with $\hat{G}$ corresponding to the Hamiltonian of two independent spins subject to localized magnetic fields ${\rm B}^k_{\mathcal{L}}$ and ${\rm B}^k_{\mathcal{R}}$ which randomly occur with a probability p_k.

The purpose now is to establish which phase has actually been applied. In other words, the phase discrimination game translates in a state discrimination one. The two states $|\Psi^1_{\rm LR}\rangle$ and

$|\Psi^2_{\rm LR}\rangle$ are in general not orthogonal: in order to discriminate them, a positive operator-valued measure (POVM) [162, 16] has to be chosen. I look for a POVM described by a set of operators $\{\hat{\Pi}_1, \hat{\Pi}_2\}$, each of which is associated to an outcome of the measurement: if I obtain 1, associated to the operator $\hat{\Pi}_1$, I conclude that the state coming of the box is $|\Psi^1_{\rm LR}\rangle$, if the result is 2, associated to the operator $\hat{\Pi}_2$, the state is $|\Psi^2_{\rm LR}\rangle$. The optimal POVM can be obtained by minimizing the probability of making an error in the discrimination, that is the probability of obtaining the result associated to $\hat{\Pi}_k$ when the state was $|\Psi^{k'}_{\rm LR}\rangle$ with $k' \neq k$. Such a probability is [162, 163]

$$P_{\rm err} = p_1 \langle \Psi^1_{\rm LR}|\hat{\Pi}_2|\Psi^1_{\rm LR}\rangle + p_2 \langle \Psi^2_{\rm LR}|\hat{\Pi}_1|\Psi^2_{\rm LR}\rangle. \tag{7.10}$$

Using the property $\sum_k \hat{\Pi}_k = \mathbb{I}$ [16], I can rewrite Eq. (7.10) as follows

$$P_{\rm err} = p_1 - {\rm Tr}\left[(p_1|\Psi^1_{\rm LR}\rangle\langle\Psi^1_{\rm LR}| - p_2|\Psi^2_{\rm LR}\rangle\langle\Psi^2_{\rm LR}|)\hat{\Pi}_1\right]. \tag{7.11}$$

The minimization of $P_{\rm err}$ is obtained when $\hat{\Pi}_1$ is the projector onto the positive eigenvector of the operator $\Delta = p_1|\Psi^1_{\rm LR}\rangle\langle\Psi^1_{\rm LR}| - p_2|\Psi^2_{\rm LR}\rangle\langle\Psi^2_{\rm LR}|$. Choosing a rotated orthonormal basis $|0\rangle$ and $|1\rangle$ (with $|0\rangle$ slicing in half the angle between $|\Psi^1_{\rm LR}\rangle$ and $|\Psi^2_{\rm LR}\rangle$), I can write

$$|\Psi^1_{\rm LR}\rangle = \cos\theta|0\rangle + \sin\theta|1\rangle,\ |\Psi^2_{\rm LR}\rangle = \cos\theta|0\rangle - \sin\theta|1\rangle. \tag{7.12}$$

The positive eigenvalue of Δ and the associated eigenvector are respectively

$$\begin{aligned} \lambda_+ &= \frac{1}{2}(p_1 - p_2 + \sqrt{1 - 4p_1p_2|\langle\Psi^1_{\rm LR}|\Psi^2_{\rm LR}\rangle|^2}, \\ |+\rangle &= \frac{1}{\mathcal{N}_+}a(|\Psi^1_{\rm LR}\rangle + |\Psi^2_{\rm LR}\rangle) + b(|\Psi^1_{\rm LR}\rangle - |\Psi^2_{\rm RL}\rangle), \end{aligned} \tag{7.13}$$

where $\mathcal{N}_+ = \sqrt{\cos^2\theta\sin^2\theta + [\lambda_+(p_1 - p_2)\cos^2\theta]^2}$, $a = \sin(\theta)/2$ and $b = [\lambda_+ - (p_1 - p_2)\cos^2\theta]/(2\sin\theta)$. The optimal POVM, dependent on the spatial overlap of the two spins, is therefore $\{|+\rangle\langle+|, \mathbb{I} - |+\rangle\langle+|\}$ which gives the probability of error

$$\begin{aligned} P_{\rm err} &= \frac{1}{2}\left(1 - \sqrt{1 - 4p_1p_2|\langle\Psi^1_{\rm LR}|\Psi^2_{\rm LR}\rangle|^2}\right) \\ &= \frac{1}{2} - \sqrt{\frac{1}{4} - p_1p_2\left|\frac{|lr'|^2e^{i\omega_{\downarrow\uparrow}\phi_{12}} + |l'r|^2e^{i\omega_{\uparrow\downarrow}\phi_{12}}}{\mathcal{N}^2_{\rm LR}}\right|^2}, \end{aligned} \tag{7.14}$$

where $\phi_{12} = \phi_1 - \phi_2$. The probability of error depends on the indistinguishability and, for the chosen initial state, is independent of the statistics of particles. Our approach also allows us to evidence the effects of particle statistics on the game efficiency starting from a different initial state, as shown in the next section.

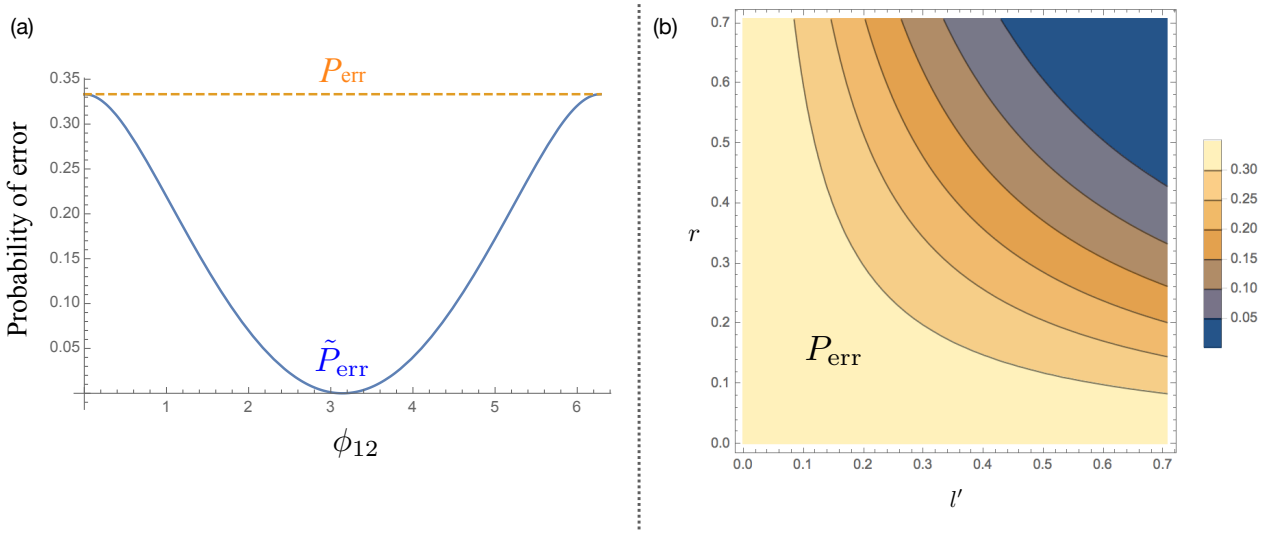

Figure 7.3: **Probability of error in the phase discrimination game. (a)**: Probability of error in function of the phase difference ϕ_{12}, with $p_1 = 1/3$, $|l|^2 = |r'|^2 = \frac{1}{2}$, and $\omega_{\downarrow\uparrow} - \omega_{\uparrow\downarrow} = 1$. The orange dashed line corresponds to $P_{\rm err}$ (Eq. 7.14) when there is no overlap ($l'r = 0$) or, analogously, to the case with distinguishable particles. The blue one corresponds to $\tilde{P}_{\rm err}$ (Eq. 7.15), i.e. to the case of spatial overlap with $|l'|^2 = |r|^2 = \frac{1}{2}$. **(b)**: Contour plot of $P_{\rm err}$ (Eq. 7.14) in function of r and l', with $\phi_{12} = \pi$, $p_1 = 1/3$, $|l|^2 = |r'|^2 = \frac{1}{2}$, and $\omega_{\downarrow\uparrow} - \omega_{\uparrow\downarrow} = 1$.

Let me fix $|l|^2 = |r'|^2 = 1/2$: when the two particles spatially overlap with $|l'|^2 = |r|^2 = \frac{1}{2}$, Eq. (7.14) reduces to

$$\tilde{P}_{\rm err} = \frac{1}{2}\left(1 - \sqrt{1 - 4p_1p_2\cos^2\left[\left(\frac{\omega_{\downarrow\uparrow} - \omega_{\uparrow\downarrow}}{2}\right)\phi_{12}\right]}\right), \tag{7.15}$$

which is zero when $\left(\frac{\omega_{\downarrow\uparrow} - \omega_{\uparrow\downarrow}}{2}\right)\phi_{12} = \pi/2$. The behavior of $P_{\rm err}$ is displayed in Fig. 7.3. In particular in Fig.7.3 (a) I show, as a function of the phase difference, $\tilde{P}_{\rm err}$ (blue solid line) and the probability of error $P_{\rm err}$ for spatially separated particles ($l', r = 0$, orange dashed line). This latter case is analogous to that of non-identical particles. Among the two, $\tilde{P}_{\rm err}$ is always smaller. For non-overlapping spins, being the state incoherent, the best guess is to suppose that the most probable phase ϕ_2 has been applied. The optimal probability of success is $P_{\rm succ} = p_2$ and so $P_{\rm err} = 1 - P_{\rm succ} = p_1$ (see orange dashed line in Fig. 7.3(a)). In Fig. 7.3 (b) a contour plot of $P_{\rm err}$ in terms of l' and r is shown, in the case $\phi_{12} = \pi$. The optimal choice to minimize $P_{\rm err}$ is to have two overlapping identical spins with $|l'|^2 \sim |r|^2 \sim 1/2$.

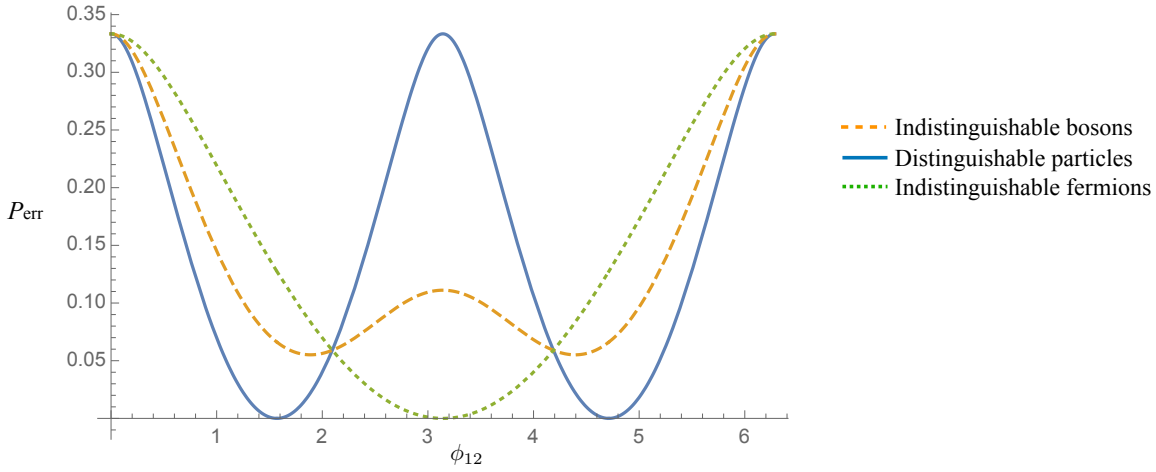

Figure 7.4: **Role of particle statistics in the phase discrimination game**. Probability of error in function of ϕ_{12} with $|l|^2 = |r'|^2 = 1/2$ for identical particles initially prepared in the state of Eq.(7.16): distinguishable (blue solid line) and indistinguishable with $|l'|^2 = |r|^2 = 1/2$ (orange-dashed line for bosons and green dotted line for fermions), with $a = b$, $\omega_{\downarrow\uparrow} = 3$, $\omega_{\uparrow\downarrow} = 2$ and $\omega_{\downarrow\downarrow} = 1$.

7.4.1 Role of particle-statistics

The phase discrimination game, within the elementary state of Eq.(7.6), is independent of particle statistics. However, for a generic state this characteristic is not maintained. As an example, let us consider the following state

$$|\Phi\rangle = \frac{1}{\mathcal{N}^{\Phi}}|\psi\downarrow, \psi' s\rangle, \tag{7.16}$$

where $|s\rangle = a\,|\uparrow\rangle + b\,|\downarrow\rangle$, with $a, b \in \mathbb{R}$, and $\mathcal{N}^{\Phi}$ the normalization constant. Projecting $|\Phi\rangle$ in the operational subspace spanned by the basis $\mathcal{B}^{\text{IP}} = \{|\text{L}\sigma, \text{R}\tau\rangle\,,\ \sigma, \tau = \downarrow, \uparrow\}$, I obtain

$$|\Phi_{\text{LR}}\rangle = \frac{1}{\mathcal{N}^{\Phi}_{\text{LR}}}(|\text{L}\downarrow, \text{R}s'\rangle + a\eta l' r\,|\text{L}\uparrow, \text{R}\downarrow\rangle), \tag{7.17}$$

where $|s'\rangle = alr'\,|\uparrow\rangle + b(lr' + \eta l' r)\,|\downarrow\rangle$, $\mathcal{N}^{\Phi}_{\text{LR}} = \sqrt{a^2(|lr'|^2 + |l'r|^2) + b^2|lr' + \eta l' r|^2}$. The state of Eq. (7.16) is coherent in $\mathcal{B}^{\text{IP}}$ (see Eq. (7.17)) and in the chosen framework of spatially localized measurements, a contribution to the coherence due only to indistinguishability can be identified when particles spatially overlap ($l'r \neq 0$). The latter indistinguishability-enabled contribution plays a statistics-dependent operational role in a phase discrimination game. Let us send $|\Phi_{\text{LR}}\rangle$ in the previously introduced box, in which a unitary transformation $U_k = e^{i\hat{G}\phi_k}$ applies to the state one of the phases $\{\phi_k\}_{k=1,2}$ with a probability p_k and $\hat{G}$ is the generator of

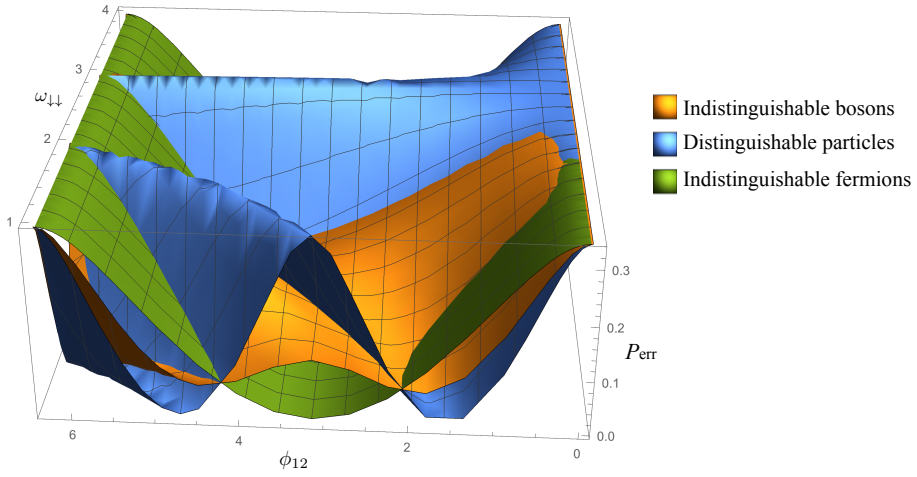

Figure 7.5: **Role of particle statistics in the phase discrimination game**. Three-dimensional (3D) plot of the probability of error with $|l|^2 = |r'|^2 = 1/2$ for identical particles initially prepared in the state of Eq.(7.16): distinguishable (blue) and indistinguishable with $|l'|^2 = |r|^2 = 1/2$ (orange for bosons and green for fermions) in function of ϕ_{12} and of $\omega_{\downarrow\downarrow}$, with $|l|^2 = |r'|^2 = 1/2$, $a = b$, $\omega_{\downarrow\uparrow} = 3$, $\omega_{\uparrow\downarrow} = 2$.

the transformation previously used. I thus obtain

$$\begin{aligned} |\Phi^k_{\text{LR}}\rangle &= U_k|\Phi_{\text{LR}}\rangle \\ &= \frac{1}{\mathcal{N}^{\Phi}_{\text{LR}}}[a(lr'e^{i\omega_{\downarrow\uparrow}\phi_k}|\text{L}\downarrow,\text{R}\uparrow\rangle + \eta l're^{i\omega_{\uparrow\downarrow}\phi_k}|\text{L}\uparrow,\text{R}\downarrow\rangle) \\ &+ b(lr' + \eta l'r)e^{i\omega_{\downarrow\downarrow}\phi_k}|\text{L}\downarrow,\text{R}\downarrow\rangle]. \end{aligned} \tag{7.18}$$

When the state comes out of the box, it is in a classical mixture

$$\rho^{out}_{\Phi} = \sum_{k=1,2} p_k|\Phi^k_{\text{LR}}\rangle\langle\Phi^k_{\text{LR}}|, \tag{7.19}$$

which represents our ignorance of which phase has been applied to the state. Using the first line of Eq. (7.14), in which $|\Psi^i_{\text{LR}}\rangle$ is substituted by $|\Phi^i_{\text{LR}}\rangle$, the probability of making an error in the discrimination game is now

$$P_{\text{err}} = \frac{1}{2}\left(1 - \sqrt{1 - 4p_1p_2\left|\frac{1}{\mathcal{N}^2_{RL}}[a^2(|lr'|^2e^{i\omega_{\downarrow\uparrow}\phi_{12}} + |l'r|^2e^{i\omega_{\uparrow\downarrow}\phi_{12}}) + b^2|lr' + \eta l'r|^2e^{i\omega_{\downarrow\downarrow}\phi_{12}}]\right|^2}\right), \tag{7.20}$$

where $\phi_{12} = \phi_1 - \phi_2$. From Figs. 7.4 and 7.5 it is easy to see that for certain ranges of the parameters ϕ_{12} and $\omega_{\sigma\tau}$ ($\sigma, \tau = \downarrow, \uparrow$), the probability of error using indistinguishable particles is considerably smaller than the one associated to distinguishable ones. In particular, in these ranges, *fermions are more advantageous than bosons*.

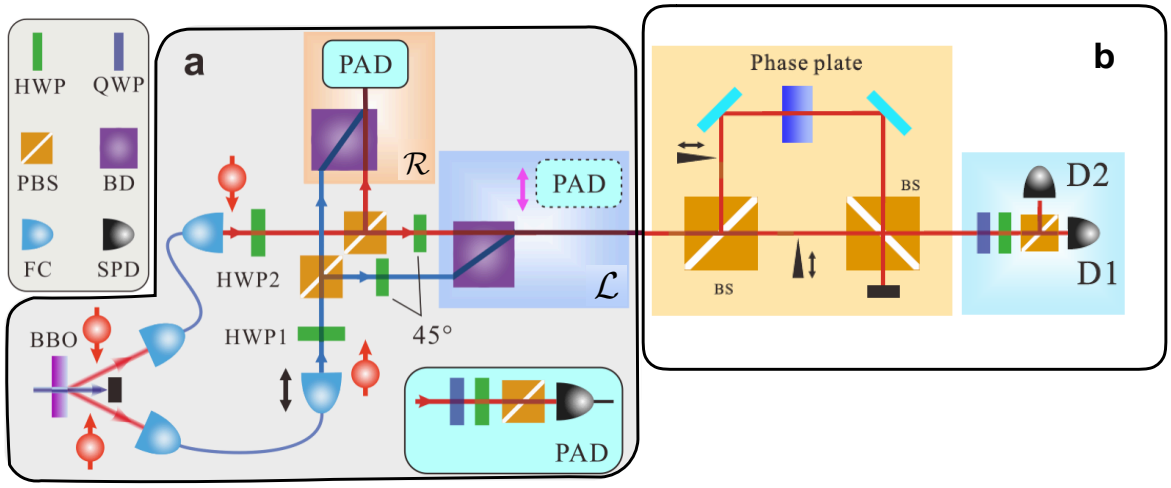

Figure 7.6: Sketch of the experimental proposal.

7.5 Sketch of the experimental proposal

An experimental proposal has been presented by the research group of Professor Guan-Can Guo of the University of Science and Technology of China, in order to characterize coherence of IP states due to their indistinguishability and to operationally use it to implement phase discrimination protocols. In Figure 7.6 the designed setup is presented. In particular, in the block (a) the setup for the generation of IP states with a sLOCC-tunable spatial indistinguishability in two spatially separated regions $\mathcal{L}$ and $\mathcal{R}$ is designed and in the block (b) the sketch of the apparatus implementing the phase discrimination game is proposed, where a sequence of non-polarizing beam splitter (BS) and of two movable shutters determine the classical probabilities of applying or not a phase on the states obtained in the block (a). A final part in block (b) implements the POVM measurements. The experiment is in progress at the CAS Key Laboratory of Quantum Information.

7.6 Discussions

In this Chapter I have defined the coherence of a couple of two-level IP in the framework of spatially localized operations and classical communication (sLOCC). I have shown that while independently prepared distinguishable particles are incoherent under local operations, the analogous configuration with indistinguishable particles can exhibit quantum coherence. Therefore, *the IP spatial indistinguishability is a source of coherence*. One can naturally identify (in the sLOCC framework) the contribution to coherence exclusively due to the spatial overlap of single-particle wave functions. The incoherent operations, as the CNOT gate, known for NIP particles are straightforwardly generalized to systems of IP.

I have then applied the above results in the context of quantum metrology. In particular, I have presented a phase discrimination protocol, for which I can explicitly demonstrate the *operational advantage of using indistinguishable rather than distinguishable particles*. This significantly reduces the error probability of guessing the phase by means of the optimal POVM. Moreover, I have shown that:*particle statistics affects coherence and the efficiency in a phase-discrimination game*.

Chapter 8

Deformations of identical particle states

8.1 Introduction

In this Chapter I will introduce, for both pure and mixed states, a class of transformations of quantum systems, that I name *deformations*. In systems of nonidentical particles (NIP), a global transformation, where one acts in the same way on each part of the system, is represented by a unitary operator. An example of this is a block space translation of the system. If, instead, one acts differently on each part of the systems, by changing the relative relations among parts, I will speak about a NIP *deformation* of the system and it continues to be represented by a unitary operator.

On the other hand, the situation completely changes when one considers identical particles (IP). In fact, while global transformations of the system remain always represented by unitary operators, I will show that IP *deformations* are represented by nonunitary operators, even if the action on each single part of the system remains unitary.

I finally will present some physical consequences of the IP-deformations on some IP states, which are the generalization of the NIP Werner and Bell diagonal states for a varying degree of indistinguishability (introduced in Section 3.5 of Chapter 3).

8.2 Elementary deformation of pure states

Let me start by considering a system of N NIP with the single-particle orthonormal basis $\{|k\rangle\}$, where k indicates a given set of eigenvalues of single-particle commuting observables. Consider the N-particles orthonormal basis $\{|\varphi_i^{(N)}\rangle = |1_i\rangle \otimes |2_i\rangle \otimes ... \otimes |N_i\rangle\}_{\rm NIP}$, where the position of each single-particle state in the global state acts as a particle physical label. The system is prepared in the state $|\Phi^{(N)}\rangle = \sum_i \phi^i |\varphi_i^{(N)}\rangle$ in which ϕ^i is the probability amplitude of finding the system in the state $|\varphi^{(N)}\rangle$.

Consider a class of N-particle transformations $\{D^{(N)}_{a_1,a_2,...,a_N}\}$, where the subscripts $\{a_i\}$ represent physical parameters characterizing the transformation. These operations act in general differently unitarily on each single-particle state as follows

$$D^{(N)}_{a_1,a_2,...,a_N} |\Phi^{(N)}\rangle = \sum_i \phi^i \, |U^{(1)}_{a_1} 1_i\rangle \otimes |U^{(1)}_{a_2} 2_i\rangle \otimes ... \otimes |U^{(1)}_{a_N} N_i\rangle \, , \tag{8.1}$$

where in general $a_n \neq a_m$ and $U^{(1)}_{a_n}$ represents the unitary action of $U^{(N)}_{a_1,a_2,...,a_N}$ in the single-particle subspace. I call the operations defined in Eq.(8.1) *elementary deformations*. As an example, let me consider an operation in which each particle is translated in space for a different vectorial quantity so that the system is "spatially deformed". If in Eq. (8.1), the 1-particle unitary operations $U^{(1)}_{a_i}$ are linear combinations of different unitary operations, Eq. (8.1) generalizes to

$$D^{(N)} = \sum_{\vec{a}} c_{\vec{a}} D^{(N)}_{\vec{a}}, \tag{8.2}$$

with $\vec{a} = a_1, ..., a_N$ and $c_{\vec{a}}$ arbitrary coefficients, constitute a group, in general non unitary ($(D^{(N)})^\dagger \neq {D^{(N)}}^{-1}$). *Composed deformations* $C^{(N)}$ on a N-particle system can be obtained by sequentially performing different deformations of the form of Eq. 8.1 (e.g. a rotation followed by a reflection), as follows

$$C^{(N)} = \prod_{\vec{a}} D^{(N)}_{\vec{a}}. \tag{8.3}$$

Introducing the notation $D^{(N)}_{a_1,...,a_N} \, | \cdot \rangle := | \cdot \rangle_D$, Eq. (8.1) can be written in the following compact form $|\Phi^{(N)}\rangle_D = \sum_i \phi^i \, |\varphi^{(N)}_i\rangle_D$. The basis of the deformed elementary states $\{|\varphi^{(N)}\rangle_D\}$ is orthonormal and $|\Phi^{(N)}\rangle_D$ is normalized. Finally the probability to find $|\Phi^{(N)}\rangle_D$ in $|\varphi^{(N)}_i\rangle_D$ is always ϕ^i. *In other words, for NIP a deformation of this type is a unitary transformation.*

On the other hand, consider now a system of distinguishable IP. Eq. (8.1) becomes

$$D^{(N)}_{a_1,...,a_N} |\Phi^{(N)}\rangle = \sum_i \phi^i \, |U^{(1)}_{a_1} 1_i, U^{(1)}_{a_2} 2_i, ...\rangle \, , \tag{8.4}$$

where each N-particle elementary state in the linear combination is written in the no-label formalism (see Chapter 2), thus it is an overall object which cannot be decomposed in terms of tensor products.

Take, as an example, the case $N = 2$: the scalar product $\langle 1_j, 2_j | 1_i, 2_i \rangle = \delta_{ij}$ (see Section 2.2 of Chapter 2). After a deformation, the scalar product of the i-th deformed state with the j-th one is

$$\langle U^{(1)}_{a_1} 1_j, U^{(1)}_{a_2} 2_j | U^{(1)}_{a_1} 1_i, U^{(1)}_{a_2} 2_i \rangle = \delta_{ij} + \langle 1_j | U^{(1)\dagger}_{a_1} U^{(1)}_{a_2} | 2_i \rangle \langle 2_j | U^{(1)\dagger}_{a_2} U^{(1)}_{a_1} | 1_i \rangle. \tag{8.5}$$

The presence of the second term in the RHS of Eq. (8.5) makes the difference with the analo-

gous NIP case. This term is in general different from zero, thus $D^{(N)}_{a_1,\ldots,a_N}$ does not preserves the scalar products: in other words, *the deformation is not in general a unitary operation for IP. The introduced class of N-particle deformations is unitary for NIP and not unitary for IP.*
From now on, I will consider IP systems.
The set of the deformed N-particles vectors $\{|\varphi_i^{(N)}\rangle_D\}$ remains complete but, in general, non-orthonormal and the state $|\Phi^{(N)}\rangle_D$ results unnormalized. After a deformation, ϕ^i are not anymore the probability to find $|\Phi^{(N)}\rangle_D$ in $|\varphi_i^{(N)}\rangle_D$. In order to obtain probability amplitudes one must normalize both the deformed state and the deformed basis. Thus, considering the following scalar product

$$ {}_D\langle\varphi_i^{(N)}|\Phi^{(N)}\rangle_D = \sum_j a_{ij}\phi^j = \phi_i, \tag{8.6}$$

where I introduced the coefficient $a_{ij} = {}_D\langle\varphi_i^{(N)}|\varphi_j^{(N)}\rangle_D$, one has ${}_D\langle\Phi^{(N)}|\Phi^{(N)}\rangle_D = \sum_i \phi^{i*}\phi_i := \mathcal{N}$ and ${}_D\langle\varphi_i^{(N)}|\varphi_i^{(N)}\rangle_D = \mathcal{N}_i$. The normalized deformed elementary states are $|\bar{\varphi}_i^{(N)}\rangle_D = |\varphi_i^{(N)}\rangle_D / \sqrt{\mathcal{N}_i}$ and in this basis the normalized deformed state $|\bar{\Phi}^{(N)}\rangle_D$ is

$$ |\bar{\Phi}^{(N)}\rangle_D = \sum_i \frac{\phi^i\sqrt{\mathcal{N}_i}}{\sqrt{\mathcal{N}}} |\bar{\varphi}_i^{(N)}\rangle_D . \tag{8.7}$$

By using Eqs. (8.6) and (8.7), one obtains that the probability amplitude of finding the state $|\bar{\Phi}^{(N)}\rangle_D$ in the state $|\bar{\varphi}_i^{(N)}\rangle_D$ is

$$ \begin{aligned} \bar{\phi}_i = {}_D\langle\bar{\varphi}_i^{(N)}|\bar{\Phi}^{(N)}\rangle_D &= \sum_j a_{ij}\frac{\phi^j}{\sqrt{\mathcal{N}\mathcal{N}_i}} \\ &= \frac{\phi_i}{\sqrt{\mathcal{N}\mathcal{N}_i}}. \end{aligned} \tag{8.8}$$

If the transformed complete basis $\{|\bar{\varphi}_j^{(N)}\rangle_D\}$ is orthogonal, i.e. ${}_D\langle\bar{\varphi}_i^{(N)}|\bar{\varphi}_j^{(N)}\rangle_D = \delta_{ij}$, the probability amplitudes are $\bar{\phi}_i = \phi^i\sqrt{\mathcal{N}_i}/\sqrt{\mathcal{N}}$.

8.3 Elementary deformation of mixed states

The previous results can be extended to the case of a generic mixed N-IP mixed state

$$ \rho^{(N)} = \sum_{ij} w^{ij} |\varphi_i^{(N)}\rangle \langle\varphi_j^{(N)}| , \tag{8.9}$$

written in the orthonormal basis $\{|\varphi_i\rangle\}$. Applying an N-particle deformation $D^{(N)}_{a_1,...,a_N}$, one obtains the following normalized deformed state

$$\bar{\rho}^{(N)}_D = \sum_{ij} \frac{w^{ij}\sqrt{\mathcal{N}_i\mathcal{N}_j}}{\mathrm{Tr}[\rho^{(N)}_D]} \, |\bar{\varphi}^{(N)}_i\rangle_D \, \langle\bar{\varphi}^{(N)}_j| \, . \tag{8.10}$$

expressed in terms of the elementary normalized states. The population of each state $|\bar{\varphi}^{(N)}_i\rangle_D$ becomes

$$\begin{aligned} p_i = \ {}_D\langle\bar{\varphi}^{(N)}_i|\bar{\rho}^{(N)}_D|\bar{\varphi}^{(N)}_i\rangle_D &= \sum_{kj} \frac{w^{kj}a_{ik}a_{ji}}{\mathrm{Tr}[\rho^{(N)}_D]\,\mathcal{N}_i} \\ &= \frac{w_{ii}}{\mathrm{Tr}[\rho^{(N)}_D]\,\mathcal{N}_i}, \end{aligned} \tag{8.11}$$

where, as in the previous section $a_{ij} =_D \langle\varphi^{(N)}_i|\varphi^{(N)}_j\rangle_D$ and $w_{ii} = \sum_{kj} w^{kj}a_{ik}a_{ji}$. If the complete set of states $\{|\bar{\varphi}^{(N)}_i\rangle_D\}$ is orthogonal, populations are $p_i = \dfrac{w^{ii}\mathcal{N}_i}{\mathrm{Tr}[\rho^{(N)}_D]}$.

From Eqs. (8.10) and (8.11), it emerges that the deformation can be obtained by applying a convex quasi-linear map [164]. In fact, given a convex set of density matrices ρ_i and $p_i \in [0,1]$, with $\sum_i p_i = 1$, and the state $\rho = \sum_i p_i\rho_i$, the deformation map $\mathcal{D}$ acts as

$$\mathcal{D}[\rho] = \frac{D\rho D^\dagger}{\mathrm{Tr}[DD^\dagger\rho]} = \sum_i \bar{p}_i\mathcal{D}[\rho_i], \tag{8.12}$$

with

$$\bar{p}_i = p_i\frac{\mathrm{Tr}[DD^\dagger\rho_i]}{\mathrm{Tr}[DD^\dagger\rho]} \ \text{ and } \ \mathcal{D}[\rho_i] = \frac{D\rho_iD^\dagger}{\mathrm{Tr}[D^\dagger D\rho_i]}. \tag{8.13}$$

where $D \equiv D_{\vec{a}}$ (being $\vec{a} = a_1, ..., a_N$ the set of physical parameters associated to the deformation).

8.4 Applications

In this section, I will treat the effects of the spatial deformations of two paradigmatic states, the Werner and the Bell-diagonal states, generalizing them to the case of indistinguishable particles. Finally I will shown how deformations influence the internal energy variation of IP systems.

8.4.1 Deformation of the Werner state

Consider two spatially separated identical qubits, one in the spatial state $|\psi\rangle$ and the other one in $|\psi'\rangle$, prepared in the Werner state W [22]

$$W = (1-p)\,|i\rangle\,\langle i| + \frac{p}{4}\mathbb{I}, \tag{8.14}$$

where $|i\rangle$ is one of the four orthonormal Bell states

$$\begin{aligned} |2_\pm\rangle &= \frac{1}{\sqrt{2}}(|\psi\downarrow,\psi'\downarrow\rangle \pm |\psi\uparrow,\psi'\uparrow\rangle), \\ |1_\pm\rangle &= \frac{1}{\sqrt{2}}(|\psi\downarrow,\psi'\uparrow\rangle \pm |\psi\uparrow,\psi'\downarrow\rangle). \end{aligned} \tag{8.15}$$

and $\mathbb{I} = \sum_{i=1_\pm,2_\pm} |i\rangle\,\langle i|$ is the identity operator. Physically, this state describes the presence, with a probability p, of a white noise [17, 16], represented by the term $\mathbb{I}/4$, in the initial preparation of a Bell state $|i\rangle$. Let me now apply a deformation $D^{(2)}_{\psi,\psi'}$, acting only on the spatial degrees of freedom ψ and ψ', which modifies the shape of the 1-particle wave functions such that $|U^{(1)}_\psi\psi\rangle := |\tilde{\psi}\rangle$ and $|U^{(1)}_{\psi'}\psi'\rangle := |\tilde{\psi}'\rangle$ spatially overlap, as follows

$$|\psi\sigma,\psi'\tau\rangle_D = |(U^{(1)}_\psi\psi)\sigma,(U^{(1)}_{\psi'}\psi')\tau\rangle = |\tilde{\psi}\sigma,\tilde{\psi}'\tau\rangle\,. \tag{8.16}$$

If $|\tilde{\psi}\rangle$ and $|\tilde{\psi}'\rangle$ are not orthogonal, the set $\{|i\rangle_D\}$ of the deformed Bell states becomes unnormalized but it remains orthogonal. I now define the deformed *IP-Bell states*, that is the generalization to IP, for any spatial overlap of the 1-particle wave functions, of the Bell states for distinguishable particles of Eq. (8.15), as

$$\begin{aligned} |\bar{2}_\pm\rangle_D &:= \frac{1}{\sqrt{2\mathcal{N}_{2_\pm}}}(|\psi\downarrow,\psi'\downarrow\rangle_D \pm |\psi\uparrow,\psi'\uparrow\rangle_D), \\ |\bar{1}_\pm\rangle_D &:= \frac{1}{\sqrt{2\mathcal{N}_{1_\pm}}}(|\psi\downarrow,\psi'\uparrow\rangle_D \pm |\psi\uparrow,\psi'\downarrow\rangle_D), \end{aligned} \tag{8.17}$$

with $\mathcal{N}_{2_\pm} = \mathcal{N}_{1_+} = (1+\eta|\langle\tilde{\psi}|\tilde{\psi}'\rangle|^2)$ and $\mathcal{N}_{1_-} = (1-\eta|\langle\tilde{\psi}|\tilde{\psi}'\rangle|^2)$.
Deforming the state of Eq. (8.14) as $D^{(2)}_{\psi,\psi'}WD^{(2)\dagger}_{\psi,\psi'}$, I define the deformed *IP-Werner state* as

$$\bar{W}_D := \frac{1}{\mathcal{N}}\left((1-p)\mathcal{N}_i\,|\bar{i}\rangle_D\,\langle\bar{i}| + \frac{p}{4}\sum_{k=1_\pm,2_\pm}\mathcal{N}_k\,|\bar{k}\rangle_D\,\langle\bar{k}|\right), \tag{8.18}$$

where $\mathcal{N}$ is such that $\mathrm{Tr}[\bar{W}_D] = 1$ and $|\bar{i}\rangle_D$ are the IP-Bell states of Eq. (8.17). The state $\bar{W}_D$ reduces to the standard Werner state for NIP when there is no spatial overlap between particles or the shifted single-particle wavefunctions are orthogonal. The state $\bar{W}_D$ can be physically

obtained after the action of a depolarizing channel on the i-th IP-Bell state [69].

The deformation not only modifies the population $(1-p)\mathcal{N}_i$ of the pure deformed state $|\bar{i}\rangle_D$ that we want to prepare, but also influences the effect of the environment on the system: in fact, in contrast to what happens with the Werner state for distinguishable particles, $\mathbb{I}_D = \sum_{k=1_\pm,2_\pm} \mathcal{N}_k |\bar{k}\rangle_D \langle\bar{k}|$ does not have the properties of the identity operator,i.e. acting on a two-particle state, it does not leave it unchanged. As a result, $\mathbb{I}_D$ is not a white noise as for the standard Werner state of Eq. (8.14), but a coloured one. As shown in Chapter 6, spatial deformations of the Werner state, modifying the degree of spatial indistinguishability of particles (see Section 3.5 of Chapter 3), determine a noise-free nonlocal quantum entanglement preparation.

8.4.2 Decoupling induced by deformations

The previous theory of spatial deformations gives the opportunity to recover, in a formal way, some physical behaviours of IP quantum systems as function of the continuous variation of the spatial indistinguishability. I shall present an example.

Consider two spatially separated identical qubits, one in the spatial state $|\psi\rangle$ and the other one in $|\psi'\rangle$ and let me prepare them in the Bell-diagonal state

$$\rho = \sum_{i=1_\pm,2_\pm} p^i |i\rangle \langle i| , \tag{8.19}$$

where $|i\rangle$ is one of the four orthonormal Bell states of Eq. (8.15) and p^i is the probability that the system occupies the i-th Bell state, with $\sum_i p^i = 1$.

Let me now apply a 2-particle spatial deformation on the system such that the deformed 1-particle wave functions $|\tilde{\psi}\rangle$ and $|\tilde{\psi}'\rangle$ spatially overlap. One thus obtains the *IP Bell-diagonal state*, that is the generalization to IP, for any spatial overlap of the 1-particle wave functions, of the Eq. (8.19), whose expression is

$$\bar{\rho}_D = \frac{1}{\mathcal{N}} \sum_{i=1_\pm,2_\pm} p^i \mathcal{N}_i |\bar{i}\rangle_D \langle\bar{i}| , \tag{8.20}$$

where

$$\begin{aligned} &\mathcal{N}_{2_\pm} = \mathcal{N}_{1_+} = (1+\eta|\langle\tilde{\psi}|\tilde{\psi}'\rangle|^2), \\ &\mathcal{N}_{1_-} = (1-\eta|\langle\tilde{\psi}|\tilde{\psi}'\rangle|^2) \\ &\mathcal{N} = \sum_i p^i \mathcal{N}_i \end{aligned} \tag{8.21}$$

and $|\bar{i}\rangle_D$ are the IP-Bell states of Eq. 8.17. The population of each state $|\bar{i}\rangle_D$ is

$$\bar{p}^i = p^i \mathcal{N}_i / \mathcal{N} \tag{8.22}$$

with $\sum_i \bar{p}^i = 1$. The state of Eq. (8.20) reduces to the standard one for distinguishable particles of Eq. (8.19) when particles are spatially separated.

Now I will show an interesting aspect consequence of deformations, that is how some states "decouple" from the physical processes because of the fermionic and bosonic statistics. The state of Eq. (8.20) takes into account the bosonic and fermionic behaviour of the system: in fact, the population of each of the four IP-Bell states satisfies all the requirements of the particle statistics, as continuous functions of the indistinguishability. In fact, for bosons ($\eta = 1$), when the deformed 1-particle wave functions are such that $|\tilde{\psi}\rangle \longrightarrow |\tilde{\psi}'\rangle$, one physically expects that the Bell state $|\bar{1}_-\rangle$ of Eq. (8.17) tends to decouple from all the physical processes, since it becomes an antisymmetric combination under exchange of the two particles. Consistently with that, in the classical mixture of Eq. (8.20), its population is such that it continuously decreases increasing the spatial overlap of the deformed spatial wave functions, up to the limit in which

$$\lim_{\tilde{\psi} \longrightarrow \tilde{\psi}'} \bar{p}^{1-} = 0, \tag{8.23}$$

since $\mathcal{N}_{1_-} \longrightarrow 0$ (Eq.(8.22)).

Analogously, for fermions ($\eta = -1$), in the same limit the states $|\bar{2}_\pm\rangle$ and $|\bar{1}_+\rangle$ are physically not allowed: in fact, the first two ones are excluded for the Pauli exclusion principle, containing fermions with the same pseudospin, and the latter becomes a symmetric combination under exchange of the two fermions. Consistently with that, their populations in the IP-Bell diagonal state decrease, increasing the spatial overlap of the deformed spatial wavefunctions, up to the limit in which

$$\lim_{\tilde{\psi} \longrightarrow \tilde{\psi}'} \bar{p}^k = 0, \qquad k = 1_+, 2_\pm, \tag{8.24}$$

since $\mathcal{N}_{1_+} \longrightarrow 0$ (Eq.(8.22)).

All the four Bell states exist for both bosons and fermions but, incresing their spatial overlap with a deformation, the probability amplitudes of occupying some of them decreases up to zero[1]. Such a type of decoupling is ordinarily imposed, when one considers systems of bosons or fermions, as an initial condition. This decoupling can be followed, by means of sLOCC, as function of the continuously variable spatial indistinguishability (introduced in Chapter 3). In fact, suppose that the 1-particle states appearing in the state of Eq. (8.20) have the following

[1]This point of view recalls the way in which Quantum Field Theory treats the longitudinal mode of massive photons, when the mass goes to zero. It describes the absence of this third degree of freedom showing that it exists, but the probability amplitude of emitting a photon with the longitudinal mode tends to zero in the zero mass limit [165, 166].

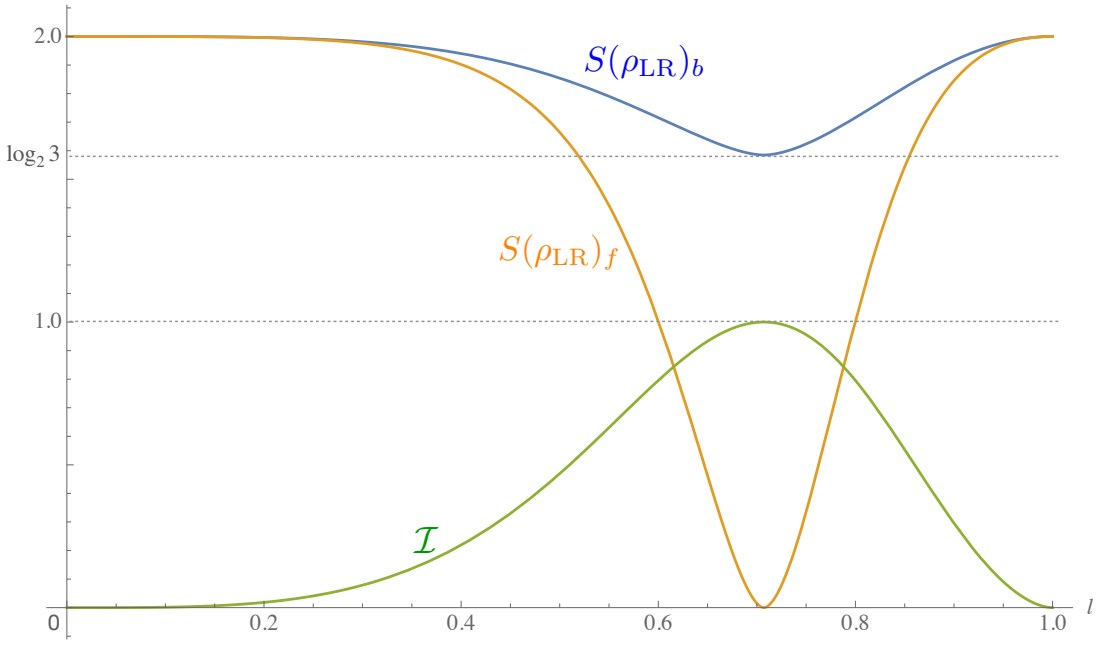

Figure 8.1: Von Neumann Entropy of $\rho_{\rm LR}$ for both bosons ($S(\rho_{\rm LR})_b$, blue curve) and fermions ($S(\rho_{\rm LR})_f$, orange curve), and degree of spatial indistinguishability ($\mathcal{I}$, green curve) in function of the probability amplitude l, when $p^i = 1/4,\ \forall i$ and $r' = l$.

specific form

$$|\tilde{\psi}\rangle = l\,|{\rm L}\rangle + r\,|{\rm R}\rangle\,,\ |\tilde{\psi}'\rangle = l'\,|{\rm L}\rangle + r'\,|{\rm R}\rangle\,, \tag{8.25}$$

and project Eq. (8.20) in the subspace spanned by $\mathcal{B}_{\rm LR} = \{|{\rm L}\sigma, {\rm R}\tau\rangle\,;\ \sigma,\tau = \downarrow,\uparrow\}$, where $|{\rm L}\rangle$ and $|{\rm R}\rangle$ are specific quantum states peaked in correspondence of two spatially separated regions $\mathcal{L}$ and $\mathcal{R}$, obtaining $\rho_{\rm LR} = \Pi^{(2)}_{\rm LR}\rho\Pi^{(2)}_{\rm LR}/{\rm Tr}(\Pi^{(2)}_{\rm LR}\rho)$, where we have used the projector $\Pi^{(2)}_{\rm LR} = \sum_{\sigma,\tau=\uparrow,\downarrow} |{\rm L}\sigma, {\rm R}\tau\rangle\langle {\rm L}\sigma, {\rm R}\tau|$. I recall the degree of spatial indistinguishability, introduced in Eq.(3.15) of Section 3.5

$$\mathcal{I} = -\sum_i^2 p^{(i)}_{\rm LR}\log_2 p^{(i)}_{\rm LR}, \tag{8.26}$$

where $p^{(1)}_{\rm LR} = |lr'|^2/(|lr'|^2 + |l'r|^2)$ and $p^{(2)}_{\rm LR} = 1 - p^{(1)}_{\rm LR}$. By assuming that the probability amplitude of finding $|\tilde{\psi}\rangle$ in $|{\rm L}\rangle$ is always equal to the one to find $|\tilde{\psi}'\rangle$ in $|{\rm R}\rangle$, i.e. $r' = l$, the behaviour of $\mathcal{I}$ is shown by the green curve of Figure 8.1. When l is 0 or 1, particles do not spatially overlap, so their indistinguishability is null. It reaches the maximum value when $l = 1/\sqrt{2}$.

The von Neumann entropy of $\rho_{\rm LR}$ is $S(\rho_{\rm LR}) = -\sum_i \lambda^{\rm LR}_i \log_2 \lambda^{\rm LR}_i$, where $\lambda^{\rm LR}_i$ are the eigenvalues of $\rho_{\rm LR}$, and in Figure8.1 its behaviour is shown in function of the probability amplitude l for both bosons (blue curve) and fermions (orange curve), in the particular case in which $r' = l$ and $\bar{p}^i = 1/4$, $\forall i$. The two curves physically represent how the von Neumann entropy behaves

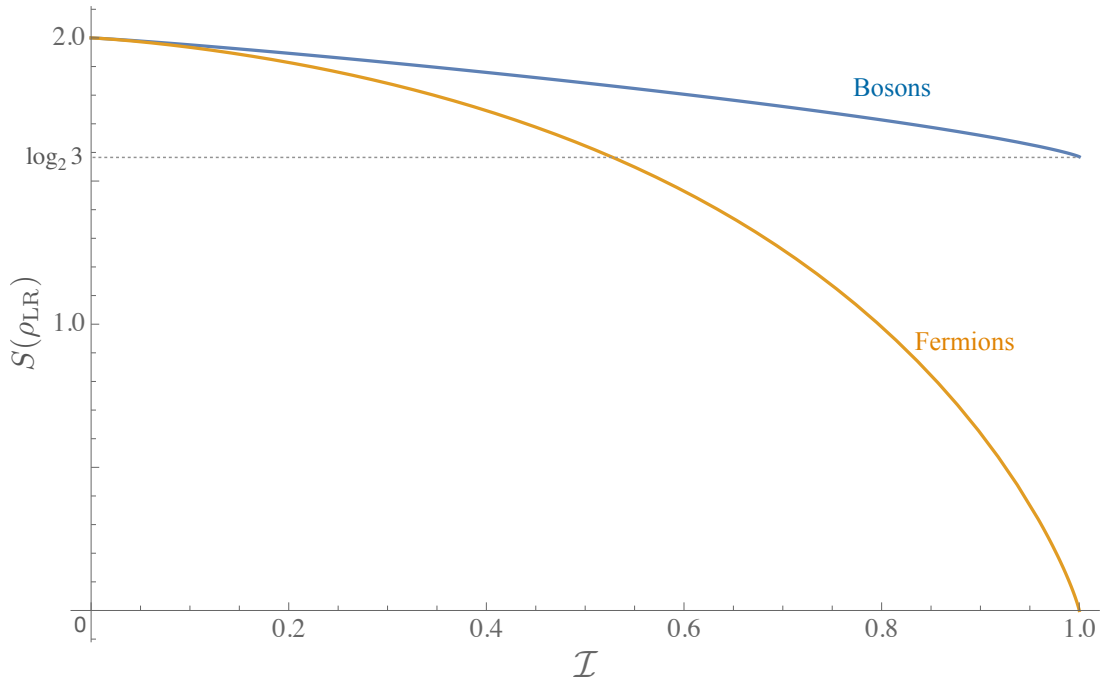

Figure 8.2: Von Neumann Entropy of ρ_{LR} in function of the degree of spatial indistinguishability $\mathcal{I}$ for bosons (blue curve) and fermions (orange curve) when $p^i = 1/4,\ \forall i$ and $r' = l$.

by changing the spatial indistinguishability of $|\tilde{\psi}\rangle$ and $|\tilde{\psi}'\rangle$. When l is 0 or 1, particles in the two 1-particle states $|\tilde{\psi}\rangle$ and $|\tilde{\psi}'\rangle$ are completely spatially distinguishable ($\mathcal{I}_{\mathrm{LR}} = 0$) and $\bar{\rho}_D$ of Eq. (8.20) is the maximally mixed state: the 2-particle system occupies with the same probability the four Bell states and $S(\rho_{\mathrm{LR}})$ joints for both bosons and fermions, as expected, the maximal entropy for a system of two qubits, i.e. $S(\rho_{\mathrm{LR}}) = 2$ (Holevo bound [167]). Increasing l, the spatial overlap of $|\tilde{\psi}\rangle$ and $|\tilde{\psi}'\rangle$ increases and some of the deformed IP-Bell states tend to become unphysical. For bosons only three generalized Bell states tend be populated for $|\tilde{\psi}\rangle \longrightarrow |\tilde{\psi}'\rangle$ (Eq. (8.23)): $\mathcal{I}_{\mathrm{LR}} \longrightarrow 1$ and the system behaves like a qutrit, in fact $S(\rho_{\mathrm{LR}})$ joints the maximal value achievable for a qutrit, i.e. $S(\rho_{\mathrm{LR}}) = \log_2 3$ (Holevo bound [167]), as shown by the blue curve in Fig.8.1. On the other hand, for fermions the state of Eq. (8.20) tends to the pure state $|1_-\rangle\langle 1_-|$ (Eq. (8.24)) and $S(\rho_{\mathrm{LR}})$ reaches zero (orange curve in Fig.8.1). When the spatial indistinguishability $\mathcal{I}$ (green curve in Fig.8.1) reaches 1, i.e. for $l = 1/\sqrt{2}$, entropy is minimum for both bosons and fermions . Finally, when the wave functions of the two IP tend to become exactly the same, the initial 2-qubit mixed state is analogous to the maximally mixed state of a qutrit, for bosons, and to a 2-qubit pure state, for fermions. In Figure 8.2 the behaviour of von Neumann entropy of ρ_{LR} as a function of the degree of spatial indistinguishability $\mathcal{I}_{\mathrm{LR}} := \mathcal{I}$ for both bosons and fermions is shown.

The chosen sLOCC framework gives also the possibility to give a measure of the mutual information [16] for the IP-Bell diagonal state. I recall that the quantum mutual information

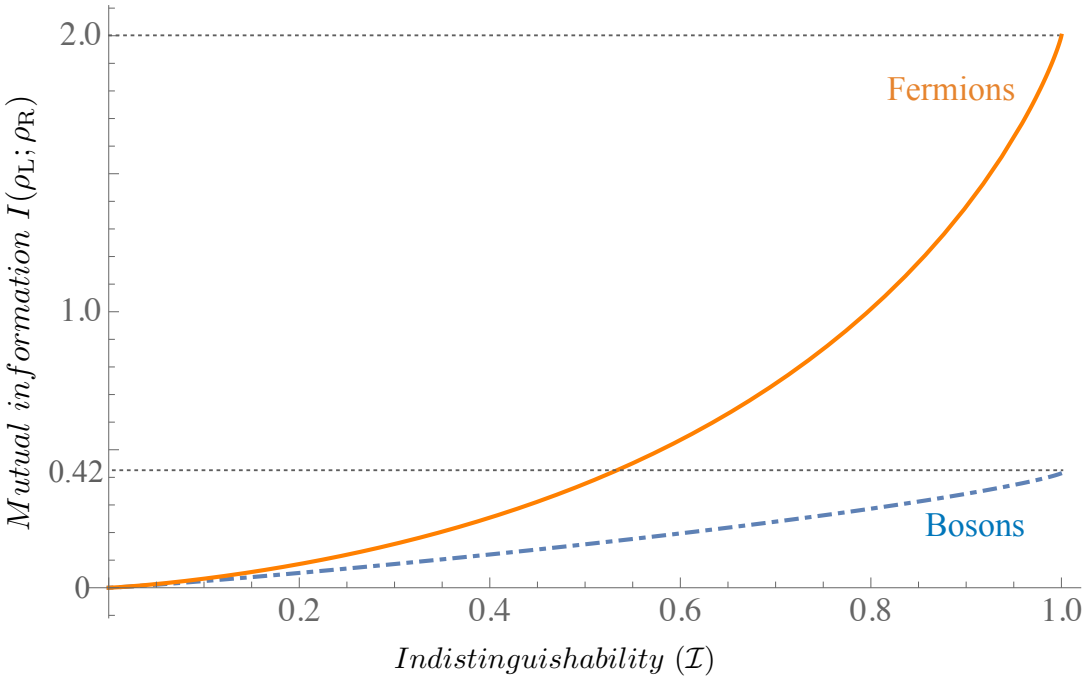

Figure 8.3: sLOCC-based Mutual information for the IP Bell-diagonal state of Eq. (8.20) when $p^i = 1/4\ \forall i$ in function of the degree of IP spatial indistinguishability.

expresses how much uncertainty one has about a composite system, expressed by its von Neumann, by looking at all the system, with respect to the uncertainty that one has by looking at the subsystems. Or differently formulated: quantum mutual information of a bipartite system is the average information which one obtains about a subsystem after a measurement performed on the other subsystem [16]. The mutual information for the IP Bell-diagonal state is

$$I(\rho_{\mathrm{L}};\rho_{\mathrm{R}}) = S(\rho_{\mathrm{L}}) + S(\rho_{\mathrm{R}}) - S(\rho_{\mathrm{LR}}) \tag{8.27}$$

where $\rho_{\mathrm{L}} = \mathrm{Tr}_{\mathrm{R}}(\rho_{\mathrm{LR}})$ and $\rho_{\mathrm{R}} = \mathrm{Tr}_{\mathrm{L}}(\rho_{\mathrm{LR}})$ are the 1-particle reduced density matrices localized in $\mathcal{L}$ and $\mathcal{R}$ respectively.

Thanks to the sLOCC framework, also initially overlapping IP become addressable in separate locations and mutual information can be directly linked to their spatial indistinguishability linked to the initial spatial overlap.

The behaviour of $I(\rho_{\mathrm{L}};\rho_{\mathrm{R}})$ in function of the degree of spatial indistinguishability is shown in Figure 8.3. For both bosons and fermions, the mutual information is zero when $\mathcal{I}$ is zero. In fact, in this case, from Eq. (8.22) one sees that the populations of the for Bell states are $\bar{p}^i = p^i = 1/4$, $\forall i$: a Bell diagonal state for distinguishable particles is separable when all the population are less than 1/2. Therefore the IP-Bell diagonal state does not present quantum correlations and a measure on $\mathcal{L}$ does not give me any information about the system in $\mathcal{R}$. By increasing the

spatial indistinguishability, on the other hand, correlations between the overlapping particles arise, increasing the value of the mutual information. For fermions it reaches the maximum value, since the system occupies only the maximally entangled IP-Bell state $|1_{-}\rangle$.

8.4.3 Quantum thermodynamical first principle for identical particles

Operations on a quantum system can have different effects, e.g. either changes in the energy spectrum or in the energy eigenvalues or both. Let me consider for example a spin 1/2 in null magnetic field: by switching on the field, changes are in the eigenvalues, not in the eigenstates. On the other hand, if we consider the rotation along x of a spin 1/2 along z, the eigenvalues are always $\pm 1/2$ but the eigenstates are different. Finally, a double-well potential with a finite central barrier presents changes on both energy eigenvalues and eigenstates by changing the barrier's height.

Suppose to have a system of two spatially nonoverlapping IP, whose hamiltonian is $H = \sum_i \epsilon^i \left|\varphi_i^{(2)}\right\rangle \left\langle\varphi_i^{(2)}\right|$, where ϵ_i and $\left|\varphi_i^{(2)}\right\rangle$ are the energy eigenvalues and the 2-particle eigenvectors, respectively. The system is in the two-particle mixed state $\rho^{(2)} = \sum_i w^i \left|\varphi_i^{(2)}\right\rangle \left\langle\varphi_i^{(2)}\right|$. I now suppose to deform adiabatically the system in such a way that at the end the Hamiltonian has the most general form $H_D = \sum_i \epsilon_D^i \mathcal{N}_i \left|\bar{\varphi}_i^{(2)}\right\rangle_D \left\langle\bar{\varphi}_i^{(2)}\right|$, where the new energy eigenvalues have a contribution ϵ_D^i due to the changes in the old eigenvalues and $\mathcal{N}_i$ due to the deformation of the eigenstates. $\left|\bar{\varphi}_i^{(2)}\right\rangle_D$ are the normalized deformed states, following the notation introduced in Section 8.2. The states $\{\left|\bar{\varphi}_i^{(2)}\right\rangle_D\}$ are supposed orthonormal, as a result they remain eigenstates of the deformed hamiltonian. According to the adiabatic theorem, the system will be in the deformed state $\bar{\rho}_D^{(2)} = \sum_i p^i \left|\bar{\varphi}_i^{(N)}\right\rangle_D \left\langle\bar{\varphi}_i^{(N)}\right|$, where $p^i = \dfrac{w^i \mathcal{N}_i}{\mathcal{N}}$ and $\mathcal{N} = \sum_i w^i \mathcal{N}_i$: in other words, it remains in a classical mixture of the eigenstates of the hamiltonian of the system after the transformation. The internal energy of the system is $U = \mathrm{Tr}[\bar{\rho}_D^{(2)} H_D] = p_i \epsilon_D^i \mathcal{N}_i$. From the expression of U I have,

$$\begin{aligned} dU = &\underbrace{\sum_i \frac{\epsilon_D^i w^i \mathcal{N}_i}{\mathcal{N}} \left(2d\mathcal{N}_i - \frac{\mathcal{N}_i}{\mathcal{N}} \sum_j w^j d\mathcal{N}_j \right)}_{\mathrm{A}} \\ &- \underbrace{\sum_i \frac{\epsilon_D^i w^i (\mathcal{N}_i)^2}{\mathcal{N}^2} \sum_j \mathcal{N}_j dw^j}_{\mathrm{B}} \\ &+ \sum_i \underbrace{\frac{(\mathcal{N}_i)^2}{\mathcal{N}} (\epsilon_D^i dw^i + w^i d\epsilon_D^i))}_{\mathrm{C}}. \end{aligned} \tag{8.28}$$

The A and B terms are intrinsically linked to the identity of particles. In fact, if particles are nonidentical one has that $\mathcal{N}_i = 1$ and $\mathcal{N} = \sum_i w^i = 1$. As a result, $d\mathcal{N}_i = 0$ and

$\sum_j dw^i = d\sum_j w^j = 0$ (in other words, the sum of the variations of the populations w^i is 1, since for NIP the deformation is unitary), therefore only the C term is present, becoming $dU = \sum_i (\epsilon^i dw^i + w^i d\epsilon^i)$, as expected.

From Eq. (8.28) it results that is present a further contribution to the internal energy variation due only to the indistinguishability.

8.5 Discussions

In this Chapter, I presented a class of operations, called *deformations* which are always unitary for NIP, while can be non unitary for IP depending on their spatial configuration. I have then presented some applications showing the effects of deformations on paradigmatic states, that is the Werner and Bell-diagonal states. It emerged that the white noise of Werner state becomes a coloured noise when particles becomes indistinguishable; in the case of the Bell diagonal state, one sees that, as a consequence of the deformations, some of the Bell states decouple from the rest of the system, not anymore contributing to physical processes. Finally, I have shown that IP indistinguishability affects the first principle of quantum thermodynamics, introducing a statistics-dependent variation of the internal energy of a deformed state.

Chapter 9

Conclusions

Quantum identical particles (IP) have always attracted interest not only for their fundamental differences from their classical counterpart, but also for the interesting features of their quantum states compared to the ones of nonidentical particles (NIP). They are also the main components of quantum platforms used for quantum information processes and quantum computing [71, 72, 75]. Therefore, the attention for their properties has increased with the aim of optimize the existent quantum technologies and to conceive new ones.

Quantum information theory basically relies on the concept of entanglement, a feature coming from the possibility of creating quantum states as linear combinations of different multiparticle configurations [17].

Therefore, both from the fundamental and experimental points of view, it is interesting to understand the interplay between the quantum nature of IP and their entanglement. However, in the attempt to reach this goal, some difficulties have come to the light. Although the IP unaddressability (they are "*quanta without individuality*" [57]), in quantum mechanics the standard approach (SA) treats them as they are nonidentical, by attributing them unobservable (mock) labels and symmetrizing their quantum states with respect to these labels. Bosonic and fermionic statistics then arise associated to the symmetric and antisymmetric structure, respectively, of quantum states, while problems emerge in the characterization of entanglement between IP. In fact, because of the presence of mock labels, all the IP states possess an unseparable structure which is recognised as entangled by using the known tools for NIP [14]. However the doubt is that this type of entanglement is a consequence of the symmetrization postulate and so it is entirely or partially fictitious. A case when the whole unphysical nature of this formal entanglement is evident is the one of independently prepared and space-like separated IP: according to the usual tools to quantify entanglement of NIP, they are always "formally" entangled, although it is "physically" natural that it is not the case. No measurements performed on one electron in the universe is affected by the mere presence of another electron in another remote part of the universe separated by the first by a spacelike interval, if they never interacted before.

The most obnoxious problem arises in the quantification and exploitation of the entanglement of spatially overlapping IP, where particle statistics directly influences their quantum behaviour. In fact, in this case, the SA-symmetrization postulate with respect to unphysical labels is necessary. The difficulties arise from the fact that, because of particle unaddressability, not only local operations and classical communication (LOCC) cannot be operationally used to exploit IP correlations (rendering unapplicable many of the entanglement witnesses and quantifiers known for NIP), but even it is not clear how to separate, for a given amount of entanglement, the "operationally exploitable" entanglement from the "unphysical" one.

Several different theories have been developed to this purposes. Some of them have evidenced that there is an *intrinsic* entanglement, coming from the structure of quantum states [24], and a *measurement-induced* one, coming from the interplay between quantum states and observables [44]. The latter characterizes only systems of IP. The problem is that there is no agreement among these theories about the entanglement of spatially overlapping independently prepared IP. Some theories [26, 23, 24], that use the particle-based SA approach, introduced new criteria to affirm that when noninteracting particles are in the same site with opposite internal degrees of freedom, they are not entangled. However this is in contrast to the fact that in this case the presence of correlations has been experimentally shown [31]. Others introduce new definitions of entanglement in terms of the structure of observables, thus not at the state level but at that of the operators [44, 28, 27, 168], in this way substituting the concept of particle partial trace with the concept of partial trace with respect to a subalgebra. Still others resort to the second quantization (to avoid the problems arising from the mock labels of the first quantization formalism) giving new forms of entanglement [29], valid only for IP, and proposing new meachanisms to characterize it, such as the extraction procedure [155]. Nevertheless, the debate is still open.

A new particle-based formalism to treat IP, named *no-label approach*, has been introduced [33]. It has the advantage of not using labels to address particles, avoiding in this way all the misunderstandings and inconsistencies coming from the corresponding SA. It has been firstly applied to the case of two IP, showing that it is possible to use the same notions known for NIP to characterize their entanglement. In this new approach, it clearly comes out that IP quantum correlations strictly depend both on spatial overlap among particles and on spatially localised measurements. It gives the possibility to recover the result, as already experimentally shown [31], that two IP in the same site with opposite pseudospins present correlations. Also a formulation of the Schmidt decomposition (SD) of bipartite quantum systems has been given with the added advantage of treating bosons and fermions on the same footing, in this way showing the universal validity (both for NIP and IP) of the SD [35]. Within this approach, it turns out that spatial indistinguishability acts as a catalyst of IP W states, which are extremely useful in quantum information because of their robustness against the interaction with the environment

[36]. Moreover, always for two IP systems, it has led to the introduction of a new operational framework that characterizes the dependence of IP entanglement on spatial overlap in a Bell-like scenario and to use this entanglement to implement quantum teleportation [34].

The first part of this thesis treats in Chapter 1 some of the problems discussed above in the characterization of IP entanglement. In Chapters 2 and 3, original results about the foundations of the no-label formalism for a generic number N of IP are presented.

In the second part of the thesis, some original conceptual and practical consequences of particle indistinguishabiliy are presented, exploiting the tools provided by the no-label formalism.

I now shall collect the main results I have obtained.

Part I: Background and new formalism for identical particles

- ***Generalization of the no-label approach to many identical particles.***

The no-label approach for a number N of IP is presented [39], starting from the derivation, by first principles, of the basic particle statistics-dependent element, i.e. the probability amplitude between N-particle states. In this context, bosons and fermions are treated on the same footing and the usual tools known for NIP, such as the partial trace and the von Neumann entropy, recover their physical meaning and validity in the characterization of the entanglement of a bipartition of N IP. Moreover, generalized products between IP states of different dimensions, named *dot* and *wedge* products, have been introduced. This allowed us to connect the no-label approach and second quantization language, in particular obtaining the commutation rules of N-particle creation and annihilation operators by the N-particles probability amplitudes. It has been shown that, as a consequence of spatial overlap, it is not possible to directly generalize to IP some paradigmatic NIP states. For example, the W states for IP are replaced by a new type of states named spin exchanged states (SPES). It emerged also that, the well known attitude of separating the spatial and spin part for the IP states in the SA [67], here can be restated directly in the language of transition amplitudes. Finally, systems of three identical qubits have been treated [169], showing that a measurement-induced entanglement can arises, when particles are independently prepared and spatially separated, and that furthermore spatial overlap is a source of intrinsic entanglement.

- ***Introduction of an entropic measure for spatial indistinguishability***

It has been presented an operational framework based on spatially localized operations and classical communication (sLOCC) for N IP, in order to characterize, in a Bell-like scenario, the exploitable entanglement due to spatial overlap [69]. It consists in choosing N separate spatial regions in each of which the probability of finding at least one particle is different from zero. As a result, a clear dependence of the operational entanglement on the spatial overlap of particles emerges. This framework has given the lead to define the entanglement of formation also of

a generic (mixed) state of IP, analogously to the case of NIP. Finally the difference between *identity* and *indistinguishability* has been underlined: the first is an intrinsic property of particles of the same species, the second is a property depending not only on the system but also on the type of measurements that are performed on it. A measure of the amount of indistinguishability has been introduced within sLOCC. This measure, that is of entropic type, permits to associate it to the overlap of one-particle wave functions. Since these last ones can be continuously tuned, we get an experimentally friendly way to control the amount of indistinguishability and to show the dependence from it of the relevant quantities.

Part II: Consequences of indistinguishability: concepts and applications

- ***Experimental control of photon entanglement and teleportation***

An experiment which utilizes the sLOCC framework to measure and exploit quantum indistinguishability of two IP has been designed and completed. The setup, that we have theoretically proposed and that has been successively constructed, can be seen as a modified Hanbury Brown and Twiss experiment [40, 85], in which the polarization of photons have to be initialized and their spatal degrees of freedom are suitably controlled. By tuning the spatial degrees of freedom of two initially uncorrelated photons with opposite pseudospins, by means of measurements in two separate spatial regions, it has been possible to control their degree of indistinguishability and to produce an indistinguishability-dependent non local polarization entanglement. It has been shown that entanglement increases with indistinguishability which is quantified by the entropic measure presented in Chapter 3. Finally it has been proved that this type of entanglement is enough to successfully implement, with fidelities above the classical threshold (82-90%), quantum teleportation of the state of another distinguishable photon.

- ***Entanglement transfer***

A new way to obtain entanglement transfer in a large-scale quantum network has been presented, which is fundamentally activated by IP spatial indistinguishability [62]. It emerged that, compared to the standard entanglement swapping, the present process, when one uses fermions, enables remote entanglement among distant nodes: (i) with no distribution of initial entangled pairs and (ii) without performing Bell measurements. The process only requires local counting of independently-prepared IP. In such a way we overcome the drawbacks encountered in the usual entanglement transfer procedures during the initial preparation stage [122] and the final measurement phase [113, 109, 124, 125, 126, 127, 128, 129]. The process with fermions has been compared to the corresponding one with bosons and with distinguishable pairs of particles: the result is that fermions are the more advantageous.

- ***Protection from noise of entanglement preparation***

The entanglement of formation of the IP Werner state has been analysed as function of spatial indistinguishability and of the environmental noise [69]. Controlling particle spatial overlap, it emerged a lower bound for the entropic degree of indistinguishability ($\simeq 0.76$) beyond which the generated entanglement is nonlocal and completely unaffected by noise. The main result of this Chapter is that indistinguishability behaves analogously to a *topological resource* of quantum platforms made of identical qubits, enabling noise-free entanglement generation that violates the CHSH-Bell inequality.

- ***Operationally useful quantum coherence***

Quantum coherence for a system of two IP with 2-level internal degrees of freedom has been defined [61]. It emerged by sLOCC that while quantum states of independently prepared and distinguishable particles are incoherent under local operations, the analogous states with indistinguishable particles can exhibit quantum coherence. In other words, *IP spatial indistinguishability is a source of coherence*. It has been highlighted that all the concepts and tools characterising the Resource Theory of coherence for NIP can be translated to IP. An application in quantum metrology has been presented, consisting in a phase-discrimination protocol: it has been shown that coherence due to the spatial indistinguishability significantly reduces the error probability of guessing the phase by means of the optimal generalized Helstrom measurement. The efficiency of the phase-discrimination game is affected by particle statistics. A proposal to experimentally implement our theoretical scheme has been done from the Huang-Can Guo's research group, in China and the experimental work is in progress.

- ***Deformations of N-identical particle systems.***

There are transformations on many-particle systems which are implemented by acting differently on each particle. While they are unitary for NIP, they result in general, as a consequence of particle indistinguishability, nonunitary for IP. We have analysed this type of operations on IP Werner and Bell-diagonal states. In the Werner case, where the environment is represented by a white noise term, deformations change this last into a coloured one (this is in contrast with NIP case where these deformations leave the noise spectrum unchanged). The Bell-diagonal case permits to clearly evidence the appearance, because of deformations, of a new phenomenon, that is the decoupling of certain states from physical processes. This manifests itself in the fact that the probability of finding the system in these states becomes zero even if initially was not. The decoupling is a consequence of particle statistics which does not allow some physical configurations. It is clear that such a phenomenon can play a role when, for example, thermodynamics of partially overlapping IP systems is considered. Finally, a formulation of the first principle of thermodynamics for IP has been given, showing the contribution to the variation of the internal energy caused by particle indistinguishability.

Chapter 10

Acknowledgements

Questa tesi di dottorato è il risultato di un percorso scientifico ed umano durato 3 anni, da cui ho imparato che una delle cose più importanti nella vita è lavorare a qualcosa che ti renda felice. Tanti altri sono stati gli insegnamenti che ho tratto, soprattutto grazie alle persone che più mi sono state accanto e che adesso desidero ringraziare.

Ringrazio il Prof. Giuseppe Compagno, per aver accettato di intraprendere questo percoso scientifico insieme a me, per avermi aiutata a saper guardare a ciò che è veramente rilevante ed essenziale in un percorso di ricerca e per essere stato il migliore esempio che potessi desiderare di sano entusiasmo di fronte al proprio lavoro. Nessuno più di lui si illumina quando parla di Fisica. Lo ringrazio anche per avere enormemente ampliato le mie conoscenze in ambito culinario e cinematografico, facendo in modo che questo percorso diventasse un'occasione di crescita su più fronti.

Ringrazio il Dr. Rosario Lo Franco, per avermi fatta sentire subito parte integrante del gruppo e per avermi incoraggiata sempre. Le sue risate e la sua spensieratezza, unite alla sua passione per il lavoro e alla sua preparazione, mi hanno insegnato che quando il lavoro è unito al divertimento, si impara e si produce più di quanto si possa immaginare.

I miei ringraziamenti vanno anche al Prof. Antonino Messina, per aver supervisionato il mio lavoro durante il primo periodo del mio dottorato. Mi ha aiutata, scientificamente, nel far crescere il mio spirito critico, e umanamente, nel trasmettermi quanto credesse in me.

Grazie anche al Prof. Bruno Bellomo, con cui ho avuto il piacere di collaborare per un intero progetto. La sua precisione scientifica e la sua disponibilità sono davvero stati essenziali!

Ringrazio il Prof. Massimo Palma, per avere "reindossato i vecchi abiti da caposquadriglia scout", dandomi supporto in qualche momento complicato. In quanto grande appassionato di Harry Potter come me, voglio ringraziarlo per avermi aiutata a ricordare che "la felicità la si può trovare anche negli attimi più tenebrosi, se solo uno si ricorda di accendere la luce".

I miei ringraziamenti non possono non andare alla Prof. Marina Guccione per la sua infinita dolcezza, per i nostri caffè e per le nostre chiacchierate. E' stata davvero preziosa durante questi

tre anni, accompagnandomi durante scelte molto importanti.

Ringrazio La Prof. Anna Napoli e il Dr. Benedetto Militello per la loro disponibilità scientifica e umana quando è stato necessario. Grazie per le lunghe conversazioni e per essermi stati vicini quando sentivo il bisogno di affrontare nuove tematiche di ricerca.

Sono grata al Prof. Gerardo Adesso, che ha supervisionato il mio lavoro mentre ero in visiting all'Università di Nottingham, per avermi accolta nel proprio gruppo di ricerca, in cui si respira aria di costante crescita scientifica. I loro group meetings mi hanno insegnato che la collaborazione, anche in ambiti scientifici molto diversi, arricchisce enormemente il modo in cui si fa ricerca ed è fonte di entusiasmo. E' stato davvero un piacere trascorrere un mese e mezzo con loro.

A tal proposito, un ringraziamento va ai miei colleghi di Nottingham Carmine, Davide, Nicola e Mauro per aver reso il mio periodo a Nottigham davvero divertente e speciale. E ovviamente, ringrazio Fabio per essere stato un compagno di scrivania e di caffè ideale.

I'd like to thank my dear friend Rosemary Rosser, for giving me the opportunity to live in her colored and wonderful house in Nottingham, for our conversations also in French and for her making me feel so at home. Rosemary, her dog Anbu, her cats Blake and Hugo and her son Krishna have been my "english family".

I thank my colleague Farzam Nosrati, for our scientific discussions and for its contagious enthusiasm. The work with him taught me a lot!

E' adesso il momento di ringraziare il collega e amico Dario Cilluffo. E' stata una fortuna per me averlo al mio fianco in ufficio ogni giorno, perchè con la sua pazienza, le sue infinite conoscenze e la sua simpatia, ha rappresentato un punto di riferimento. Grazie per aver migliorato il mio rapporto con Mathematica e per tutte le chiacchierate scientifiche, anche in mezzo alla Natura.

Ringraziamenti speciali vanno anche alla mia carissima amica e collega Nadia Milazzo, che è stata la migliore compagna di studi di sempre e un'amica insostituibile. La fisica è più bella quando la affrontiamo insieme.

Ringrazio i miei amici e colleghi Vincenzo de Michele, Gabriele Coniglio, Antonino Madonia e Simona Mazzola: abbiamo condiviso anni di studio, lavoro e divertimento che porterò sempre con me.

Un ringraziamento speciale va anche alla mia cara amica Olga Sambataro, un'anima affine: la nostra passione per la fotografia ha rappresentato per me un rifugio e le nostre discussioni sul futuro lavorativo mi hanno sempre aiutato a capire cosa volessi fare realmente.

Naturalmente, ringrazio Gabriele, per avermi dato la spinta decisiva per cambiare punto di vista quando tutto sembrava difficile, per avermi ascoltata e capita sempre. Lo ringrazio per il legame unico che abbiamo e per essere la mia dose di colore quotidiano: questa tesi esiste anche grazie a lui.

E infine non posso che ringraziare dal profondo del cuore mia madre e dedicarle questa tesi. Il suo sostegno è stato essenziale, la sua forza è stata la mia. Le sono grata per esserci stata in ogni momento, bello o negativo, di questo dottorato, tenendomi sempre per mano. Lei è il mio regalo ed è per sempre.

Appendix A

Appendix A

Here I give the explicit derivation of equation (2.32).

- I first consider the action of $a(m',n')a^\dagger(m,n)$ on a generical N-particle state $|\phi^{(N)}\rangle$ (see equation (2.1)). Using equation (2.18)) I find:

$$\begin{aligned} a(m',n')a^\dagger(m,n)|\phi^{(N)}\rangle &= a(m',n')|m,n,1,2,...,N\rangle = \\ &= (\langle m'|m\rangle\langle n'|n\rangle + \eta\langle m'|n\rangle\langle n'|n\rangle)|\phi^{(N)}\rangle + \\ &+ \sum_{k=1}^{N}\eta^{k-1}\langle m'|k\rangle\sum_{j<k}\eta^{j-1}\langle n'|j\rangle|m,n,\not{j},\not{k}\rangle + \\ &+ \sum_{k=1}^{N}\eta^{k-1}\langle m'|k\rangle\sum_{j>k}\eta^{j-2}\langle n'|j\rangle|m,n,\not{k},\not{j}\rangle \end{aligned}$$

  where $|m,n,\not{k},\not{j}\rangle = |m,n,1,...\not{k}...,\not{j}...,N\rangle$.

- The action of $a^\dagger(m,n)a(m',n')$ on the same state is

$$\begin{aligned} a^\dagger(m,n)a(m',n')|\phi^{(N)}\rangle =& a^\dagger(m,n)\sum_{k=1}^{N}\eta^{k-1}\langle m'|k\rangle\sum_{j<k}\eta^{j-1}\langle n'|j\rangle|\not{j},\not{k}\rangle + \\ &+ a^\dagger(m,n)\sum_{k=1}^{N}\eta^{k-1}\langle m'|k\rangle\sum_{j>k}\eta^{j-2}\langle n'|j\rangle|\not{k},\not{j}\rangle = \\ &= \sum_{k=1}^{N}\eta^{k-1}\langle m'|k\rangle\sum_{j<k}\eta^{j-1}\langle n'|j\rangle|m,n,\not{j},\not{k}\rangle + \\ &+ \sum_{k=1}^{N}\eta^{k-1}\langle m'|k\rangle\sum_{j>k}\eta^{j-2}\langle n'|j\rangle|m,n,\not{k},\not{j}\rangle. \end{aligned}$$

From above equations I get

$$a(m',n')a^{\dagger}(m,n) - a^{\dagger}(m,n)a(m',n') = \langle m'|m\rangle\langle n'|n\rangle + \eta\langle m'|n\rangle\langle n'|m\rangle$$

which is the first rule of equation (2.32). Similarly, the relations in the second line of equation (2.32) can be straightforwardly proven.

Appendix B

Appendix B

B.1 Shared intermediate nodes with fermions

The four-fermion global state $|\Psi_{\mathrm{f}}^{(4)}\rangle$ is

$$\begin{aligned}|\Psi_{\mathrm{f}}^{(4)}\rangle =&\frac{1}{3}(|\mathrm{A}\downarrow,\mathrm{A}\uparrow,\mathrm{M}\downarrow,\mathrm{M}\uparrow\rangle+|\mathrm{A}\downarrow,\mathrm{A}\uparrow,\mathrm{M}\downarrow,\mathrm{B}\uparrow\rangle\\&+|\mathrm{A}\downarrow,\mathrm{A}\uparrow,\mathrm{B}\downarrow,\mathrm{M}\uparrow\rangle+|\mathrm{A}\downarrow,\mathrm{A}\uparrow,\mathrm{B}\downarrow,\mathrm{B}\uparrow\rangle\\&+|\mathrm{A}\downarrow,\mathrm{M}\uparrow,\mathrm{M}\downarrow,\mathrm{B}\uparrow\rangle+|\mathrm{A}\downarrow,\mathrm{M}\uparrow,\mathrm{B}\downarrow,\mathrm{B}\uparrow\rangle\\&+|\mathrm{M}\downarrow,\mathrm{A}\uparrow,\mathrm{B}\downarrow,\mathrm{M}\uparrow\rangle+|\mathrm{M}\downarrow,\mathrm{A}\uparrow,\mathrm{B}\downarrow,\mathrm{B}\uparrow\rangle\\&+|\mathrm{M}\downarrow,\mathrm{M}\uparrow,\mathrm{B}\downarrow,\mathrm{B}\uparrow\rangle).\end{aligned} \tag{B.1}$$

The sLOCC here consists in counting one particle in A and one in B (this entails having two particles in M) and allowing for classical communication of the outcomes. Projecting therefore the above prepared state onto the subspace spanned by the basis $\mathcal{B}_{\mathrm{f}} = \{|\mathrm{A}\,\sigma,\mathrm{M}\uparrow,\mathrm{M}\downarrow,\mathrm{B}\tau\rangle\}$ $(\sigma,\tau=\downarrow,\uparrow)$, I find the post-selected state

$$|\Psi_{\mathrm{f,PS}}^{(4)}\rangle = |\mathrm{M}\uparrow,\mathrm{M}\downarrow\rangle \wedge |1_{\mathrm{AB}}^{-}\rangle\,, \tag{B.2}$$

which is obtained with probability $P_{\mathrm{f}}(4) = |\langle\Psi_{\mathrm{f,PS}}^{(4)}|\Psi_{\mathrm{f}}^{(4)}\rangle|^2 = 2/9$ and where

$$|1_{\mathrm{AB}}^{-}\rangle = \frac{|\mathrm{A}\downarrow,\mathrm{B}\uparrow\rangle - |\mathrm{A}\uparrow,\mathrm{B}\downarrow\rangle}{\sqrt{2}} \tag{B.3}$$

is one of the maximally entangled Bell states (the number 1 in the ket indicates the number of excited spins in the state).

The scheme presented for the minimum core with four particles can be extended to the case of $n = 2N$ particles, where N is the number of involved particle pairs. The generalized scheme

with $k = N - 1$ shared intermediate nodes M_i ($i = 1, \ldots, k$) is displayed in Fig. 5.1 of the main text.

Each j-th pair ($j = 1, \ldots, N$) has opposite pseudospins and (delocalized) spatial mode $|\alpha_j\rangle$, with $|\alpha_1\rangle = (|\mathrm{A}\rangle + |\mathrm{M}_1\rangle)/\sqrt{2}$, $|\alpha_N\rangle = (|\mathrm{M}_k\rangle + |\mathrm{B}\rangle)/\sqrt{2}$ and $|\alpha_j\rangle = (|\mathrm{M}_{j-1}\rangle + |\mathrm{M}_j\rangle)/\sqrt{2}$ for $j = 2, \ldots, k$. I take as the initially prepared n-fermion state $|\Psi_{\mathrm{f}}^{(n)}\rangle$ the one obtained from $|\alpha_1 \downarrow, \alpha_1 \uparrow, \ldots, \alpha_N \downarrow, \alpha_N \uparrow\rangle$ by eliminating, because of the Pauli exclusion principle, the terms with two particles in the same node with the same pseudospin. The normalization constant $\mathcal{N}_{\mathrm{f}}$ of $|\Psi_{\mathrm{f}}^{(n)}\rangle$ can be conveniently expressed as $\mathcal{N}_{\mathrm{f}} = \sqrt{\det(\mathcal{M}^{(n)})}$ where $\det(\mathcal{M}^{(n)})$ is the determinant of the $n \times n$ matrix

$$\mathcal{M}^{(n)} = \begin{pmatrix} \langle \alpha_1 \downarrow | \alpha_1 \downarrow \rangle & \cdots & \langle \alpha_1 \downarrow | \alpha_N \uparrow \rangle \\ \vdots & \ddots & \vdots \\ \langle \alpha_N \uparrow | \alpha_1 \downarrow \rangle & \cdots & \langle \alpha_N \uparrow | \alpha_N \uparrow \rangle \end{pmatrix}, \tag{B.4}$$

defined in the n-dimensional one-particle basis $\{|\alpha_1 \downarrow\rangle, |\alpha_1 \uparrow\rangle, \ldots, |\alpha_N \downarrow\rangle, |\alpha_N \uparrow\rangle\}$.

The sLOCC framework is once again realized by counting one particle in each of the nodes A and B (this entails that two particles are in each node M_i), also allowing for classical communication of the counting outcomes. The post-selected global state results to be

$$|\Psi_{\mathrm{f,PS}}^{(n)}\rangle = |\Psi_{\mathrm{M}_1}^{-}, \Psi_{\mathrm{M}_2}, \ldots, \Psi_{\mathrm{M}_k}, 1_{\mathrm{AB}}^{-}\rangle, \tag{B.5}$$

where $|\Psi_{\mathrm{M}_i}\rangle = |\mathrm{M}_i \uparrow, \mathrm{M}_i \downarrow\rangle$ and $|1_{\mathrm{AB}}^{-}\rangle$ is a maximally entangled Bell state of Eq. (B.3). The probability to obtain the state above, that is the success probability of the remote entanglement transfer process, is given by $P_{\mathrm{f}}(n) = |\langle \Psi_{\mathrm{f,PS}}^{(n)} | \Psi_{\mathrm{f}}^{(n)} \rangle|^2$. It is straightforward to show that its explicit expression as a function of the number of fermions is (Figure B.1, orange points)

$$P_{\mathrm{f}}(n) = \frac{1}{2^{n-1}\det(\mathcal{M}^{(n)})}. \tag{B.6}$$

B.2 Shared intermediate nodes with bosons

The four-boson global state $|\Psi_{\mathrm{b}}^{(4)}\rangle$ is

$$|\Psi_{\mathrm{b}}^{(4)}\rangle = \frac{1}{5}|(\mathrm{A} + \mathrm{M}) \downarrow, (\mathrm{A} + \mathrm{M}) \uparrow, (\mathrm{M} + \mathrm{B}) \downarrow, (\mathrm{M} + \mathrm{B}) \uparrow\rangle. \tag{B.7}$$

The basis for sLOCC, corresponding to counting two particles in the shared intermediate mode M and one particle in each mode A and B, is $\mathcal{B}_{\mathrm{b}} = \left\{ \frac{|\mathrm{A}\ \sigma, \mathrm{M}\ \tau, \mathrm{M}\ \sigma', \mathrm{B}\ \tau'\rangle}{\mathcal{N}_{\tau\sigma'}} \right\}$ ($\sigma, \tau, \sigma', \tau' = \downarrow, \uparrow$) where $\mathcal{N}_{\tau\sigma'} = \sqrt{1 + \langle \tau | \sigma' \rangle}$. The four-boson post-selected state, after projection onto $\mathcal{B}_{\mathrm{b}}$ (also

allowing for classical communication), is then

$$|\Psi^{(4)}_{\rm b,PS}\rangle = \frac{1}{\sqrt{6}}(|{\rm A}\downarrow,{\rm M}\uparrow,{\rm M}\uparrow,{\rm B}\downarrow\rangle + |{\rm A}\downarrow,{\rm M}\uparrow,{\rm M}\downarrow,{\rm B}\uparrow\rangle + |{\rm A}\uparrow,{\rm M}\uparrow,{\rm M}\downarrow,{\rm B}\downarrow\rangle + |{\rm A}\uparrow,{\rm M}\downarrow,{\rm M}\downarrow,{\rm B}\uparrow\rangle), \tag{B.8}$$

which is found with probability $P_{\rm b}(4) = |\langle\Psi^{(4)}_{\rm b,PS}|\Psi^{(4)}_{\rm b}\rangle|^2 = 6/25$.

In the M-subspace, the Bell basis for bosons is given by the three states $|\Phi^{\pm}_{\rm M}\rangle = (|{\rm M}\downarrow,{\rm M}\downarrow\rangle \pm |{\rm M}\uparrow,{\rm M}\uparrow\rangle)/2$ and $|\Psi_{\rm M}\rangle = |{\rm M}\uparrow,{\rm M}\downarrow\rangle$. The post-selected state $|\Psi^{(4)}_{\rm b,PS}\rangle$ can be then expressed in terms of this Bell basis as

$$|\Psi^{(4)}_{\rm b,PS}\rangle = \frac{|\Psi_{\rm M},1^{+}_{\rm AB}\rangle + |\Phi^{+}_{\rm M},2^{+}_{\rm AB}\rangle - |\Phi^{-}_{\rm M},2^{-}_{\rm AB}\rangle}{\sqrt{3}}, \tag{B.9}$$

where in each term the particles in the distant sites A and B are in a Bell state (see Eq. (B.18)). Therefore, each outcome of the joint Bell measurement successfully realizes the entanglement swapping over the distant nodes A and B.

The four-particle bosonic protocol can be extended, analogously to the standard ES, by a cascaded procedure [118]. The scheme is again that of Fig. 5.2 with n independently-prepared identical bosons and $k = N-1$ intermediate nodes ($N = n/2$ is the number of particle pairs).

The initially prepared n-boson state is

$$|\Psi^{(n)}_{\rm b}\rangle = \frac{1}{\mathcal{N}_b}|\alpha_1\downarrow,\alpha_1\uparrow,\alpha_2\downarrow,\alpha_2\uparrow,\ldots,\alpha_N\downarrow,\alpha_N\uparrow\rangle, \tag{B.10}$$

where the normalization constant $\mathcal{N}_b = \sqrt{{\rm perm}(\mathcal{M}^{(n)})}$, with ${\rm perm}(\mathcal{M}^{(n)})$ being the permanent of the matrix of Eq. (B.4).

By counting two particles in each intermediate node and one in each of the distant nodes A and B, also allowing for classical communication of the counting outcomes, one gets the post-selected state $|\Psi^{(n)}_{\rm b,PS}\rangle$. Bell measurements are then performed step by step on each intermediate node ${\rm M}_i$ ($i = 1,...,k$) to transfer entanglement over A and B. The type of the final Bell state transferred over A and B will depend on the consecutive outcomes of the cascaded Bell measurements. The success probability of the protocol is obtained by $P_{\rm b}(n) = |\langle\Psi^{(n)}_{\rm b,PS}|\Psi^{(n)}_{\rm b}\rangle|^2$. Its explicit expression as a function of the number of bosons is (Figure B.1, blue triangles)

$$P_{\rm b}(n) = \frac{3^{\frac{n}{2}-1}}{2^{n-1}{\rm perm}(\mathcal{M}^{(n)})}. \tag{B.11}$$

In order to be more explicit concerning the cascaded procedure leading to the Bell states over A and B, I treat the case with $n = 6$ bosons ($N = 3$ pairs) and two shared intermediate nodes ${\rm M}_1$, ${\rm M}_2$. From the initially prepared state $|\Psi^{(6)}_{\rm b}\rangle$, easily obtained from Eq. (B.10), the

sLOCC framework counting two particles in the intermediate nodes and one particle in each of the far nodes A and B, including classical communication, leads to the post-selected state

$$\begin{aligned} |\Psi^{(6)}_{\mathrm{b,PS}}\rangle &= \frac{\sqrt{2}}{3}(|\Psi_{\mathrm{M}_1}, 2^+_{\mathrm{AM}_2}\rangle + |\Phi^+_{\mathrm{M}_1}, 2^+_{\mathrm{AM}_2}\rangle \\ &\quad - |\Phi^-_{\mathrm{M}_1}, 2^-_{\mathrm{AM}_2}\rangle) \wedge |1^+_{\mathrm{M}_2\mathrm{B}}\rangle\,, \end{aligned} \tag{B.12}$$

where the relevant Bell states are analogous to those given after Eq. (B.8) and in Eq. (B.18). A first Bell measurement has to be performed on the intermediate node M_1 in order to entangle bosons in A and M_2. Any outcome is good for continuing the protocol. Let us suppose, without loss of generality, that the result of this first Bell measurement is $|\Phi^-_{\mathrm{M}_1}\rangle$. From $|\Psi^{(6)}_{\mathrm{b,PS}}\rangle$ above, one sees that the remaining four bosons are left into the state $-|2^-_{\mathrm{AM}_2}, 1^+_{\mathrm{M}_2\mathrm{B}}\rangle$. This state, suitably normalized and expressed in terms of the Bell basis in the node M_2, assumes the form

$$|\Psi^{(4)}\rangle_{\mathrm{AM_2B}} = \frac{|\Phi^+_{\mathrm{M}_2}, 1^-_{\mathrm{AB}}\rangle + |\Phi^-_{\mathrm{M}_2}, 1^+_{\mathrm{AB}}\rangle + |\Psi_{\mathrm{M}_2}, 2^-_{\mathrm{AB}}\rangle}{\sqrt{3}}. \tag{B.13}$$

It is now clear that a second Bell measurement on the intermediate node M_2 has the final effect to transfer a Bell state over the far nodes A and B. Thus, for six bosons, two cascaded Bell measurements realize the desired entanglement swapping protocol. This procedure can be continued analogously for successive steps with more particles.

B.3 Separated intermediate nodes

Here, I report the calculations regarding the scheme above, depicted in Fig. 5.3 . The prepared state $|\Psi^{(4)}\rangle$ can be written as the superposition of 16 terms

$$\begin{aligned} |\Psi^{(4)}\rangle =& \frac{1}{4}(|\mathrm{A}\downarrow, \mathrm{A}\uparrow, \mathrm{D}\downarrow, \mathrm{D}\uparrow\rangle + |\mathrm{A}\downarrow, \mathrm{A}\uparrow, \mathrm{D}\downarrow, \mathrm{B}\uparrow\rangle \\ &+ |\mathrm{A}\downarrow, \mathrm{A}\uparrow, \mathrm{B}\downarrow, \mathrm{D}\uparrow\rangle + |\mathrm{A}\downarrow, \mathrm{A}\uparrow, \mathrm{B}\downarrow, \mathrm{B}\uparrow\rangle \\ &+ |\mathrm{A}\downarrow, \mathrm{C}\uparrow, \mathrm{D}\downarrow, \mathrm{D}\uparrow\rangle + |\mathrm{A}\downarrow, \mathrm{C}\uparrow, \mathrm{D}\downarrow, \mathrm{B}\uparrow\rangle \\ &+ |\mathrm{A}\downarrow, \mathrm{C}\uparrow, \mathrm{B}\downarrow, \mathrm{D}\uparrow\rangle + |\mathrm{A}\downarrow, \mathrm{C}\uparrow, \mathrm{B}\downarrow, \mathrm{B}\uparrow\rangle \\ &+ |\mathrm{C}\downarrow, \mathrm{A}\uparrow, \mathrm{D}\downarrow, \mathrm{D}\uparrow\rangle + |\mathrm{C}\downarrow, \mathrm{A}\uparrow, \mathrm{D}\downarrow, \mathrm{B}\uparrow\rangle \\ &+ |\mathrm{C}\downarrow, \mathrm{A}\uparrow, \mathrm{B}\downarrow, \mathrm{D}\uparrow\rangle + |\mathrm{C}\downarrow, \mathrm{A}\uparrow, \mathrm{B}\downarrow, \mathrm{B}\uparrow\rangle \\ &+ |\mathrm{C}\downarrow, \mathrm{C}\uparrow, \mathrm{D}\downarrow, \mathrm{D}\uparrow\rangle + |\mathrm{C}\downarrow, \mathrm{C}\uparrow, \mathrm{D}\downarrow, \mathrm{B}\uparrow\rangle \\ &+ |\mathrm{C}\downarrow, \mathrm{C}\uparrow, \mathrm{B}\downarrow, \mathrm{D}\uparrow\rangle + |\mathrm{C}\downarrow, \mathrm{C}\uparrow, \mathrm{B}\downarrow, \mathrm{B}\uparrow\rangle). \end{aligned} \tag{B.14}$$

In the linear combination of Eq. (B.14), there are contributions in which two particles occupy the same site. I perform sLOCC in the form of a post-selection counting a single particle

in each site A, B and classically communicating their outcomes to each other (notice that a single particle in A entails one particle in C and a single particle in B implies one particle in D). This post-selection corresponds to project the global four-particle state $|\Psi^{(4)}\rangle$ onto the subspace spanned by the spatially localized basis $\mathcal{B} = \{|\mathrm{A}\ \sigma, \mathrm{C}\ \tau, \mathrm{D}\ \sigma', \mathrm{B}\ \tau'\rangle\}$, by the projector $\hat{\Pi}_{\mathrm{ACDB}} = \sum_{\sigma,\tau,\sigma',\tau'=\downarrow,\uparrow} |\mathrm{A}\ \sigma, \mathrm{C}\ \tau, \mathrm{D}\ \sigma', \mathrm{B}\ \tau'\rangle\langle \mathrm{A}\ \sigma, \mathrm{C}\ \tau, \mathrm{D}\ \sigma', \mathrm{B}\ \tau'|$. The post-selected (projected) state is thus obtained as

$$|\Psi^{(4)}_{\mathrm{PS}}\rangle = \hat{\Pi}_{\mathrm{ACDB}}|\Psi^{(4)}\rangle/\mathcal{N}, \tag{B.15}$$

where $\mathcal{N} = \sqrt{\langle\Psi^{(4)}|\hat{\Pi}_{\mathrm{ACDB}}|\Psi^{(4)}\rangle} = 1/2$. Its explicit expression is

$$\begin{aligned} |\Psi^{(4)}_{\mathrm{PS}}\rangle =& \frac{1}{\sqrt{2}}(|\mathrm{A}\downarrow, \mathrm{C}\uparrow\rangle + \eta|\mathrm{A}\uparrow, \mathrm{C}\downarrow\rangle) \\ & \wedge \frac{1}{\sqrt{2}}(|\mathrm{D}\downarrow, \mathrm{B}\uparrow\rangle + \eta|\mathrm{D}\uparrow, \mathrm{B}\downarrow\rangle), \end{aligned} \tag{B.16}$$

This state is obtained with probability $P(4) = |\langle\Psi^{(4)}_{\mathrm{PS}}|\Psi^{(4)}\rangle|^2 = 1/4$. Notice that in this sLOCC framework, the prepared state $|\Psi^{(4)}\rangle$ can be written as $|\Psi^{(4)}\rangle = |\alpha\downarrow, \alpha\uparrow\rangle \wedge |\beta\downarrow, \beta\uparrow\rangle$, from which one then obtains particle entanglement between (A, C) and (D, B), as evidenced in Eq. (B.16). This is linked to the concept of indistinguishability as a resource by sLOCC introduced in Ref. [34]. Since the sites (A, C) and (D, B) are separated, the identical particles can be distinguished by their spatial location. Once got the post-selected state $|\Psi^{(4)}_{\mathrm{PS}}\rangle$, the entanglement swapping proceeds following the lines of the standard protocol for distinguishable particles [114]. A Bell measurement is therefore performed on the intermediate nodes (C, D) to obtain entanglement over the far nodes A and B. In fact, one can write

$$\begin{aligned} |\Psi^{(4)}_{\mathrm{PS}}\rangle = \frac{1}{2}[&|1^{+}_{\mathrm{CD}}, 1^{+}_{\mathrm{AB}}\rangle - |1^{-}_{\mathrm{CD}}, 1^{-}_{\mathrm{AB}}\rangle \\ &+ \eta|2^{+}_{\mathrm{CD}}, 2^{+}_{\mathrm{AB}}\rangle - \eta|2^{-}_{\mathrm{CD}}, 2^{-}_{\mathrm{AB}}\rangle], \end{aligned} \tag{B.17}$$

where

$$\begin{aligned} |1^{\pm}_{\mathrm{IJ}}\rangle &= \frac{1}{\sqrt{2}}(|\mathrm{I}\downarrow, \mathrm{J}\uparrow\rangle \pm |\mathrm{I}\uparrow, \mathrm{J}\downarrow\rangle), \\ |2^{\pm}_{\mathrm{IJ}}\rangle &= \frac{1}{\sqrt{2}}(|\mathrm{I}\downarrow, \mathrm{J}\downarrow\rangle \pm |\mathrm{I}\uparrow, \mathrm{J}\uparrow\rangle), \end{aligned} \tag{B.18}$$

with IJ=AB, CD. The result of the Bell measurement does not depend on the particle statistics, as expected from the fact that the post-selected state describes identical particles in separated spatial regions under sLOCC.

The previous protocol can be straightforwardly extended to multiple entanglement swapping

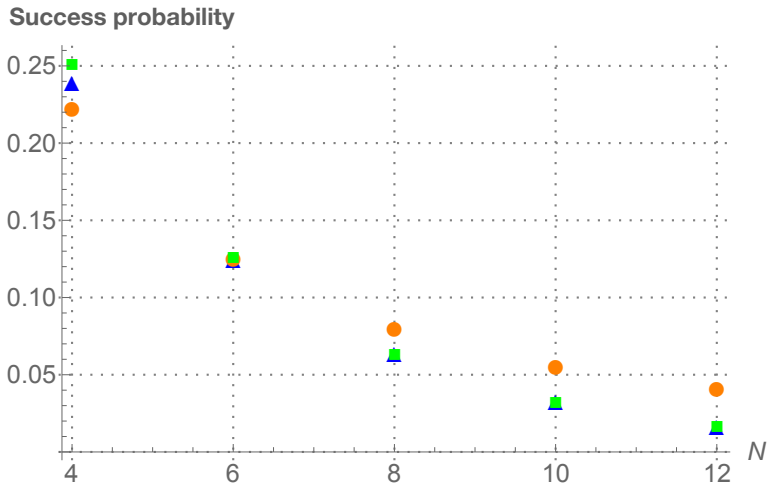

Figure B.1: Success probability to implement multiple entanglement transfer as a function of the number of particles n, for separated nodes with either bosons or fermions ($P(n)$, green squares) and for shared intermediate nodes with fermions ($P_{\mathrm{f}}(n)$, orange points) and with bosons ($P_{\mathrm{b}}(n)$, blue triangles).

(with $n = 2N$ independently prepared particles, being N the number of involved particle pairs), in analogy to the case of distinguishable particles [118], by a cascaded procedure with a success probability $P(n) = 1/2^{\frac{n}{2}}$ (Figure B.1, green squares).

B.4 Probabilities of success

We finally compare the efficiency of the protocol for the various cases treated above, given the prepared state before post-selection. I have already shown that, in the case of separated nodes, the success probability for both bosons and fermions is $P(n) = 1/2^{\frac{n}{2}}$ (see green squares in Fig. B.1). In the case of shared intermediate nodes, the success probabilities $P_{\mathrm{f}}(n)$ for fermions and $P_{\mathrm{b}}(n)$ for bosons decrease as a function of the particle number similarly to $P(n)$, as displayed in Fig. B.1 (orange points and blue triangles, respectively). From the experimental viewpoint, one has to take into account that the requirement of Bell measurements further hinders the protocol efficiency [109, 113, 124, 125, 126, 127, 128, 129]. Therefore, the fermionic process results in being not only qualitatively different, but also more advantageous from a practical viewpoint than the other procedures that necessarily require Bell measurements.

Bibliography

[1] L. Amico, R. Fazio, A. Osterloh, and V. Vedral, "Entanglement in many-body systems," *Rev. Mod. Phys*, vol. 80, pp. 517–576, 2008.

[2] F. Benatti, S. Alipour, and A. T. Rezakhani, "Dissipative quantum metrology in many-body systems of identical particles," *New J. Phys.*, vol. 16, p. 015023, 2014.

[3] M. Cramer, A. Bernard, N. Fabbri, L. Fallani, C. Fort, S. Rosi, F. Caruso, M. Inguscio, and M. B. Plenio, "Spatial entanglement of bosons in optical lattices," *Nat. Comm.*, vol. 4, p. 2161, 2013.

[4] V. Giovannetti, S. Lloyd, and L. Maccone, "Quantum-enhanced measurements: Beating the standard quantum limit," *Science*, vol. 306, pp. 1330–1336, 2004.

[5] I. Bloch, J. Dalibard, and W. Zwerger, "Many-body physics with ultracold gases," *Rev. Mod. Phys.*, vol. 80, no. 3, pp. 885–964, 2008.

[6] M. Anderlini, P. J. Lee, B. L. Brown, J. Sebby-Strabley, W. D. Phillips, and J. Porto, "Controlled exchange interaction between pairs of neutral atoms in an optical lattice," *Nature*, vol. 448, no. 7152, pp. 452–456, 2007.

[7] J. R. Petta, A. C. Johnson, J. M. Taylor, E. A. Laird, A. Yacoby, M. D. Lukin, C. M. Marcus, M. P. Hanson, and A. C. Gossard, "Coherent manipulation of coupled electron spins in semiconductor quantum dots," vol. 309, pp. 2180–2184, 2005.

[8] Z. B. Tan, D. Cox, T. Nieminen, P. Lähteenmäki, D. Golubev, G. B. Lesovik, and P. J. Hakonen, "Cooper pair splitting by means of graphene quantum dots," *Phys. Rev. Lett.*, vol. 114, p. 096602, 2015.

[9] A. Crespi, L. Sansoni, G. D. Valle, A. Ciamei, R. Ramponi, F. Sciarrino, P. Mataloni, S. Longhi, and R. Osellame, "Particle statistics affects quantum decay and Fano interference," *Phys. Rev. Lett.*, vol. 114, p. 090201, 2015.

[10] C. Reimer *et al.*, "Generation of multiphoton entangled quantum states by means of integrated frequency combs," *Science*, vol. 351, pp. 1176–1180, 2016.

[11] R. Zia, J. A. Schuller, A. Chandran, and M. L. Brongersma, "Plasmonics: the next chip-scale technology," *Materials Today*, vol. 9, pp. 20–27, 2006.

[12] C. E. Susa, J. H. Reina, and R. Hildner, "Plasmon-assisted quantum control of distant emitters," *Physics Letters A*, vol. 378, 2014.

[13] A. Castellini, H. R. Jauslin, B. Rousseaux, D. Dzsotjan, G. C. des Francs, A. Messina, and S. Guérin, "Quantum plasmonics with multi-emitters: application to stimulated raman adiabatic passage," *The European Physical Journal D*, vol. 72, 2018.

[14] A. Peres, *Quantum Theory: Concepts and Methods*. Dordrecht, The Netherlands: Springer, 1995.

[15] C. Cohen-Tannoudji, B. Diu, and F. Laloe, *Quantum mechanics. Vol. 2.* Paris, France: Willey-VCH, 2005.

[16] J. Audretsch, *Entangled Systems*. Bonn, Germany: WILEY-VCH, 2007.

[17] R. Horodecki, P. Horodecki, M. Horodecki, and K. Horodecki, "Quantum entanglement," *Rev. Mod. Phys.*, vol. 81, no. 2, pp. 865–942, 2009.

[18] V. Giovannetti, S. Lloyd, and L. Maccone, "Quantum metrology," *Phys. Rev. Lett.*, vol. 96, 2006.

[19] A. K. Ekert, "Quantum cryptography based on bell's theorem," *Phys. Rev. Lett.*, vol. 67, 1991.

[20] C. H. Bennett, G. Brassard, C. Crépeau, R. Jozsa, A. Peres, and W. K. Wootters, "Teleporting an unknown quantum state via dual classical and Einstein-Podolsky-Rosen channels," *Phys. Rev. Lett.*, vol. 70, pp. 1895–1899, 1993.

[21] C. L. Degen, F. Reinhard, and P. Cappellaro, "Quantum sensing," *Rev. Mod. Phys.*, vol. 89, 2017.

[22] R. F. Werner, "Quantum states with Einstein-Podolsky-Rosen correlations admitting a hidden-variable model," *Phys. Rev. A*, vol. 40, no. 8, p. 4277, 1989.

[23] G. Ghirardi and L. Marinatto, "General criterion for the entanglement of two indistinguishable particles," *Phys. Rev. A*, vol. 70, p. 012109, 2004.

[24] M. C. Tichy, F. Mintert, and A. Buchleitner, "Essential entanglement for atomic and molecular physics," *J. Phys. B: At. Mol. Opt. Phys.*, vol. 44, p. 192001, 2011.

[25] J. Schliemann, J. I. Cirac, M. Kus, M. Lewenstein, and D. Loss, "Quantum correlations in two-fermion systems," *Phys. Rev. A*, vol. 64, p. 022303, 2001.

[26] K. Eckert, J. Schliemann, D. Bruss, and M. Lewenstein, "Quantum correlations in systems of indistinguishable particles," *Ann. Phys.*, vol. 299, no. 1, pp. 88–127, 2002.

[27] F. Benatti, R. Floreanini, F. Franchini, and U. Marzolino, "Remarks on entanglement and identical particles," *Open Systems & Information Dynamics*, vol. 24, 2017.

[28] F. Benatti, R. Floreanini, and U. Marzolino, "Sub-shot-noise quantum metrology with entangled identical particles," *Annals of Physics*, vol. 325, 2010.

[29] H. M. Wiseman and J. A. Vaccaro, "Entanglement of indistinguishable particles shared between two parties," *Phys. Rev. Lett.*, vol. 91, p. 097902, 2003.

[30] U. Marzolino and A. Buchleitner, "Quantum teleportation with identical particles," *Phys. Rev. A.*, vol. 91, p. 032316, 2015.

[31] A. Kaufman, B. Lester, M. Foss-Feig, M. Wall, A. Rey, and C. Regal, "Entangling two transportable neutral atoms via local spin exchange," *Nature*, vol. 527, no. 7577, pp. 208–211, 2015.

[32] E. Chitambar, D. Leung, L. Mančinska, M. Ozols, and A. Winter, "Everything you always wanted to know about locc (but were afraid to ask)," *Communications in Mathematical Physics*, vol. 328, 2014.

[33] R. Lo Franco, "Nonlocality threshold for entanglement under general dephasing evolutions: a case study," *Quantum Inform. Process.*, vol. 15, pp. 2393–2404, 2016.

[34] R. Lo Franco and G. Compagno, "Indistinguishability of elementary systems as a resource for quantum information processing," *Phys. Rev. Lett.*, vol. 120, p. 240403, 2018.

[35] S. Sciara, R. Lo Franco, and G. Compagno, "Universality of Schmidt decomposition and particle identity," *Sci. Rep.*, vol. 7, p. 44675, 2017.

[36] B. Bellomo, R. Lo Franco, and G. Compagno, "N identical particles and one particle to entangle them all," *Phys. Rev. A*, vol. 96, no. 2, p. 022319, 2017.

[37] S. Chin and J. Huh, "Entanglement of identical particles and coherence in the first quantization language," *Phys. Rev. A*, vol. 99, 2019.

[38] A. C. Lourenço, T. Debarba, and E. I. Duzzioni, "Entanglement of indistinguishable particles: A comparative study," *Phys. Rev. A*, vol. 99, 2019.

[39] G. Compagno, A. Castellini, and R. Lo Franco, "Dealing with indistinguishable particles and their entanglement," *Phil. Trans. R. Soc. A*, vol. 376, no. 2123, p. 20170317, 2018.

[40] T. Qureshi and U. Rizwan, "Hanbury Brown-Twiss effect with wave packets," *Quanta*, vol. 6, pp. 61–69, 2017.

[41] H. Mani, V. Sreedhar, *et al.*, "Quantum entanglement in one-dimensional anyons," *arXiv preprint arXiv:1910.02654*, 2019.

[42] C. Cohen-Tannoudji, B. Diu, and F. Laloe, *Quantum mechanics. Vol. 1.* Paris, France: Willey-VCH, 2005.

[43] J. J. Sakurai, J. Napolitano, *et al.*, *Modern quantum mechanics*, vol. 185. Pearson Harlow, 2014.

[44] A. Balachandran, T. Govindarajan, A. R. de Queiroz, and A. Reyes-Lega, "Entanglement and particle identity: A unifying approach," *Phys. Rev. Lett.*, vol. 110, p. 080503, 2013.

[45] F. Benatti, R. Floreanini, and U. Marzolino, "Entanglement robustness and geometry in systems of identical particles," *Phys. Rev. A*, vol. 85, p. 042329, 2012.

[46] P. Blasiak and M. Markiewicz, "Entangling three qubits without ever touching," *arXiv preprint arXiv:1807.05546*, 2018.

[47] M. H. Kolodrubetz and J. R. Petta, "Coherent holes in a semiconductor quantum dot," *Science*, vol. 325, no. 5936, pp. 42–43, 2009.

[48] Z. B. Tan, D. Cox, T. Nieminen, P. Lähteenmäki, D. Golubev, G. B. Lesovik, and P. J. Hakonen, "Cooper pair splitting by means of graphene quantum dots," *Phys. Rev. Lett.*, vol. 114, p. 096602, Mar 2015.

[49] F. Martins *et al.*, "Noise suppression using symmetric exchange gates in spin qubits," *Phys. Rev. Lett.*, vol. 116, p. 116801, 2016.

[50] M. C. Tichy, F. de Melo, M. Kus, F. Mintert, and A. Buchleitner, "Entanglement of identical particles and the detection process," *Fortschr. Phys.*, vol. 61, p. 225, 2013.

[51] F. Benatti, R. Floreanini, and K. Titimbo, "Entanglement of identical particles," *Open Syst. Inf. Dyn.*, vol. 21, p. 1440003, 2014.

[52] S. D. Bartlett and H. M. Wiseman, "Entanglement constrained by superselection rules," *Physical review letters*, vol. 91, 2003.

[53] N. Schuch, F. Verstraete, and J. I. Cirac, "Quantum entanglement theory in the presence of superselection rules," *Physical Review A*, vol. 70, p. 042310, 2004.

[54] N. Killoran, M. Cramer, and M. B. Plenio, "Extracting entanglement from identical particles," *Phys. Rev. Lett.*, vol. 112, p. 150501, 2014.

[55] F. Herbut and M. Vujicic, "Irrelevance of the pauli principle in distant correlations between identical fermions," *Journal of Physics A: Mathematical and General*, vol. 20, 1987.

[56] Y. Omar, "Indistinguishable particles in quantum mechanics: an introduction," *Contemporary Physics*, vol. 46, pp. 437–448, 2005.

[57] E. Schrödinger, *Statistical thermodynamics*. Courier Corporation, 1989.

[58] R. Lo Franco and G. Compagno, "Quantum entanglement of identical particles by standard information-theoretic notions," *Sci. Rep.*, vol. 6, p. 20603, 2016.

[59] A. C. Lourenço, T. Debarba, and E. I. Duzzioni, "Entanglement of indistinguishable particles: A comparative study," *Physical Review A*, vol. 99, 2019.

[60] S. Chin and J. Huh, "Entanglement of identical particles and coherence in the first quantization language," *Phys. Rev. A*, vol. 99, 2019.

[61] A. Castellini, R. Lo Franco, L. Lami, A. Winter, G. Adesso, and G. Compagno, "Indistinguishability-enabled coherence for quantum metrology," *Phys. Rev. A*, vol. 100, 2019.

[62] A. Castellini, B. Bellomo, G. Compagno, and R. Lo Franco, "Activating remote entanglement in a quantum network by local counting of identical particles," *Phys. Rev. A*, vol. 99, 2019.

[63] R. Penrose, *The Road to Reality*. New York: Knopf Doubleday Publishing Group, 2007.

[64] R. Horodecki, P. Horodecki, M. Horodecki, and K. Horodecki, "Quantum entanglement," *Rev. Mod. Phys.*, vol. 81, no. 2, pp. 865–942, 2009.

[65] F. Benatti, R. Floreanini, F. Franchini, and U. Marzolino, "Remarks on entanglement and identical particles," *Open Sys. Inform. Dyn.*, vol. 24, p. 1740004, 2017.

[66] M. Walter, D. Gross, and J. Eisert, "Multi-partite entanglement," *arXiv:1612.02437 [quant-ph]*.

[67] E. Lifshitz, LD, and S. L. (JB), *Quantum Mechanics; Non-relativistic Theory*. Pergamon Press, 1965.

[68] L. Amico, R. Fazio, A. Osterloh, and V. Vedral, "Entanglement in many-body systems," *Rev. Mod. Phys*, vol. 80, pp. 517–576, 2008.

[69] F. Nosrati, A. Castellini, G. Compagno, and R. L. Franco, "Control of noisy entanglement preparation through spatial indistinguishability," *arXiv preprint arXiv:1907.00136*, 2019.

[70] A. Trabesinger, "Quantum computing: towards reality," *Nature*, vol. 543, p. S1, 2017.

[71] T. D. Ladd, F. Jelezko, R. Laflamme, Y. Nakamura, C. Monroe, and J. L. O?Brien, "Quantum computers," *Nature*, vol. 464, pp. 45–53, 2010.

[72] X.-L. Wang *et al.*, "Experimental ten-photon entanglement," *Phys. Rev. Lett.*, vol. 117, p. 210502, 2016.

[73] R. Barends *et al.*, "Superconducting quantum circuits at the surface code threshold for fault tolerance," *Nature*, vol. 508, pp. 500–503, 2014.

[74] A. D. Cronin, J. Schmiedmayer, and D. E. Pritchard, "Optics and interferometry with atoms and molecules," *Rev. Mod. Phys.*, vol. 81, pp. 1051–1129, 2009.

[75] D. Braun, G. Adesso, F. Benatti, R. Floreanini, U. Marzolino, M. W. Mitchell, and S. Pirandola, "Quantum-enhanced measurements without entanglement," *Rev. Mod. Phys.*, vol. 90, p. 035006, 2018.

[76] G. C. Ghirardi, L. Reusch, and T. Weber, "Entanglement and properties of composite quantum systems: a conceptual and mathematical analysis," *J. Stat. Phys.*, vol. 108, p. 49, 2002.

[77] N. Brunner, D. Cavalcanti, S. Pironio, V. Scarani, and S. Wehner, "Bell nonlocality," *Rev. Mod. Phys.*, vol. 86, pp. 419–478, 2014.

[78] R. Horodecki, P. Horodecki, and M. Horodecki, "Violating bell inequality by mixed spin-12 states: necessary and sufficient condition," *Physics Letters A*, vol. 200, no. 5, pp. 340–344, 1995.

[79] F. Sciarrino, G. Vallone, A. Cabello, and P. Mataloni, "Bell experiments with random destination sources," *Phys. Rev. A*, vol. 83, no. 3, p. 032112, 2011.

[80] W. K. Wootters, "Entanglement of formation of an arbitrary state of two qubits," *Phys. Rev. Lett.*, vol. 80, pp. 2245–2248, 1998.

[81] C. H. Bennett, D. P. DiVincenzo, J. A. Smolin, and W. K. Wootters, "Mixed-state entanglement and quantum error correction," *Phys. Rev. A*, vol. 54, pp. 3824–3851, Nov 1996.

[82] S. Hill and W. K. Wootters, "Entanglement of a pair of quantum bits," *Phys. Rev. Lett.*, vol. 78, pp. 5022–5025, 1997.

[83] W. K. Wootters, "Entanglement of formation of an arbitrary state of two qubits," *Phys. Rev. Lett.*, vol. 80, pp. 2245–2248, 1998.

[84] Y.-S. Li, B. Zeng, X.-S. Liu, and G.-L. Long, "Entanglement in a two-identical-particle system," *Phys. Rev. A*, vol. 64, p. 054302, 2001.

[85] R. Hanbury Brown and R. Q. Twiss, "A test of a new type of stellar interferometer on Sirius," *Nature*, vol. 178, pp. 1046–1048, 1956.

[86] S. Pirandola, J. Eisert, C. Weedbrook, A. Furusawa, and S. L. Braunstein, "Advances in quantum teleportation," *Nat. Photon.*, vol. 9, pp. 641–652, 2015.

[87] U. Marzolino and A. Buchleitner, "Performances and robustness of quantum teleportation with identical particles," *Proc. R. Soc. A.*, vol. 472, p. 20150621, 2016.

[88] F. Sciarrino, G. Vallone, A. Cabello, and P. Mataloni, "Bell experiments with random destination sources," *Phys. Rev. A*, vol. 83, p. 032112, 2011.

[89] J. F. Clauser, M. A. Horne, A. Shimony, and R. A. Holt, "Proposed experiment to test local hidden-variable theories," *Phys. Rev. Lett.*, vol. 23, pp. 880–884, 1969.

[90] N. Brunner, D. Cavalcanti, S. Pironio, V. Scarani, and S. Wehner, "Bell nonlocality," *Rev. Mod. Phys.*, vol. 86, pp. 419–478, 2014.

[91] N. Lütkenhaus, J. Calsamiglia, and K.-A. Suominen, "Bell measurements for teleportation," *Phys. Rev. A*, vol. 59, pp. 3295–3300, 1999.

[92] J. Calsamiglia and N. Lutkenhaus, "Maximum efficiency of a linear-optical Bell-state analyzer," *App. Phys. B-Las. Opt.*, vol. 72, pp. 67–71, 2001.

[93] S. Massar and S. Popescu, "Optimal extraction of information from finite quantum ensembles," *Phys. Rev. Lett.*, vol. 74, pp. 1259–1263, 1995.

[94] J. L. O'Brien, G. J. Pryde, A. Gilchrist, D. F. V. James, N. K. Langford, T. C. Ralph, and A. G. White, "Quantum process tomography of a controlled-not gate," *Phys. Rev. Lett.*, vol. 93, p. 080502, 2004.

[95] M. A. Nielsen and I. L. Chuang, *Quantum Computation and Quantum Information*. Cambridge: Cambridge University Press, 2010.

[96] N. Gisin and R. Thew, "Quantum communication," *Nat. Photon.*, vol. 1, no. 3, p. 165, 2007.

[97] Y. Omar, "Particle statistics in quantum information processing," *Int. J. Quantum Inform.*, vol. 3, p. 201, 2005.

[98] Y. Omar, N. Paunković, S. Bose, and V. Vedral, "Spin-space entanglement transfer and quantum statistics," *Phys. Rev. A*, vol. 65, p. 062305, 2002.

[99] N. Paunković, Y. Omar, S. Bose, and V. Vedral, "Entanglement concentration using quantum statistics," *Phys. Rev. Lett.*, vol. 88, p. 187903, 2002.

[100] S. Bose, A. Ekert, Y. Omar, N. Paunković, and V. Vedral, "Optimal state discrimination using particle statistics," *Phys. Rev. A*, vol. 68, p. 052309, 2003.

[101] S. Bose and D. Home, "Generic entanglement generation, quantum statistics, and complementarity," *Phys. Rev. Lett.*, vol. 88, no. 5, p. 050401, 2002.

[102] A. Scherer, B. C. Sanders, and W. Tittel, "Long-distance practical quantum key distribution by entanglement swapping," *Opt. Express*, vol. 19, no. 4, pp. 3004–3018, 2011.

[103] T.-Y. Ye, "Robust quantum dialogue based on the entanglement swapping between any two logical bell states and the shared auxiliary logical bell state," *Quant. Inform. Process.*, vol. 14, no. 4, pp. 1469–1486, 2015.

[104] M. Naseri, "Revisiting quantum authentication scheme based on entanglement swapping," *Int. J. Theor. Phys.*, vol. 55, no. 5, pp. 2428–2435, 2016.

[105] Q.-C. Sun, Y.-L. Mao, Y.-F. Jiang, Q. Zhao, S.-J. Chen, W. Zhang, W.-J. Zhang, X. Jiang, T.-Y. Chen, L.-X. You, *et al.*, "Entanglement swapping with independent sources over an optical-fiber network," *Phys. Rev. A*, vol. 95, no. 3, p. 032306, 2017.

[106] B. Jacobs, T. Pittman, and J. Franson, "Quantum relays and noise suppression using linear optics," *Phys. Rev. A*, vol. 66, no. 5, p. 052307, 2002.

[107] J.-W. Pan, D. Bouwmeester, H. Weinfurter, and A. Zeilinger, "Experimental entanglement swapping: entangling photons that never interacted," *Phys. Rev. Lett.*, vol. 80, no. 18, p. 3891, 1998.

[108] H. de Riedmatten, I. Marcikic, J. A. W. van Houwelingen, W. Tittel, H. Zbinden, and N. Gisin, "Long-distance entanglement swapping with photons from separated sources," *Phys. Rev. A*, vol. 71, p. 050302, May 2005.

[109] T. Yang, Q. Zhang, T.-Y. Chen, S. Lu, J. Yin, J.-W. Pan, Z.-Y. Wei, J.-R. Tian, and J. Zhang, "Experimental synchronization of independent entangled photon sources," *Phys. Rev. Lett.*, vol. 96, no. 11, p. 110501, 2006.

[110] R. Kaltenbaek, R. Prevedel, M. Aspelmeyer, and A. Zeilinger, "High-fidelity entanglement swapping with fully independent sources," *Phys. Rev. A*, vol. 79, p. 040302, Apr 2009.

[111] E. Megidish, A. Halevy, T. Shacham, T. Dvir, L. Dovrat, and H. Eisenberg, "Entanglement swapping between photons that have never coexisted," *Phys. Rev. Lett.*, vol. 110, no. 21, p. 210403, 2013.

[112] Q.-C. Sun, Y.-F. Jiang, Y.-L. Mao, L.-X. You, W. Zhang, W.-J. Zhang, X. Jiang, T.-Y. Chen, H. Li, Y.-D. Huang, *et al.*, "Entanglement swapping over 100 km optical fiber with independent entangled photon-pair sources," *Optica*, vol. 4, no. 10, pp. 1214–1218, 2017.

[113] C. Hu and J. Rarity, "Loss-resistant state teleportation and entanglement swapping using a quantum-dot spin in an optical microcavity," *Phys. Rev. B*, vol. 83, no. 11, p. 115303, 2011.

[114] M. Zukowski, A. Zeilinger, M. A. Horne, and A. K. Ekert, ""event-ready-detectors" Bell experiment via entanglement swapping," *Phys. Rev. Lett.*, vol. 71, pp. 4287–4290, 1993.

[115] T. Jennewein, G. Weihs, and A. Pan, J.-W.and Zeilinger, "Experimental nonlocality proof of quantum teleportation and entanglement swapping," *Phys. Rev. Lett.*, vol. 88, p. 017903, Dec 2001.

[116] C. Branciard, N. Gisin, and S. Pironio, "Characterizing the nonlocal correlations created via entanglement swapping," *Phys. Rev. Lett.*, vol. 104, no. 17, p. 170401, 2010.

[117] S. Bose, V. Vedral, and P. L. Knight, "Multiparticle generalization of entanglement swapping," *Phys. Rev. A*, vol. 57, no. 2, p. 822, 1998.

[118] A. M. Goebel, C. Wagenknecht, Q. Zhang, Y.-A. Chen, K. Chen, J. Schmiedmayer, and J.-W. Pan, "Multistage entanglement swapping," *Phys. Rev. Lett.*, vol. 101, no. 8, p. 080403, 2008.

[119] A. Khalique, W. Tittel, and B. C. Sanders, "Practical long-distance quantum communication using concatenated entanglement swapping," *Phys. Rev. A*, vol. 88, no. 2, p. 022336, 2013.

[120] C.-Y. Lu, T. Yang, and J.-W. Pan, "Experimental multiparticle entanglement swapping for quantum networking," *Phys. Rev. Lett.*, vol. 103, p. 020501, Jul 2009.

[121] A. N. Vamivakas, B. E. Saleh, A. V. Sergienko, and M. C. Teich, "Theory of spontaneous parametric down-conversion from photonic crystals," *Phys. Rev. A*, vol. 70, no. 4, p. 043810, 2004.

[122] A. Dousse, J. Suffczyński, A. Beveratos, O. Krebs, A. Lemaître, I. Sagnes, J. Bloch, P. Voisin, and P. Senellart, "Ultrabright source of entangled photon pairs," *Nature*, vol. 466, no. 7303, p. 217, 2010.

[123] A. Scherer, R. B. Howard, B. C. Sanders, and W. Tittel, "Quantum states prepared by realistic entanglement swapping," *Phys. Rev. A*, vol. 80, p. 062310, Dec 2009.

[124] S.-W. Lee and H. Jeong, "Bell-state measurement and quantum teleportation using linear optics: two-photon pairs, entangled coherent states, and hybrid entanglement," *arXiv:1304.1214 [quant-ph]*, 2013.

[125] M. Yang, W. Song, and Z.-L. Cao, "Entanglement swapping without joint measurement," *Phys. Rev. A*, vol. 71, no. 3, p. 034312, 2005.

[126] R. Pakniat, M. H. Zandi, and M. K. Tavassoly, "On the entanglement swapping by using the beam splitter," *Eur. Phys. J. Plus*, vol. 132, no. 1, p. 3, 2017.

[127] W. P. Grice, "Arbitrarily complete Bell-state measurement using only linear optical elements," *Phys. Rev. A*, vol. 84, p. 042331, 2011.

[128] L. Zhou and Y.-B. Sheng, "Complete logic Bell-state analysis assisted with photonic Faraday rotation," *Phys. Rev. A*, vol. 92, p. 042314, 2015.

[129] Y.-B. Sheng, F.-G. Deng, and G. L. Long, "Complete hyperentangled-Bell-state analysis for quantum communication," *Phys. Rev. A*, vol. 82, p. 032318, 2010.

[130] D. Pirandola, S.and Vitali, P. Tombesi, and S. Lloyd, "Macroscopic entanglement by entanglement swapping," *Phys. Rev. Lett.*, vol. 97, p. 150403, Oct 2006.

[131] D. Press, T. D. Ladd, B. Zhang, and Y. Yamamoto, "Complete quantum control of a single quantum dot spin using ultrafast optical pulses," *Nature*, vol. 456, no. 7219, p. 218, 2008.

[132] G. Fève, A. Mahé, J.-M. Berroir, T. Kontos, B. Placais, D. Glattli, A. Cavanna, B. Etienne, and Y. Jin, "An on-demand coherent single-electron source," *Science*, vol. 316, no. 5828, pp. 1169–1172, 2007.

[133] E. Bocquillon, V. Freulon, J.-M. Berroir, P. Degiovanni, B. Plaçais, A. Cavanna, Y. Jin, and G. Fève, "Coherence and indistinguishability of single electrons emitted by independent sources," *Science*, vol. 339, p. 1054, 2013.

[134] M. Rashidi, W. Vine, T. Dienel, L. Livadaru, J. Retallick, T. Huff, K. Walus, and R. A. Wolkow, "Initiating and monitoring the evolution of single electrons within atom-defined structures," *Phys. Rev. Lett.*, vol. 121, p. 166801, 2018.

[135] J. C. Matthews, K. Poulios, J. D. Meinecke, A. Politi, A. Peruzzo, N. Ismail, K. Wörhoff, M. G. Thompson, and J. L. O'Brien, "Observing fermionic statistics with photons in arbitrary processes," *Sci. Rep.*, vol. 3, p. 1539, 2013.

[136] L. Sansoni, F. Sciarrino, G. Vallone, P. Mataloni, A. Crespi, R. Ramponi, and R. Osellame, "Two-particle bosonic-fermionic quantum walk via integrated photonics," *Phys. Rev. Lett.*, vol. 108, no. 1, p. 010502, 2012.

[137] C. Orzel, M. Walhout, U. Sterr, P. S. Julienne, and S. L. Rolston, "Spin polarization and quantum-statistical effects in ultracold ionizing collisions," *Phys. Rev. A*, vol. 59, pp. 1926–1935, 1999.

[138] E. Chitambar and G. Gour, "Quantum resource theories," *Reviews of Modern Physics*, vol. 91, no. 2, p. 025001, 2019.

[139] E. Buks, R. Schuster, M. Heiblum, D. Mahalu, and V. Umansky, "Dephasing in electron interference by a 'which-path'detector," *Nature*, vol. 391, no. 6670, p. 871, 1998.

[140] A. D. Armour and M. P. Blencowe, "Possibility of an electromechanical which-path interferometer," *Phys. Rev. B*, vol. 64, p. 035311, Jun 2001.

[141] A. S. Parkins, P. Marte, P. Zoller, O. Carnal, and H. J. Kimble, "Quantum-state mapping between multilevel atoms and cavity light fields," *Phys. Rev. A*, vol. 51, pp. 1578–1596, Feb 1995.

[142] L. Xiu, L. Hong-Cai, Y. Rong-Can, and H. Zhi-Ping, "Entanglement swapping without joint measurement via a λ-type atom interacting with bimodal cavity field," *Chin. Phys.*, vol. 16, no. 4, p. 919, 2007.

[143] R. Pakniat, M. Tavassoly, and M. Zandi, "Entanglement swapping and teleportation based on cavity qed method using the nonlinear atom–field interaction: Cavities with a hybrid of coherent and number states," *Opt. Comm.*, vol. 382, pp. 381–385, 2017.

[144] C. Bäuerle, D. C. Glattli, T. Meunier, F. Portier, P. Roche, P. Roulleau, S. Takada, and X. Waintal, "Coherent control of single electrons: a review of current progress," *Rep. Prog. Phys.*, vol. 81, no. 5, p. 056503, 2018.

[145] B. Bellomo, R. Lo Franco, and G. Compagno, "Dynamics of non-classically-reproducible entanglement," *Phys. Rev. A*, vol. 78, p. 062309, Dec 2008.

[146] A. Perez-Leija, D. Guzmán-Silva, R. d. J. León-Montiel, M. Gräfe, M. Heinrich, H. Moya-Cessa, K. Busch, and A. Szameit, "Endurance of quantum coherence due to particle indistinguishability in noisy quantum networks," *npj Quantum Information*, vol. 4, no. 1, p. 45, 2018.

[147] E. Chitambar and G. Gour, "Critical examination of incoherent operations and a physically consistent resource theory of quantum coherence," *Phys. Rev. Lett.*, vol. 117, no. 3, 2016.

[148] T. Baumgratz, M. Cramer, and M. B. Plenio, "Quantifying coherence," *Phys. Rev. Lett.*, vol. 113, no. 14, p. 140401, 2014.

[149] C. Napoli, T. R. Bromley, M. Cianciaruso, M. Piani, N. Johnston, and G. Adesso, "Robustness of coherence: an operational and observable measure of quantum coherence," *Phys. Rev. Lett.*, vol. 116, no. 15, p. 150502, 2016.

[150] M. Piani, M. Cianciaruso, T. R. Bromley, C. Napoli, N. Johnston, and G. Adesso, "Robustness of asymmetry and coherence of quantum states," *Phys. Rev. A*, vol. 93, no. 4, 2016.

[151] J. I. de Vicente and A. Streltsov, "Genuine quantum coherence," *J. Phys. A: Math. Theor.*, vol. 50, no. 4, p. 045301, 2016.

[152] A. Winter and D. Yang, "Operational resource theory of coherence," *Phys. Rev. Lett.*, vol. 116, no. 12, p. 120404, 2016.

[153] A. Streltsov, G. Adesso, and M. B. Plenio, "Colloquium: Quantum coherence as a resource," *Rev. Mod. Phys.*, vol. 89, 2017.

[154] A. Streltsov, G. Adesso, and M. B. Plenio, "Colloquium: Quantum coherence as a resource," *Rev. Mod. Phys.*, vol. 89, p. 041003, 2017.

[155] N. Killoran, M. Cramer, and M. B. Plenio, "Extracting entanglement from identical particles," *Phys. Rev. Lett.*, vol. 112, p. 150501, 2014.

[156] D. P. Pires, I. A. Silva, D. O. Soares-Pinto, and J. G. Filgueiras, "Coherence orders, decoherence, and quantum metrology," *Phys. Rev. A*, vol. 98, no. 3, 2018.

[157] K. Korzekwa, M. Lostaglio, J. Oppenheim, and D. Jennings, "The extraction of work from quantum coherence," *New J. Phys.*, vol. 18, no. 2, 2016.

[158] J. P. Santos, L. C. Céleri, G. T. Landi, and M. Paternostro, "The role of quantum coherence in non-equilibrium entropy production," *npj Quantum Information*, vol. 5, no. 1, 2019.

[159] G. C. Ghirardi, L. Marinatto, and T. Weber, "Entanglement and properties of composite quantum systems: a conceptual and mathematical analysis," *J. Stat. Phys.*, vol. 108, p. 49, 2002.

[160] D. Braun, G. Adesso, F. Benatti, R. Floreanini, U. Marzolino, M. W. Mitchell, and S. Pirandola, "Quantum-enhanced measurements without entanglement," *Rev. Mod. Phys.*, vol. 90, p. 035006, 2018.

[161] M. Ringbauer, T. R. Bromley, M. Cianciaruso, L. Lami, W. S. Lau, G. Adesso, A. G. White, A. Fedrizzi, and M. Piani, "Certification and quantification of multilevel quantum coherence," *Phys. Rev. X*, vol. 8, 2018.

[162] C. W. Helstrom, *Quantum detection and estimation theory / Carl W. Helstrom*. Academic Press New York, 1976.

[163] S. M. Barnett and S. Croke *Adv. Opt. Photon.*, vol. 1, no. 2, 2009.

[164] K. Kraus, *States, effects and operations: fundamental notions of quantum theory*. Springer, 1983.

[165] B. G.-g. Chen, D. Derbes, D. Griffiths, B. Hill, R. Sohn, and Y.-S. Ting, *Lectures of Sidney Coleman on Quantum Field Theory*. WORLD SCIENTIFIC, 2019.

[166] A. Zee, *Quantum field theory in a nutshell*, vol. 7. Princeton university press, 2010.

[167] M. A. Nielsen and I. Chuang, *Quantum computation and quantum information*. AAPT, 2002.

[168] P. Zanardi, "Quantum entanglement in fermionic lattices," *Phys. Rev. A*, vol. 65, p. 042101, 2002.

[169] A. Castellini, R. L. Franco, and G. Compagno, “Effects of indistinguishability in a system of three identical qubits,” *Proceedings*, vol. 12, 2019.